FOREWORD

This report was prepared by the Engineering Analysis Division of Computer Engineering Associates, Pasadena, California, on Air Force contract AF 33(657)-8293, under Task Number 821901, Project Number 8219. The work was administered by the Stability and Control Section, Control Criteria Branch, Flight Control Division of the Air Force Flight Dynamics Laboratory. Mr. Robert L. Swaim was project engineer for the Laboratory.

Work under the contract began in March 1962, and was concluded in August of 1963. Most of the research was carried out by Robert G. Schwendler and Jack H. Hill, and valuable contributions were made by Dr. Richard H. MacNeal, who also directed the early phases of the research activity.

This is the final report and concludes work on contract AF 33(657)-8293.

ABSTRACT

This report contains an investigation of "mode interaction" instabilities of aircraft. "Mode interaction" refers to coupling between an elastic mode and a rigid body mode of the free system. Three rather general airframe configurations are analyzed in detail. It is shown that systems which tend toward steady state divergence are particularly susceptible to mode interaction. Also, that aerodynamic damping terms can have a destabilizing effect upon a free system. The analyses show that aeroelastic systems which possess no finite frequency elastic mode can be susceptible to a finite frequency instability. Computer studies of several different airframe configurations are discussed. An appendix to the report contains stability charts for an aircraft having two rigid body modes and one elastic mode.

PUBLICATION REVIEW

This technical documentary report has been reviewed and is approved.

C. B. WESTBROOK
Chief, Control Criteria Branch
Flight Control Division
AF Flight Dynamics Laboratory

TABLE OF CONTENTS

TABLE OF CONTENTS (CONT'D)

LIST OF ILLUSTRATIONS

LIST OF ILLUSTRATIONS (CONT'D)

LIST OF TABLES

LIST OF SYMBOLS

m	Mass (lb.-sec.^{2}/in.)
I	Moment of inertia = mr^2 (lb.-sec.^{2}-in.)
r, r_e	Radii of gyration (in.)
R	Generalized mass ratio, $\frac{r^2}{r_e^2}$
k, K	Stiffnesses (in.-lb./rad. or lb./in.)
x	Distance measured from center of gravity (in.)
x_e	Distance from center of gravity to elastic axis (in.)
x_{ac}	Distance from center of gravity to aerodynamic center (in.)
$x_{n\delta}$	Distance from center of gravity to node line (in.)
x_{ae}	Distance from aerodynamic center to elastic axis = $x_{ac} - x_e$ (in.)
x_{an}	Distance from aerodynamic center to node line = $x_{ac} - x_{n\delta}$ (in.)
z	Vertical deflection of center of gravity (in.)
z_a	Vertical deflection of aerodynamic center (in.)
θ	Pitch angle of fuselage (rad.)
θ_a	Pitch angle of lifting surface (rad.)
ω	Frequency (rad./sec.)
ω_z	Plunge frequency (rad./sec.)
ω_θ	Pitch frequency (rad./sec.)
ω_o^*	Undamped pitch frequency, including residual flexibility of higher modes (rad./sec.)
ω_o	Undamped pitch frequency for rigid airframe $= \sqrt{-\frac{\frac{1}{2}\rho V^2 S C_{L_\alpha} x_{ac}}{m r^2}}$ (rad./sec.)
s	Derivative operator, d/dt (rad./sec.)

LIST OF SYMBOLS (Cont'd)

$\{\Phi\}$	Eigenvector
$[\Phi]$	Modal matrix, array of eigenvectors
ξ	Generalized coordinate deflection
$[Q]$	Aerodynamic force coefficient matrix
p	Pressure (lb./in.^{2})
q	Dynamic pressure, $\frac{1}{2} \rho V^2$ (lb./in.^{2})
ρ	Air density (lb.-sec.^{2}/in.^{4})
V	Velocity (in./sec.)
$[X]$	Flexibility matrix
$[I]$ $[I]$	Unit diagonal matrix
D	Aeroelastic index
c	Chord of lifting surface (in.)
S	Area of lifting surface (in.^{2})
C_{L_α}	Lift curve slope
C_{L_q}	Pitch damping force coefficient
C_{m_q}	Pitch damping moment coefficient
L	Lift (lb.)
M	Moment (in.-lb.)
g	Damping factor (g = 2 for a critically damped system)

LIST OF SYMBOLS (Cont'd)

Subscripts and Superscripts

e	Elastic mode or elastic axis
h, z	Plunge coordinate
θ	Pitch coordinate
r	r normal modes
D	Steady state divergence
a	Aerodynamic center
∞	Infinite frequency modes
o	Zero frequency modes

A bar "—" over a symbol is used to distinguish a nondimensionalized quantity from the corresponding dimensional quantity.

I. INTRODUCTION

The investigation of reference 1, titled "Optimum Structural Representation in Aeroelastic Analyses" was initiated as a study of the effects of elastic modes of an aeroelastic system on the low frequency response of the system. The results of that investigation provided a straight forward method of representing a system in terms of a few of its normal coordinates and the "residual flexibility" of all higher modes which proved to be an accurate approximation of the aeroelastic system for the prediction of its dynamic behavior in the frequency band from zero through the frequencies of the normal modes explicitly included in the representation.

This method of structural representation was shown to be valid in all configurations studied except in the case of "mode interaction" where no conclusions were drawn. "Mode interaction" is defined as a condition of potential or incipient aeroelastic instability involving one elastic mode and one rigid body mode of the free system.

The investigation reported here was undertaken to provide some insight into the mechanism of "mode interaction" and to provide a means of predicting the susceptibility of a given configuration to this phenomenon. Since the "mode interaction" phenomenon is definable in terms of a potential aeroelastic instability, this study was aimed particularly at the prediction and understanding of the instability rather than at prediction of the response at a subcritical speed.

Manuscript released by authors August 1963 for publication as an ASD Technical Documentary Report.

The prediction of critical velocity (flutter speed) and the system response at a subcritical speed is certainly a solvable problem for any system. Many standard references on flutter analysis and aeroelasticity present general methods which are comprehensive in their potential application. Reference 1 presents equations of motion of an aeroelastic system which are an example of a completely comprehensive analysis. Equation (3.69) of reference 1 is

$$\left[Y_{K}\right]\left\{\xi_{K}\right\} = \left[\Phi_{mK}\right]^{T}\left(\left[I\right] - \left[Q_{mm}\right]\left[X^{\infty}_{mm}\right]\right)^{-1}\left(\left[Q_{mm}\right]\left[\Phi_{mK}\right]\left\{\xi_{K}\right\} + \left\{F^{(a)}_{m}\right\}\right) \quad \text{(I-1)}$$

where:

$\left[Y_{K}\right]$ is a diagonal matrix of the generalized mass and stiffness of the normal modes, $\left[Y_{K}\right] = \left[K_{K}\right] - \omega^{2}\left[m_{K}\right]$.

$\left\{\xi_{K}\right\}$ is the vector of normal coordinate deflections.

$\left[\Phi_{mK}\right]$ is the matrix of normal mode shapes or the "modal matrix" of physical coordinates m. $\left[\Phi_{mK}\right]$ is a square matrix.

$\left[Q_{mm}\right]$ is the aerodynamic influence coefficient matrix in the physical coordinates m, defined by $\left\{F_{m}\right\} = \left[Q_{mm}\right]\left\{y_{m}\right\}$.

$\left[X^{\infty}_{mm}\right]$ is the residual flexibility matrix or a matrix defining the stiffness properties of the system which are not included in the generalized stiffnesses $\left[K_{K}\right]$.

$\left\{F^{(a)}_{m}\right\}$ is a vector of additional externally applied forces.

Equation (I-1) can provide a rigorous statement of the equations of motion of a system if <u>all</u> elastic modes of the system are included in the K coordinates and at least an excellent approximation of the system equations when the K coordinates include a reasonable number of the lowest modes of the system.

Equation (I-1) is useful in providing an accurate prediction of the dynamic response of a complicated system. Such predictions, however, do not always give an understanding of the basic mechanism of the phenomena being studied. Thus, such an equation can provide means of discovering that a given aircraft design has unsatisfactory stability and control characteristics, but unless the basic mechanism of the instability is understood by the designer, he will be unable to foresee which design changes result in improvement. The systems analysed in this study were selected so as to throw light on the basic mechanisms of mode interaction. In order to illustrate these mechanisms clearly, it was often found useful to make simplifying assumptions. Therefore the results of this study apply to more definite stability and control problems than does equation (I-1), which is very general.

Three analyses are made in this study. These analyses consider the following systems:

1. (Section II) Analysis of an airframe represented by two rigid body modes, one elastic mode, and the "residual flexibility" of all higher modes. The chief simplifying assumption of this analysis is the omission of all damping terms from the equations of motion of the system.
2. (Section III) Analysis of an airframe consisting of a simple airfoil flexibly attached to a rigid fuselage. In addition to the assumption that the fuselage is rigid, it is also assumed that the airfoil has no mass.
3. (Section IV) Analysis of an airframe having two rigid body modes and one elastic mode. This analysis omits all consideration of

residual flexibility of the higher modes of the system.

Since this study is aimed particularly at the supersonic and high subsonic velocity regime, aerodynamic lag functions were omitted in all analyses.

II. ANALYSIS OF AN AIRFRAME REPRESENTED BY TWO RIGID BODY MODES, ONE ELASTIC MODE, AND THE "RESIDUAL FLEXIBILITY" OF ALL HIGHER MODES

The "residual flexibility" approximation, derived in reference 1, in generalized modal analyses provides a means of including all stiffness properties of a system in the analyses while the mass is represented by the generalized mass of a selected number of lower-frequency normal modes. Advantages in simplicity of solution of the conventional truncated modal approach are obtained when the coordinate velocity dependent terms are omitted. The omission of these damping terms in the equations of motion will be detrimental to the accuracy of the predicted stability boundaries, but this analysis will be shown to be useful by providing some insight into the stability problems of more complex structures.

The airframe configuration considered in this analysis will be a general one defined only by the following parameters.

m = the total mass of the system.

r = the radius of gyration of the system (then mr^2 is the pitching mass moment of inertia of the airframe about its c.g.).

$r_e^2 m$ = the generalized mass of the first elastic mode of the system. Thus r_e is just a radius of gyration obtained by dividing the generalized mass of the first elastic mode by the total mass, and taking the square root.

ω_e = the undamped natural frequency of the first elastic mode.

$\begin{bmatrix} \Phi_{hr} \\ \hline \Phi_{\theta r} \end{bmatrix}$ = the modal matrix defining the mode shapes at the h (plunge) coordinates and the θ (pitch) coordinates of the system

for the r modes included. 3 modes are included, the zero frequency plunge mode (mode 1), the zero frequency pitch mode (mode 2) and the first elastic mode (mode 3).

$\begin{bmatrix} X_{hh} & X_{\theta h}^T \\ X_{\theta h} & X_{\theta\theta} \end{bmatrix}$ = the flexibility matrix of the complete free system when the zero frequency modes are restrained to zero displacement, partitioned by h and θ coordinates.

$\begin{bmatrix} X_{hh}^{\infty} & X_{\theta h}^{\infty T} \\ X_{\theta h}^{\infty} & X_{\theta\theta}^{\infty} \end{bmatrix}$ = the "residual flexibility" matrix of all elastic modes higher than the first, partitioned by h and θ coordinates. This matrix actually is not needed to define the system since (from a special case of equation (3.21) of reference 1) it is determined from system parameters listed above by the equation

$$\left[X_{ii}^{\infty}\right] = \left[X_{ii}\right] - \left[\Phi_{ir}\right]\left[\frac{1}{m_r \omega_r^2}\right]\left[\Phi_{ir}\right]^T$$

where X_{ii} is the flexibility matrix with the zero frequency modes restrained.

The aerodynamic forces included in this analysis will be defined by the following partitioned matrix equation

$$\begin{Bmatrix} F_h \\ M_\theta \end{Bmatrix} = q \begin{bmatrix} 0 & Q_{h\theta} \\ 0 & 0 \end{bmatrix} \begin{Bmatrix} h \\ \theta \end{Bmatrix} \qquad \text{(II-1)}$$

where q is the dynamic pressure $\frac{1}{2}\rho V^2$.

The equations of motion of the aeroelastic system can be written by a process of partitioning equation (I-1). The quantity $-\omega^2$ in equation (I-1) is replaced by s^2 in equation (II-2), since we look for solutions of the equations of motion having time dependence of the form e^{st}, where s may be complex.

$$\begin{bmatrix} ms^2 & 0 & 0 \\ 0 & mr^2s^2 & 0 \\ 0 & 0 & mr_e^2(s^2+\omega_e^2) \end{bmatrix} \begin{Bmatrix} \xi_1 \\ \xi_2 \\ \xi_3 \end{Bmatrix} =$$

$$\left[\begin{array}{c|c} \{\Phi_h^1\}^T & \{\Phi_\theta^1\}^T \\ \hline \{\Phi_h^2\}^T & \{\Phi_\theta^2\}^T \\ \hline \{\Phi_h^3\}^T & \{\Phi_\theta^3\}^T \end{array}\right] \left\{\left[\begin{array}{c|c} I & 0 \\ \hline 0 & I \end{array}\right] - q \left[\begin{array}{c|c} 0 & Q_{h\theta} \\ \hline 0 & 0 \end{array}\right] \left[\begin{array}{c|c} X_{hh}^{\infty} & X_{\theta h}^{\infty T} \\ \hline X_{\theta h}^{\infty} & X_{\theta\theta}^{\infty} \end{array}\right]^{-1} q \left[\begin{array}{c|c} 0 & Q_{h\theta} \\ \hline 0 & 0 \end{array}\right]\right] \left[\begin{array}{c|c|c} \{\Phi_h^1\} & \{\Phi_h^2\} & \{\Phi_h^3\} \\ \hline \{\Phi_\theta^1\} & \{\Phi_\theta^2\} & \{\Phi_\theta^3\} \end{array}\right] \begin{Bmatrix} \xi_1 \\ \xi_2 \\ \xi_3 \end{Bmatrix} \qquad \text{(II-2)}$$

Including only the non-zero terms of the matrix product on the right side of equation (II-2),

$$\begin{bmatrix} ms^2 & 0 & 0 \\ 0 & mr^2s^2 & 0 \\ 0 & 0 & mr_e^2(s^2+\omega_e^2) \end{bmatrix} \begin{Bmatrix} \xi_1 \\ \xi_2 \\ \xi_3 \end{Bmatrix} =$$

$$\begin{bmatrix} \{\Phi_h^1\}^T \\ \{\Phi_h^2\}^T \\ \{\Phi_h^3\}^T \end{bmatrix} \left\{[I] - q[Q_{h\theta}][X_{\theta h}^{\infty}]\right\}^{-1} q[Q_{h\theta}] \left[\{\Phi_\theta^1\} \mid \{\Phi_\theta^2\} \mid \{\Phi_\theta^3\}\right] \begin{Bmatrix} \xi_1 \\ \xi_2 \\ \xi_3 \end{Bmatrix} \qquad \text{(II-3)}$$

In order to shorten subsequent matrix equations we shall define an "aeroelastic aerodynamic influence coefficient matrix" $\left[\bar{Q}_{h\theta}\right]$ as follows

$$\left[\bar{Q}_{h\theta}\right] = \left\{\left[I\right] - q\left[Q_{h\theta}\right]\left[X^{\infty}_{\theta h}\right]\right\}^{-1}\left[Q_{h\theta}\right] \qquad \text{(II-4)}$$

It is well to note that $\left[\bar{Q}_{h\theta}\right]$ is a function of the dynamic pressure (q) and the number of elastic modes explicitly included in the analysis (in this case 1 mode).

The equations of motion of equation (II-3) may be further simplified by recognizing that the modal column $\left\{\Phi_{\theta}{}^{1}\right\}$, the pitching slope deflections in the rigid plunge mode, is equal to zero, and that the modal columns $\left\{\Phi_{h}{}^{1}\right\}$ and $\left\{\Phi_{\theta}{}^{2}\right\}$, the plunge deflections in the rigid plunge mode and the pitch slopes in the rigid pitch mode, are equal to $\left\{1\right\}$, a column of ones, due to normalization. The equations of motion now may be written in the form

$$0 = \begin{bmatrix} ms^2 & -\left\{1\right\}^T q\left[\bar{Q}_{h\theta}\right]\left\{1\right\} & -\left\{1\right\}^T q\left[\bar{Q}_{h\theta}\right]\left\{\Phi_{\theta}{}^{3}\right\} \\ 0 & mr^2s^2 - \left\{\Phi_{h}{}^{2}\right\}^T q\left[\bar{Q}_{h\theta}\right]\left\{1\right\} & -\left\{\Phi_{h}{}^{2}\right\}^T q\left[\bar{Q}_{h\theta}\right]\left\{\Phi_{\theta}{}^{3}\right\} \\ 0 & -\left\{\Phi_{h}{}^{3}\right\}^T q\left[\bar{Q}_{h\theta}\right]\left\{1\right\} & mr_e{}^2(s^2+\omega_e{}^2) - \left\{\Phi_{h}{}^{3}\right\}^T q\left[\bar{Q}_{h\theta}\right]\left\{\Phi_{\theta}{}^{3}\right\} \end{bmatrix} \begin{Bmatrix} \xi_1 \\ \xi_2 \\ \xi_3 \end{Bmatrix} \qquad \text{(II-5)}$$

In an effort to obtain a solution in terms of parameters for which engineers are more likely to have intuitive judgment than for the generalized modal parameters of equation (II-5), we will introduce the concepts of steady-state elastic divergence and short period mode frequency.

Conventionally the short period mode frequency is the pitching frequency exhibited by the rigid system when aerodynamic forces are included.

For this analysis we will define the "aeroelastic short period mode frequency" (ω_o^*) to be similar to the conventional definition except that the system, instead of being rigid, will include the "residual flexibility" of all elastic modes higher than the first. This frequency can be obtained from equation (II-5) by letting ξ_3 be zero, then assuming harmonic motion.

$$\omega_o^{*2} = -\left(\frac{1}{mr^2}\right) \left\{\Phi_h^2\right\}^T q \left[\bar{Q}_{h\theta}\right] \left\{1\right\} \qquad \text{(II-6)}$$

Steady-state elastic divergence is conventionally defined for a supported system as that aeroelastic instability which can occur at zero frequency and is therefore independent of the mass of the system. This simple definition cannot be applied to a free system because in this case:

1. Other potential zero-frequency instabilities exist which are not aeroelastic in nature.
2. The mass distribution of a free system must be considered.

The only reasonable definition for steady-state elastic divergence of a free system is available through the description of the elasticity of the structure when restraints are placed on the zero-frequency normal modes of the system. In this case steady-state divergence can be defined by the singularity of the matrix $\left\{\left[I\right] - q \left[Q_{mm}\right] \left[X_{mm}\right]\right\}$ where $q \left[Q_{mm}\right]$ is the matrix of aerodynamic influence coefficients and $\left[X_{mm}\right]$ is the deflection influence coefficient matrix of the structure when the zero-frequency modes are restrained. In this analysis elastic divergence is determined by the vanishing of the determinant

$$\left| \left[I\right] - q \left[Q_{h\theta}\right] \left[X_{\theta h}\right] \right|$$

which may be expanded as follows in the parameter q

$$\left|\left[I\right] - q\left[Q_{h\theta}\right]\left[X_{\theta h}\right]\right| = 1 - D_1 q + D_2 q - \ldots\ldots D_h q^h \qquad \text{(II-7)}$$

where: D_1 is the sum of the first symmetric minors of $\left[Q_{h\theta}\right]\left[X_{\theta h}\right]$ (sum of the diagonal elements).

D_2 is the sum of the second symmetric minors of $\left[Q_{h\theta}\right]\left[X_{\theta h}\right]$.

D_h is the sum of the h^{th} symmetric minor of $\left[Q_{h\theta}\right]\left[X_{\theta h}\right]$.

Then defining the "aeroelastic index" $\bar{D}$ by

$$\bar{D} = D_1 q - D_2 q^2 + \ldots\ldots D_h q^h \qquad \text{(II-8)}$$

from equation (II-7); $\bar{D}$ will equal 0 when $q = 0$ and $\bar{D}$ will equal 1 when q is the dynamic pressure at divergence.

Steady-state divergence of the free system can also be determined from equation (II-5) by letting $\xi_1 = \xi_2 = s = 0$. Then

$$mr_e^2 \omega_e^2 - \left\{\Phi_h{}^3\right\}^T q_D \left[\bar{Q}_{h\theta}\right]\left\{\Phi_\theta{}^3\right\} = 0 \qquad \text{(II-9)}$$

where q_D is the dynamic pressure at divergence. We now note that the quantity

$$\frac{1}{mr_e^2\omega_e^2}\left\{\Phi_h{}^3\right\}^T q \left[\bar{Q}_{h\theta}\right]\left\{\Phi_\theta{}^3\right\} \qquad \text{(II-10)}$$

exhibits the same known dependence on q as $\bar{D}$; that is both functions:

1. Equal 1 when $q = 0$.
2. Equal 0 when q = the dynamic pressure at divergence.
3. Are equal to $q\,QX_{h\theta}$ when applied to a system containing only 1 elastic degree of freedom, 1 pair of aerodynamic coordinates.

It is then postulated that

$$\bar{D} = \frac{1}{mr_e^2\omega_e^2}\left\{\Phi_h{}^3\right\}^T q \left[\bar{Q}_{h\theta}\right]\left\{\Phi_\theta{}^3\right\} \qquad \text{(II-11)}$$

A rigorous proof of equation (II-11) was not obtained and its validity will be tried by example problems.

The characteristic equation obtained from the determinant of the matrix coefficients of equation (II-5) is

$$s^2 \left[s^4 + As^2 + B \right] = 0 \qquad \text{(II-12)}$$

where

$$A = \omega_e^2 - \frac{1}{mr_e^2} \left\{ \Phi_h^3 \right\}^T q \left[\bar{Q}_{h\theta} \right] \left\{ \Phi_\theta^3 \right\} - \frac{1}{mr^2} \left\{ \Phi_h^2 \right\}^T q \left[\bar{Q}_{h\theta} \right] \left\{ 1 \right\}$$

$$B = - \frac{\omega_e^2}{mr^2} \left\{ \Phi_h^2 \right\}^T q \left[\bar{Q}_{h\theta} \right] \left\{ 1 \right\} + \frac{1}{m^2 r^2 r_e^2} \left\{ \Phi_h^2 \right\}^T q \left[\bar{Q}_{h\theta} \right] \left\{ \left\{ 1 \right\} \left\{ \Phi_h^3 \right\}^T q \left[\bar{Q}_{h\theta} \right] \left\{ \Phi_\theta^3 \right\} - \left\{ \Phi_\theta^3 \right\} \left\{ \Phi_h^3 \right\}^T q \left[\bar{Q}_{h\theta} \right] \left\{ 1 \right\} \right\}$$

For a configuration where the slope deflections "sensed" by the aerodynamic representation are all equal in the first elastic mode,* then the last term in equation (II-12) for the factor B is zero, since through normalization $\left\{ \Phi_\theta^3 \right\}$ can be made equal to $\left\{ 1 \right\}$. For the configuration considered in Section IV (since only 1 aerodynamic cell is included) this term is zero and probably for a rather large range of configurations this term has little importance. Therefore because this term is of doubtful significance and because its omission greatly simplifies the results of this analysis it will be assumed that

$$\left\{ 1 \right\} \left\{ \Phi_h^3 \right\}^T \left[\bar{Q}_{h\theta} \right] \left\{ \Phi_\theta^3 \right\} - \left\{ \Phi_\theta^3 \right\} \left\{ \Phi_h^3 \right\}^T \left[\bar{Q}_{h\theta} \right] \left\{ 1 \right\} = 0 \qquad \text{(II-13)}$$

*An example of this configuration is one containing a rigid lifting surface.

Then by substitution of equations (II-6), (II-11) and (II-13) into equation (II-12), the characteristic equation can be written

$$s^2 \left[s^4 + As^2 + B \right] = 0, \qquad \text{(II-14)}$$

where

$$A = \omega_e{}^2 (1 - \bar{D}) + \omega_o{}^{*2}$$

$$B = \omega_o{}^{*2} \omega_e{}^2$$

In equation (II-14) with $(1 - \bar{D}) \geq 0$, s^2 will be real and negative unless $A^2 - 4B$ is negative. If $A^2 - 4B$ is negative, then two of the roots s of equation (II-14) will have a positive real part. The system is therefore on the verge of instability when

$$A^2 = 4B.$$

Then marginal stability is given by

$$\frac{\omega_o{}^*}{\omega_e} = \pm \left(1 - \sqrt{\bar{D}} \right) ; \qquad \text{(II-15)}$$

and since both $\bar{D}$ and $\frac{\omega_o{}^*}{\omega_e}$ are always continuous functions of the dynamic pressure beginning at the origin, the lowest dynamic pressure which will satisfy equation (II-15) is given by

$$\frac{\omega_o{}^*}{\omega_e} = 1 - \sqrt{\bar{D}} \qquad \text{(II-16)}$$

Both sides of equation (II-16) are functions of the dynamic pressure. The dynamic pressure at flutter is defined as the intersection of these 2 functions.

The first observation we may make from the results of this analysis is that a strong relationship does exist between mode interaction, or

flutter resulting from coupling of the first elastic mode and the rigid body modes, and elastic divergence. This analysis shows that for free systems which fit the assumptions made, classical "elastic divergence" will not occur because a flutter instability will always exist at a velocity lower than that corresponding to divergence.

The second observation we may make from equation (II-16) is that when $\overline{D}$, the "aeroelastic index", is negative the frequency ratio is complex and therefore flutter will not occur. The significance of a negative $\overline{D}$ is that the system is losing aerodynamic effectiveness (at a given rigid body mode pitch angle, the aeroelastic deflections of the structure reduce the total lift force). This observation provides the following useful qualitative criteria for the susceptibility of a given configuration to mode interaction:

1. If a system loses aerodynamic effectiveness as velocity is increased, then mode interaction will not occur.
2. If a system increases in aerodynamic effectiveness as velocity is increased, then mode interaction will probably occur; the system will be unstable at a velocity less than that predicted for steady-state divergence. At the velocity of instability the ratio of the uncoupled short period mode frequency to the first elastic mode frequency will be less than 1.

COMPARISON WITH KNOWN SOLUTIONS

A number of aircraft were studied on the CEA analog computer in the course of this project and that reported in reference 1. Most configurations studied exhibited a flutter instability involving the rigid body modes and the first elastic mode, and in all but one of

these cases the system tended to diverge at some higher speed. One configuration, (configuration 3 of reference 1) a swept wing airplane, lost aerodynamic effectiveness as velocity increased. This configuration showed no tendency to flutter even though the short period mode frequency virtually coincided with the elastic mode frequency. The one configuration which did not tend to diverge but did exhibit mode interaction was one where finite aerodynamic damping will be shown to be a necessary parameter for flutter to occur and therefore could not be predicted by this analysis which ignored all damping terms.

These results in general coincide with the qualitative criteria drawn from this analysis; however, in most cases the aerodynamic damping appeared to have a reasonably large effect on the quantitative value of the flutter speed, precluding accurate prediction by this analysis.

Configuration 4 of reference 1, the delta winged airplane, showed very rapid variations in damping at flutter. This phenomenon usually indicates that aerodynamic damping terms have little influence on the instability because they do not vary rapidly with speed or A.C. location. The criterion of equation (II-16) was applied to configuration 4 because damping did not appear to be a controlling parameter in this case. This criterion was the only one produced in this study which was in a form applicable to this "plate-like" structure.

DESCRIPTION OF CONFIGURATION 4

The aircraft used in this comparison is identical to configuration 4 of reference 1. The geometry, mass distribution and structural parameters are repeated in this report in Figures 1 through 5. The aero-

dynamic forces were represented as follows:

1. For the purposes of describing aerodynamic forces, the wing was divided into three strips shown in Figure 6. The strips are assumed to be rigid planes whose deflection is defined by the plunge deflections at the 1/4 and 3/4 chord coordinates shown in Figure 6. The aerodynamic lift and moment on each strip are rigidly beamed to these same 1/4 and 3/4 chord coordinates of the elastic structure.

2. The aerodynamic center of each strip is located on the mean chord of the strip and aft of the effective leading edge of the strip a distance xc (c = mean chord length of strip). x was varied in the study.

3. The aerodynamic lift force on a strip is given by

$$L = \frac{1}{2} \rho V^2 S C_{L_\alpha} \left(\theta - \frac{\dot{z}}{V}\right)$$

where

$\theta = \frac{2}{c}\left(z_{\frac{1}{4}} - z_{\frac{3}{4}}\right)$ is the pitching slope of the strip (positive nose up),

z is the plunge deflection at the A.C. (positive up),

$z_{\frac{1}{4}}$ and $z_{\frac{3}{4}}$ are the plunge deflections at the 1/4 chord and 3/4 chord points of the elastic structure (positive up).

Thus

$$z = z_{\frac{1}{4}}\left(\frac{3}{2} - 2x\right) - z_{\frac{3}{4}}\left(\frac{1}{2} - 2x\right).^*$$

*This equation is given incorrectly in reference 1.

4. The aerodynamic moment about the A.C. is given by

$$M = -\frac{1}{2}\rho V^2 S \frac{\pi}{8}\frac{c^2 s\theta}{V} \text{ (positive nose up).}$$

5. The basic flight condition used in the following numerical study is described by the parameters:

Velocity = 1655 mph

Altitude = 40,000 feet

Dynamic Pressure = q_o = 11.9 lb./in.^{2}

Lift Curve Slope = C_{L_α} = 5.0 per rad.

The dynamic pressure is varied in the numerical study and is expressed as fraction of the basic value given above (q_o).

NUMERICAL COMPARISON

This configuration was simulated on the CEA passive analog computer in the project reported in reference 1. At that time it was observed to exhibit the following unusual aeroelastic properties:

1. Three distinct flutter instabilities were observed for various combinations of dynamic pressure and A.C. location. Two of these instabilities were identified as conventional flutter phenomena involving the coupling of 2 elastic modes. The third instability was the result of coupling of elastic modes and rigid body modes. It is the latter case which will be considered in this comparison.
2. The system was observed to have a much smaller stable region when the system was represented by one elastic mode than when the higher modes were included in the representation.

3. The stability of the system was sensitive to small variations in flexibility.

The application of equation (II-16) to configuration 4 involved two major steps:

1. The determination of $\frac{\omega_o^*}{\omega_e}$ for various A.C. locations and values of $\frac{q}{q_o}$. This calculation was accomplished using equations (II-6), (II-4) and the modal properties of the system presented in reference 1.
2. The calculation of D from equation (II-8) and the flexibility matrix of the system given in reference 1.

The results of these calculations are presented graphically in Figures 7 through 11 for values of x of .25, .30, .35, .375 and .40. Also included on Figures 7 through 11 are curves of the dimensionless short period mode frequency of the rigid system $\frac{\omega_o}{\omega_e}$ and the curve of $1 - \sqrt{D}$ when the elasticity of the system is represented by only the generalized flexibility of the first elastic mode. The intersection of the latter two curves defines the dynamic pressure ratio $\left(\frac{q}{q_o}\right)$ at marginal stability when the "residual flexibility" of all elastic modes higher than the first is ignored. The intersection of the upper curves defines the stability boundary for the system when all flexibility of the system is included.

The stability boundaries calculated from equation (II-16) are presented in Figure 12 along with the corresponding boundary observed in reference 1.

Curve A of Figure 12 is the low frequency stability boundary of reference 1 (dynamic pressure ratio $\left(\frac{q}{q_o}\right)$ has been substituted for the equivalent parameter "flexibility factor" of reference 1 for convenience). Curve B of Figure 12 is the stability boundary calculated from equation (II-16) including the residual flexibility of all modes of the system. Curves A and B are in substantial agreement. The discrepancy between curves A and B can be attributed to any one or all of the following reasons.

1. The approximations made in this analysis.
2. The omission of all damping terms from this analysis.
3. Experimental error in the determination of system flexibility. Discrepancies were also observed on the analog computer between the modal simulation and the "exact" representation. The stability boundaries were recorded for the "exact" representation.

Curve C of Figure 12 is the stability boundary, determined from equation (II-16), when the flexibility of the system is represented by the generalized flexibility of only the first elastic mode. The stable region above curve B is much larger than that above curve C. This fact agrees with observations of the analog computer analysis of reference 1.

It is not claimed that this comparison proves the validity of equation (II-16). However it is known that equation (II-16) is valid for very simple systems and this comparison does show that it is useful for qualitative evaluation of a complicated system. The conclusion is made that the criteria of equation (II-16) is useful in the prediction of the susceptibility of a configuration to the "mode interaction" phenomenon.

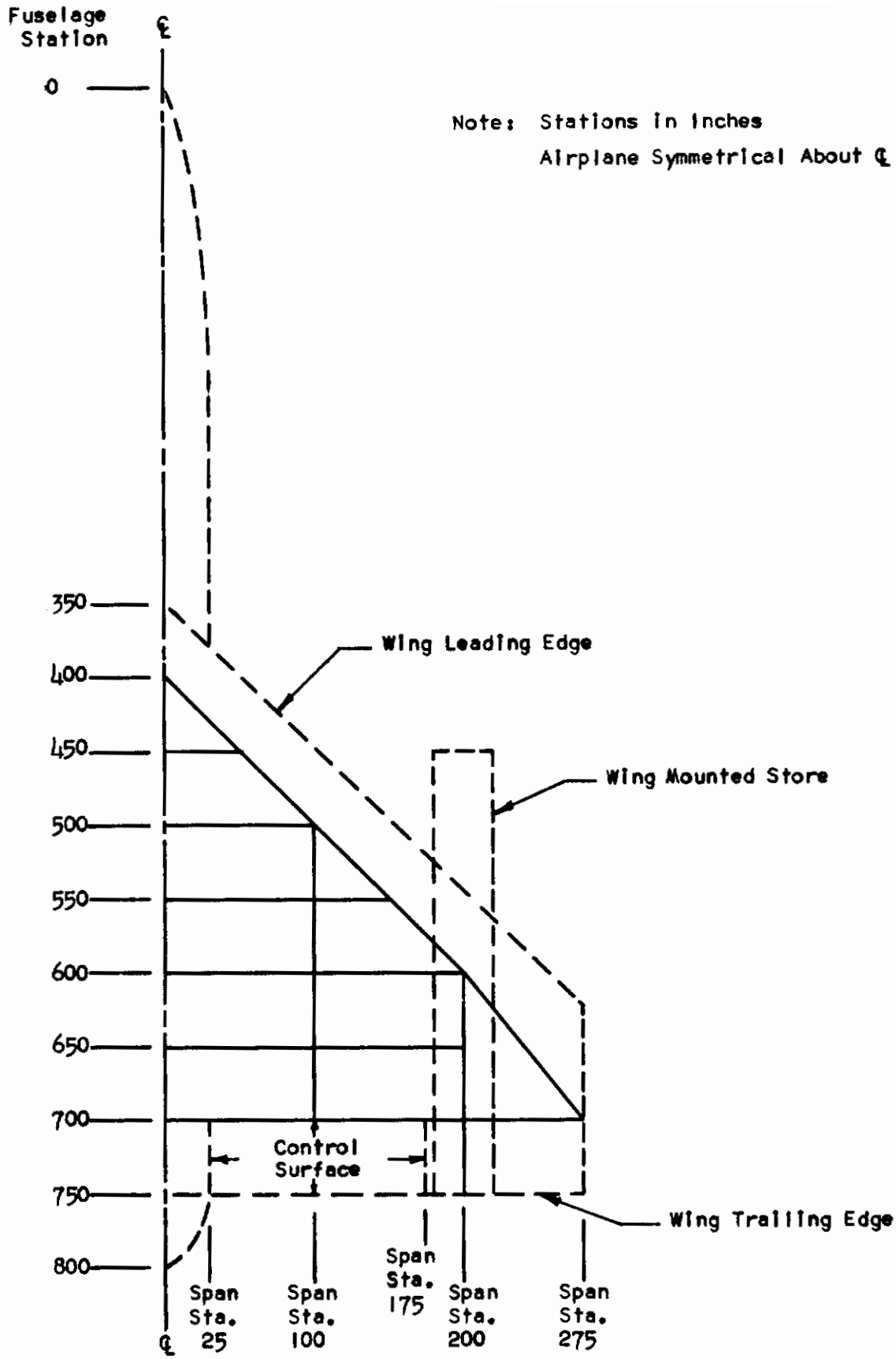

Figure 1. Configuration 4

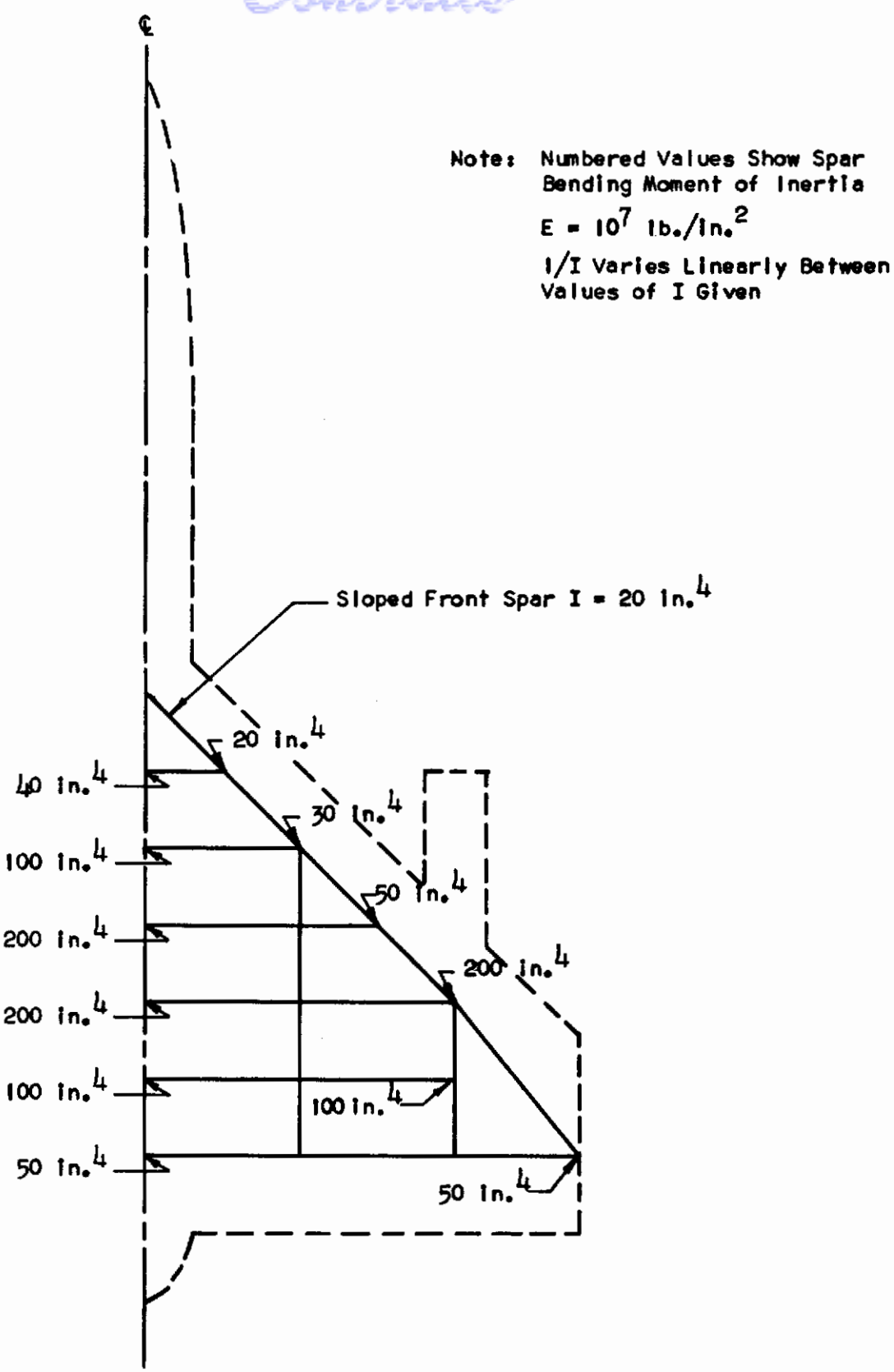

Figure 2. Spar Stiffness of Configuration 4

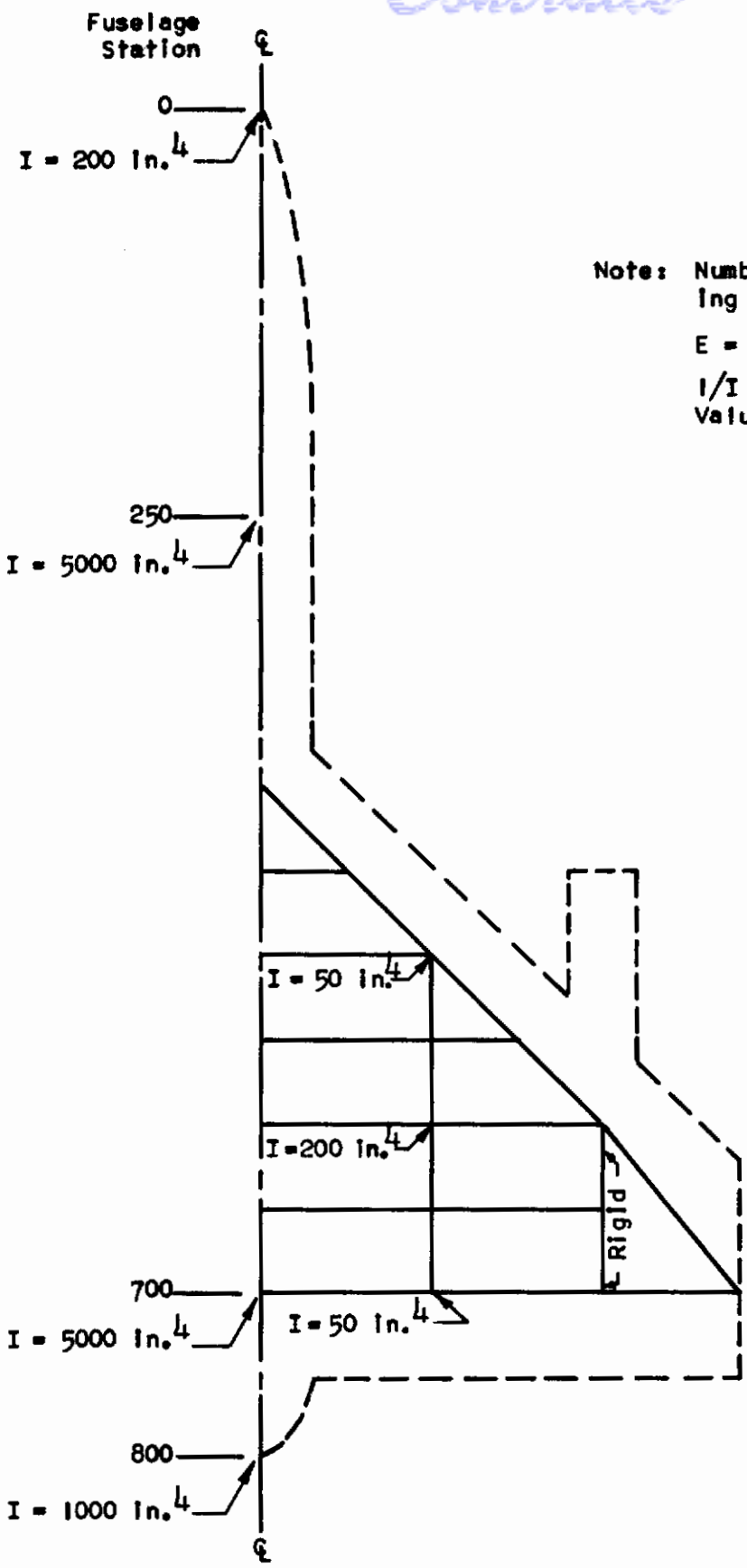

Figure 3. Fuselage and Rib Stiffness of Configuration 4

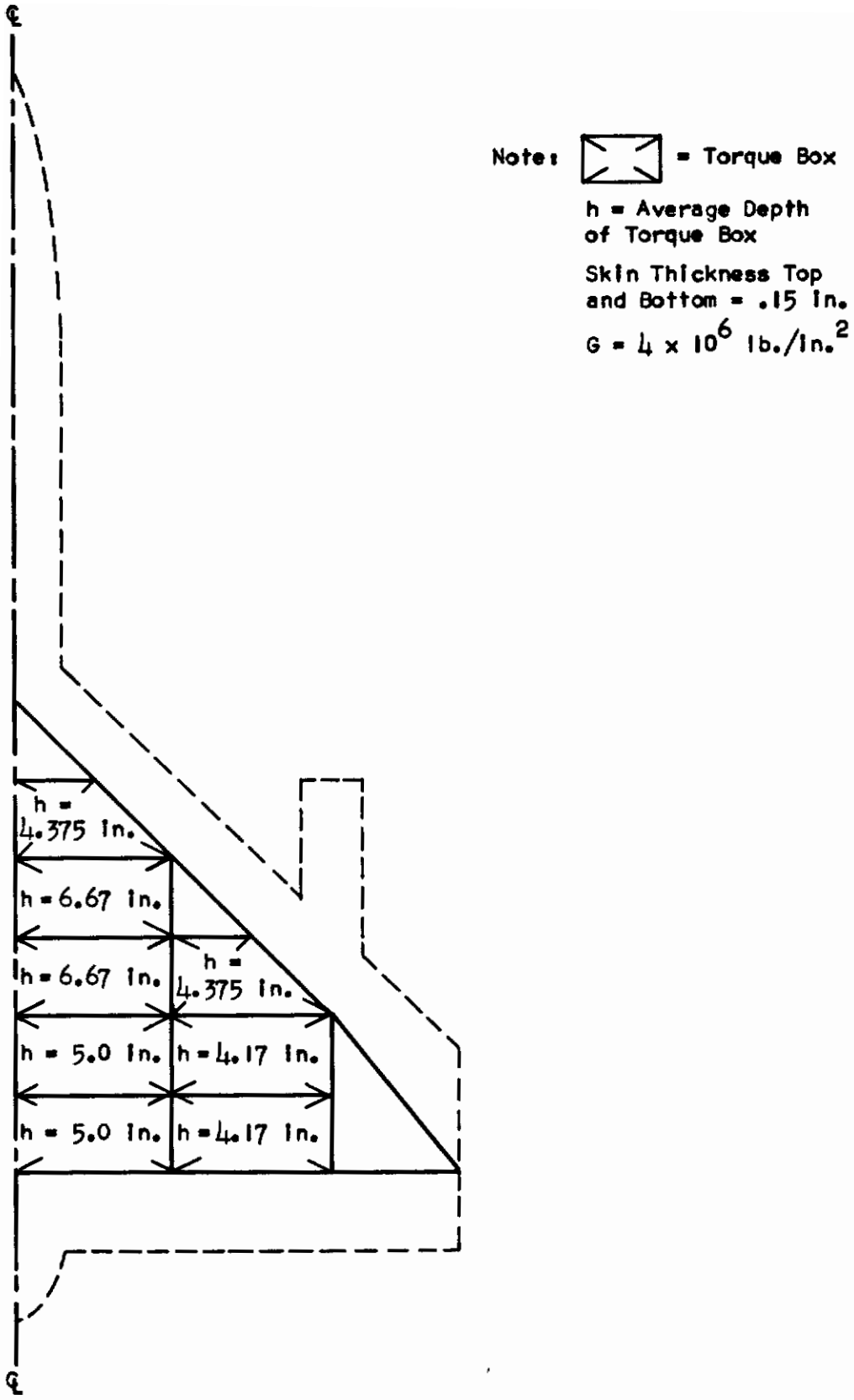

Figure 4. Torque Boxes of Configuration 4

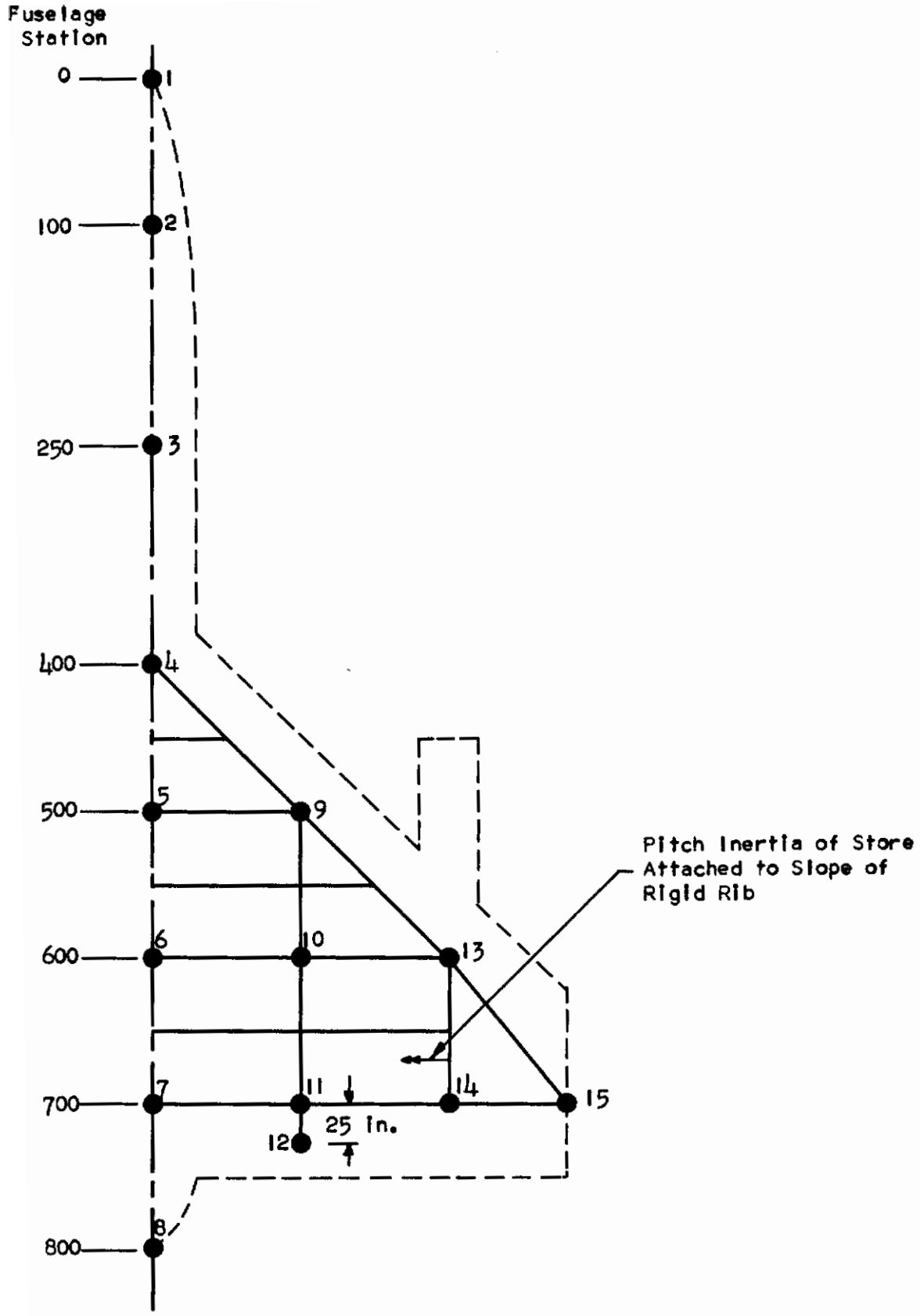

Figure 5. Mass Locations of Configuration 4

Strip	Chord	Area	Span Sta. of A.C.
I	400 in.	20,000 in.^{2}	0
II	300 in.	30,000 in.^{2}	100 in.
III	200 in.	20,000 in.^{2}	200 in.

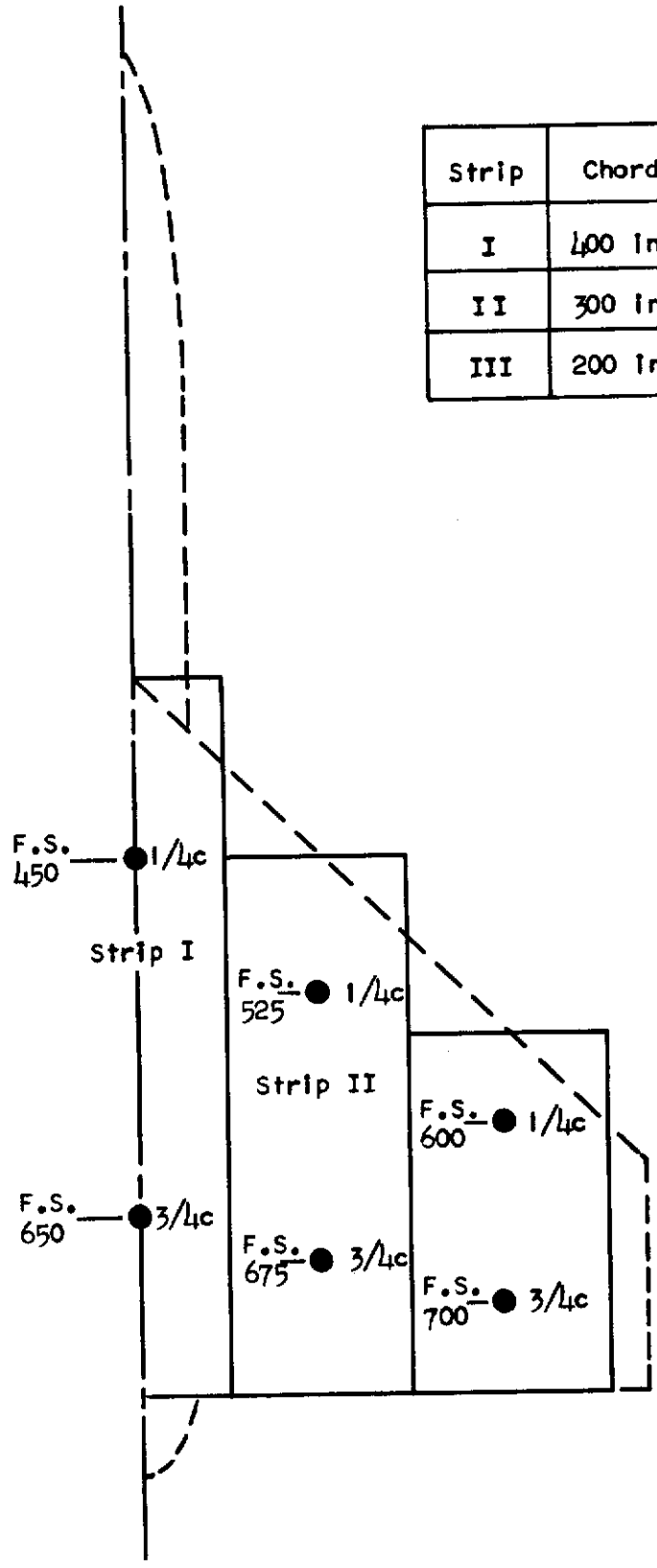

Figure 6. Aerodynamic Strips of Configuration 4

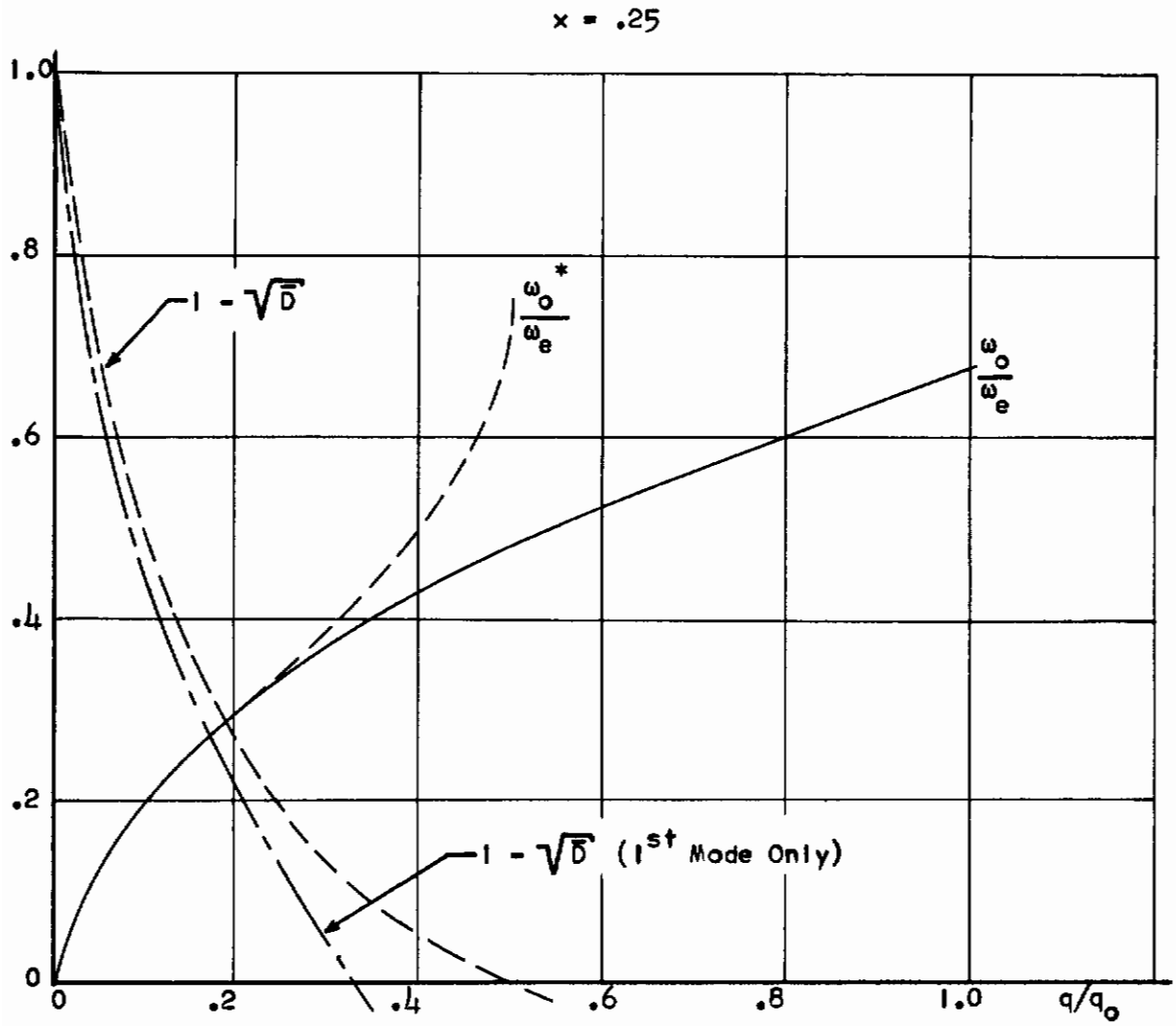

Figure 7. $1 - \sqrt{\bar{D}}$, $\frac{\omega_o^*}{\omega_e}$ and $\frac{\omega_o}{\omega_e}$ Versus Dimensionless Dynamic Pressure

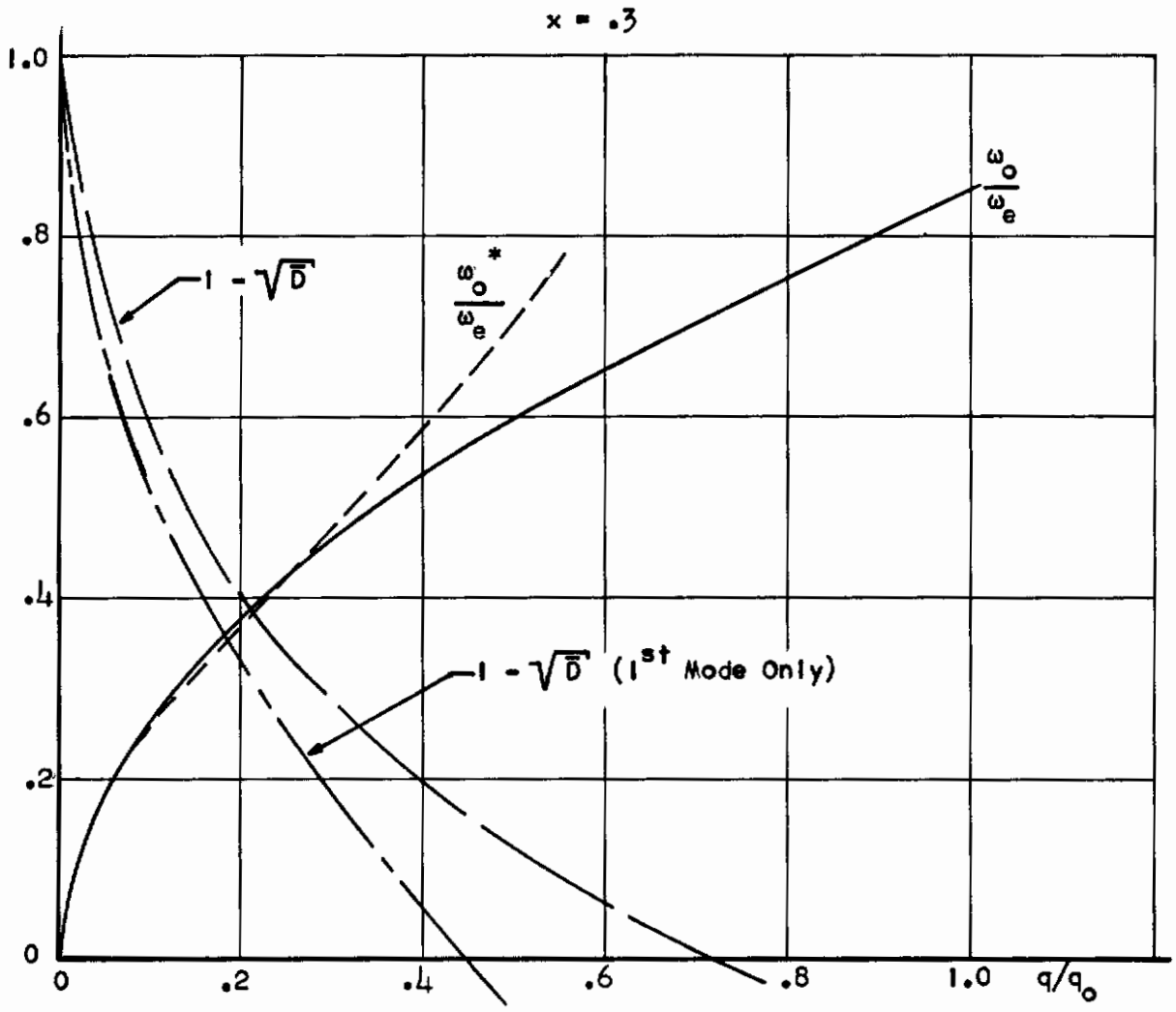

Figure 8. $1 - \sqrt{\bar{D}}$, $\frac{\omega_o^*}{\omega_e}$ and $\frac{\omega_o}{\omega_e}$ Versus Dimensionless Dynamic Pressure

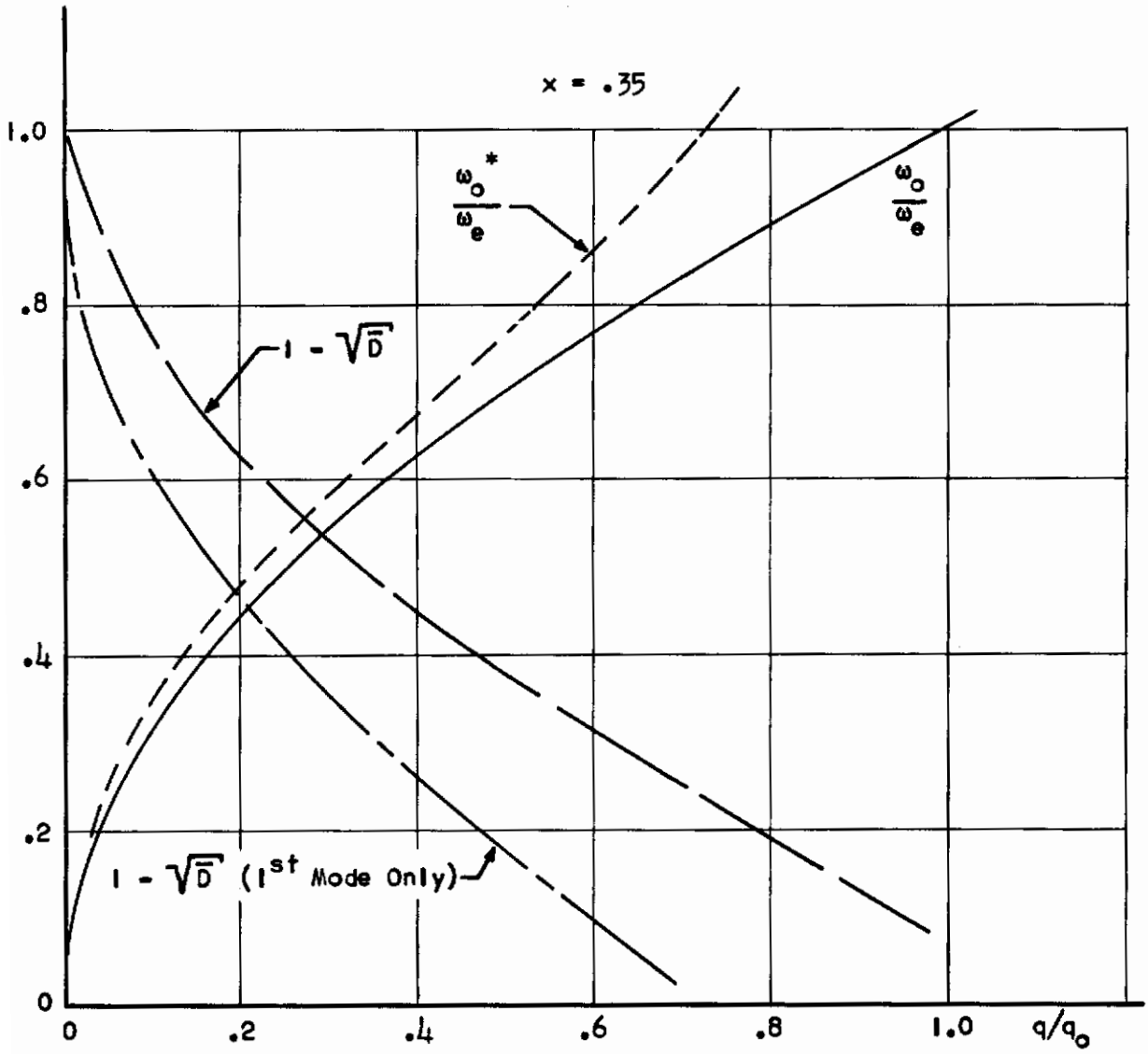

Figure 9. $1 - \sqrt{\bar{D}}$, $\frac{\omega_o^*}{\omega_e}$ and $\frac{\omega_o}{\omega_e}$ Versus

Dimensionless Dynamic Pressure

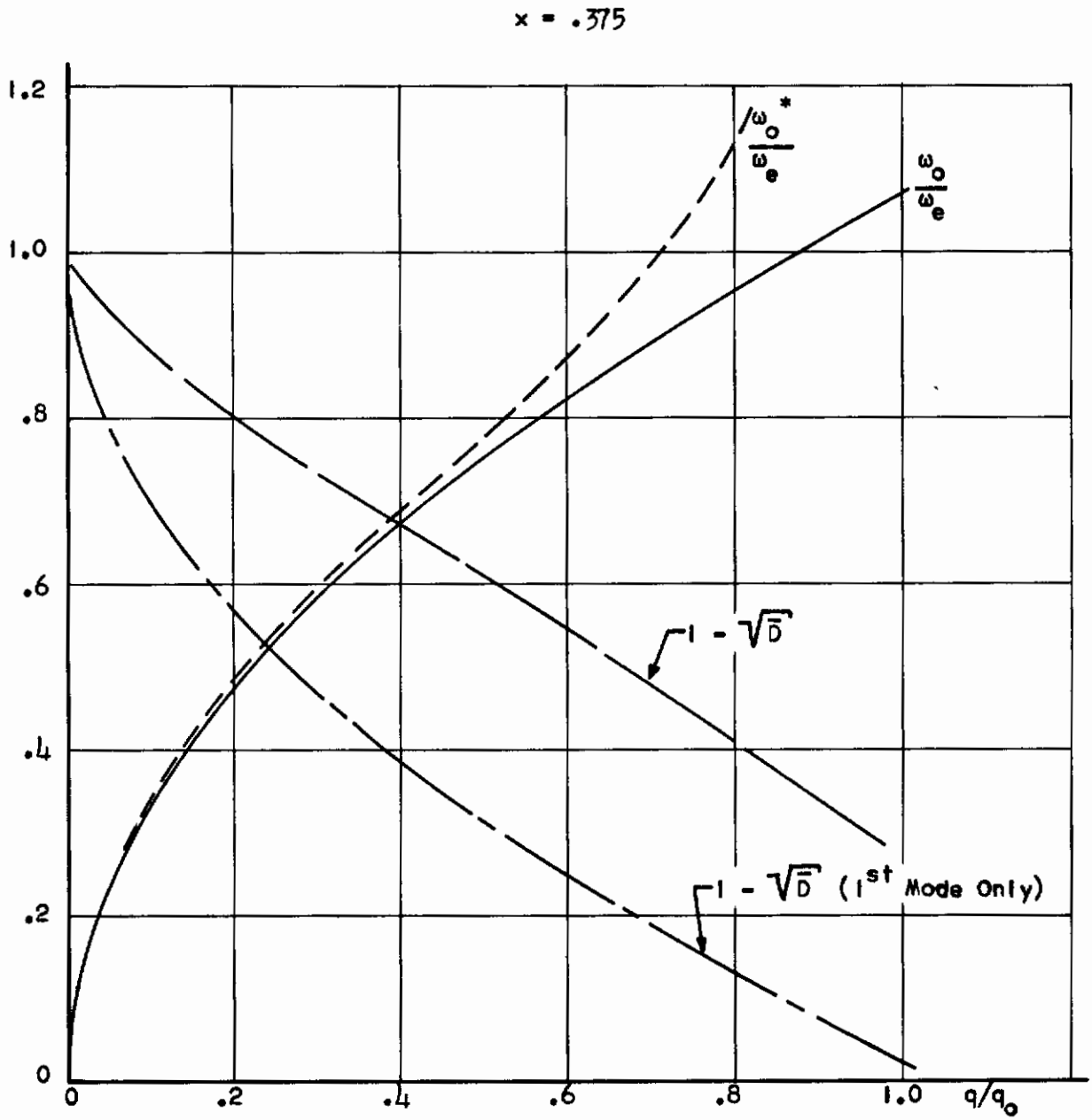

Figure 10. $1 - \sqrt{\bar{D}}$, $\frac{\omega_o^*}{\omega_e}$ and $\frac{\omega_o}{\omega_e}$ Versus Dimensionless Dynamic Pressure

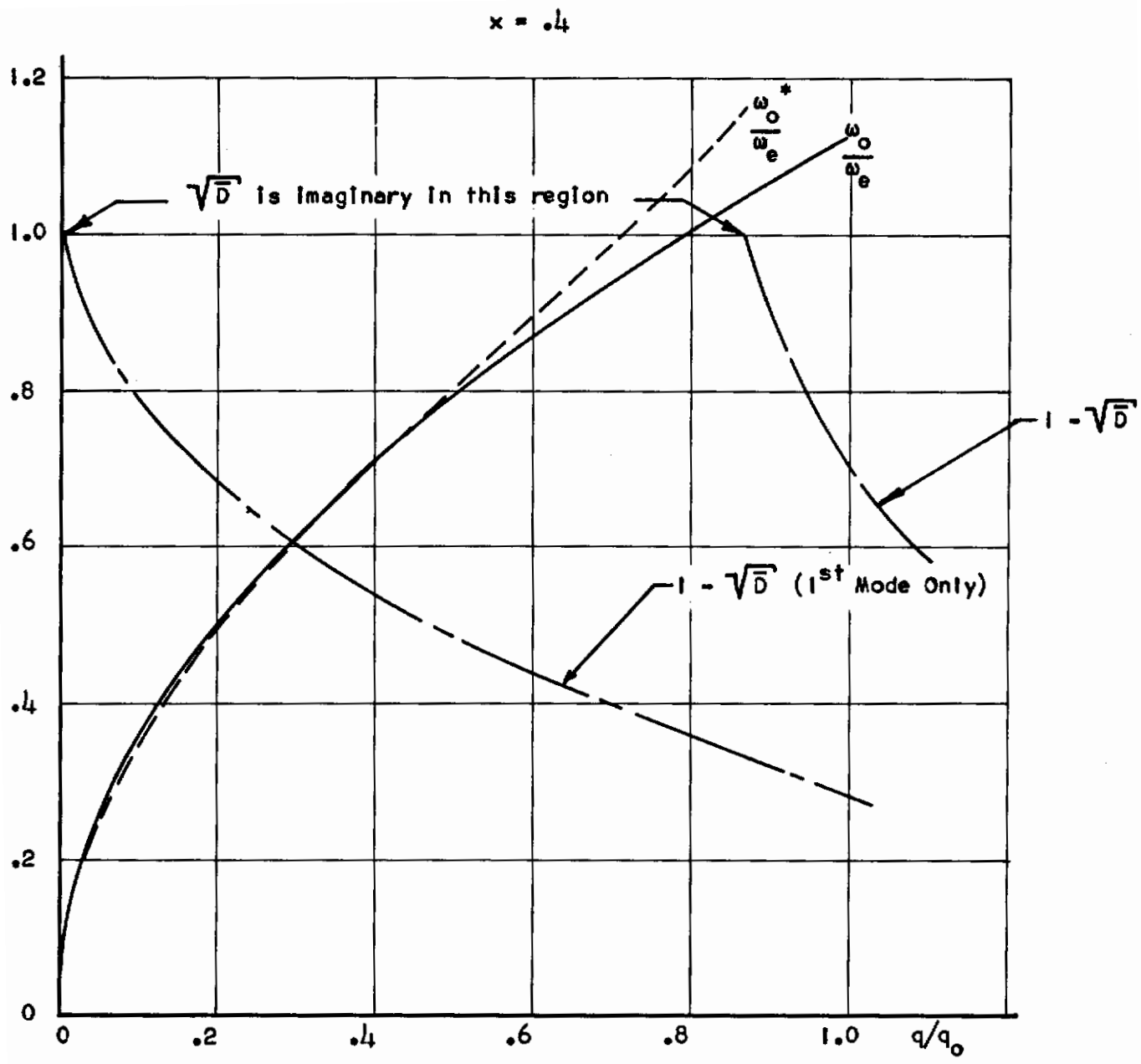

Figure 11. $1 - \sqrt{D}$, $\frac{\omega_o^*}{\omega_e}$ and $\frac{\omega_o}{\omega_e}$ Versus

Dimensionless Dynamic Pressure

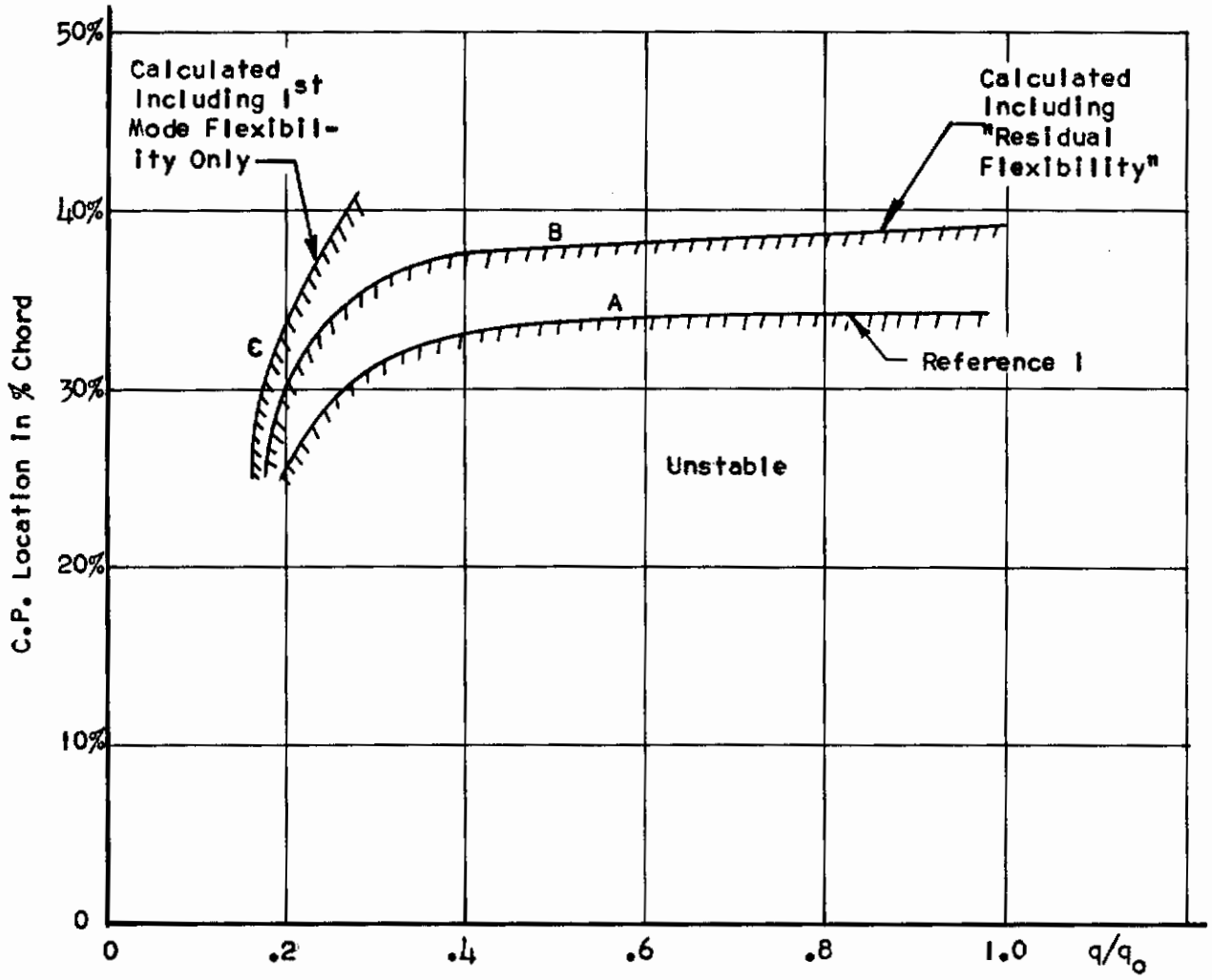

Figure 12. Stability Boundary of Configuration 4

III. ANALYSIS OF AN AIRFRAME CONSISTING OF A SIMPLE AIRFOIL FLEXIBLY ATTACHED TO A RIGID FUSELAGE

In order to place frequency coalescence methods in proper perspective, it is useful to analyze a basic aeroelastic system consisting of a simple rigid lifting surface flexibly mounted to a rigid fuselage (see Figure 13). Since we are not concerned here with conventional binary flutter, we shall assume that the inertia of the lifting surface is entirely negligible. Of course, by ignoring the inertia of the lifting surface, we leave out of account instabilities which occur because of coupling between the short period mode and a low frequency elastic mode. This type of instability will be discussed in Section IV of the report.

Clearly, if the system possesses instabilities, they are not of the type which can be predicted by frequency coalescence methods, since there is no finite frequency elastic mode which can coalesce with the short period mode. We will demonstrate that this system can exhibit three distinct types of instability.

The configuration of the system can be specified by four coordinates:

z = vertical deflection of the center of mass, positive up,

θ = pitch angle of the fuselage, positive nose up,

z_a = vertical deflection of the aerodynamic center, positive up,

θ_a = pitch angle of the lifting surface, positive nose up.

All coordinates are measured relative to an inertial reference system. The equations of motion are

$$m\ddot{z} = K(z_a - z - x_e\theta - x_{ae}\,\theta_a) = L$$

$$I\ddot{\theta} = k(\theta_a - \theta) + x_e\,K(z_a - z - x_e\theta - x_{ae}\,\theta_a)$$

$$0 = -K(z_a - z - x_e\theta - x_{ae}\,\theta_a) + L$$

$$0 = x_{ae}\,K(z_a - z - x_e\theta - x_{ae}\,\theta_a) - k(\theta_a - \theta) + M$$

The lift and moment at the aerodynamic center are

$$L = q\,S\left(C_{L_\alpha}\,\theta_a - C_{L_{\dot\alpha}}\frac{\dot z_a}{V} + C_{L_q}\frac{c\,\dot\theta_a}{V}\right)$$

$$M = q\,S\left(-C_{m_q}\frac{c^2\,\dot\theta_a}{V}\right)$$

$$q = \frac{1}{2}\rho V^2$$

(the geometrical quantities x_a, x_e, x_{ae} are defined in Figure 13).

Introducing matrix notation, these equations may be written:

$$M\begin{bmatrix} s^2+\omega_z^2 & x_e\omega_z^2 & -\omega_z^2 & x_{ae}\,\omega_z^2 \\ x_e\,\omega_z^2 & r^2s^2+r^2\omega_\theta^2+x_e^2\omega_z^2 & -x_e\,\omega_z^2 & x_e\,x_{ae}\,\omega_z^2 - r^2\,\omega_\theta^2 \\ -\omega_z^2 & -x_e\omega_z^2 & \omega_z^2 & -x_{ae}\,\omega_z^2 \\ x_{ae}\,\omega_z^2 & x_e\,x_{ae}\,\omega_z^2 - r^2\,\omega_\theta^2 & -x_{ae}\,\omega_z^2 & r^2\,\omega_\theta^2 + x_{ae}^2\,\omega_z^2 \end{bmatrix}\begin{bmatrix} z \\ \theta \\ z_a \\ \theta_a \end{bmatrix}$$

$$= q\,S\begin{bmatrix} 0 & 0 & 0 & 0 \\ 0 & 0 & 0 & 0 \\ 0 & 0 & -C_{L_\alpha}\frac{s}{V} & C_{L_\alpha} + C_{L_q}\frac{cs}{V} \\ 0 & 0 & 0 & -C_{m_q}\frac{c^2\,s}{V} \end{bmatrix}\begin{bmatrix} z \\ \theta \\ z_a \\ \theta_a \end{bmatrix} \qquad \text{(III-1)}$$

where $\omega_z^2 = \frac{K}{m}$, $\omega_\theta^2 = \frac{k}{I}$, $I = m\,r^2$.

Introduce c as a unit of length, $\frac{c}{V}$ as a unit of time, and ρSc as

a unit of mass. Then the following quantities are non-dimensional:

$$\bar{x}_e = \frac{x_e}{c} \qquad \bar{s} = \frac{cs}{V} \qquad \bar{m} = \frac{m}{\rho S c} \qquad \bar{C}_{L_\alpha} = \frac{C_{L_\alpha}}{2\bar{m}}$$

$$\bar{x}_{ae} = \frac{x_{ae}}{c} \qquad \bar{\omega}_z = \frac{c\omega_z}{V} \qquad \bar{C}_{L_q} = \frac{C_{L_q}}{2\bar{m}}$$

$$\bar{r} = \frac{r}{c} \qquad \bar{\omega}_\theta = \frac{c\omega_\theta}{V} \qquad \bar{C}_{m_q} = \frac{C_{m_q}}{2\bar{m}}$$

$$\bar{z} = \frac{z}{c}$$

$$\bar{z}_a = \frac{z_a}{c}$$

In terms of these quantities the equations of motion become

$$\begin{bmatrix} \bar{s}^2 + \bar{\omega}_z^2 & \bar{x}_e \bar{\omega}_z^2 & -\bar{\omega}_z^2 & \bar{x}_{ae} \bar{\omega}_z^2 \\ \bar{x}_e \bar{\omega}_z^2 & \bar{r}^2\bar{s}^2 + \bar{r}^2\bar{\omega}_\theta^2 + \bar{x}_e^2\bar{\omega}_z^2 & -\bar{x}_e \bar{\omega}_z^2 & \bar{x}_e \bar{x}_{ae} \bar{\omega}_z^2 - \bar{r}^2 \bar{\omega}_\theta^2 \\ -\bar{\omega}_z^2 & -\bar{x}_e \bar{\omega}_z^2 & \bar{C}_{L_\alpha}\bar{s} + \bar{\omega}_z^2 & -\bar{C}_{L_q}\bar{s} - \bar{C}_{L_\alpha} - \bar{x}_{ae}\bar{\omega}_z^2 \\ \bar{x}_{ae} \bar{\omega}_z^2 & \bar{x}_e \bar{x}_{ae} \bar{\omega}_z^2 - \bar{r}^2 \bar{\omega}_\theta^2 & -\bar{x}_{ae} \bar{\omega}_z^2 & \bar{C}_{m_q}\bar{s} + \bar{x}_{ae}^2\bar{\omega}_z^2 + \bar{r}^2\bar{\omega}_\theta^2 \end{bmatrix} \begin{bmatrix} z \\ \theta \\ \bar{z}_a \\ \theta_a \end{bmatrix} = 0, \tag{III-2}$$

and the characteristic equation is obtained by taking the determinant of the matrix of coefficients. Laplace's method of expanding a determinant (reference 3) is convenient and yields the following characteristic polynomial:

$$\bar{s}^2 \left[a_4 \bar{s}^4 + a_3 \bar{s}^3 + a_2 \bar{s}^2 + a_1 \bar{s} + a_0 \right] = 0,$$

where

$$a_4 = \bar{r}^2 \bar{C}_{m_q} \bar{C}_{L_\alpha}$$

$$a_3 = \bar{r}^2 \bar{\omega}_z^2 \bar{C}_{L_\alpha} \left(\bar{x}_{ae}^2 - \bar{x}_{ae} \frac{\bar{C}_{L_q}}{\bar{C}_{L_\alpha}} + \frac{\bar{C}_{m_q}}{\bar{C}_{L_\alpha}} \right) + \bar{r}^4 \bar{\omega}_\theta^2 \bar{C}_{L_\alpha}$$

$$a_2 = \bar{r}^4 \bar{\omega}_\theta^2 \bar{\omega}_z^2 - \bar{r}^2 \bar{\omega}_z^2 \bar{x}_{ae} \bar{C}_{L_\alpha} + (\bar{x}_e^2 + \bar{r}^2) \bar{\omega}_z^2 \bar{C}_{L_\alpha} \bar{C}_{m_q} + \bar{r}^2 \bar{\omega}_\theta^2 \bar{C}_{L_\alpha} \bar{C}_{m_q}$$

$$a_1 = \bar{r}^2 \bar{\omega}_z^2 \bar{\omega}_\theta^2 \bar{C}_{L_\alpha} \left(\bar{x}_{ac}^2 + \bar{r}^2 - \bar{x}_{ac} \frac{\bar{C}_{L_q}}{\bar{C}_{L_\alpha}} + \frac{\bar{C}_{m_q}}{\bar{C}_{L_\alpha}} \right)$$

$$a_0 = - \bar{r}^2 \bar{\omega}_z^2 \bar{\omega}_\theta^2 \bar{C}_{L_\alpha} \left(\bar{x}_{ac} - \bar{C}_{m_q} \right)$$

Before deriving any conclusions concerning the stability of the system, it is useful to introduce a fictitious frequency, ω_o, which would be the undamped short period frequency if the airframe were rigid.

$$\omega_o = \sqrt{- \frac{\left(\frac{1}{2} \rho V^2 \right) S C_{L_\alpha} x_{ac}}{m r^2}} = V \sqrt{- \frac{\frac{1}{2} \rho S C_{L_\alpha} x_{ac}}{m r^2}} \qquad \text{(III-3)}$$

The usefulness of this parameter depends upon the fact that given ω_o, the velocity V is determined and vice versa, and upon the fact that stability criteria are more conveniently expressed in terms of frequency ratios than in terms of velocity. The non-dimensional frequency corresponding to ω_o is simply

$$\bar{\omega}_o = \frac{c}{V} \omega_o = \sqrt{- \frac{\bar{x}_{ac} \bar{C}_{L_\alpha}}{\bar{r}^2}}$$

In the characteristic equation replace $\bar{C}_{L_\alpha}$ by

$$\bar{C}_{L_\alpha} = - \frac{\bar{r}^2 \bar{\omega}_o^2}{\bar{x}_{ac}}$$

and divide the equation by $\bar{r}^4 \bar{\omega}_o^4$. In this way we obtain

$$\bar{s}^2 \left[A_4 \bar{s}^4 + A_3 \bar{s}^3 + A_2 \bar{s}^2 + A_1 \bar{s} + A_o \right] = 0, \qquad \text{(III-4)}$$

$$A_4 = \frac{\bar{r}^2}{\bar{x}_{ac}^2} \frac{C_{m_q}}{C_{L_\alpha}} \tag{III-5}$$

$$A_3 = -\frac{1}{\bar{x}_{ac}} \left(\frac{\omega_z}{\omega_o}\right)^2 \left(\bar{x}_{ae}^2 - \bar{x}_{ae} \frac{C_{L_q}}{C_{L_\alpha}} + \frac{C_{m_q}}{C_{L_\alpha}}\right) - \frac{\bar{r}^2}{\bar{x}_{ac}} \left(\frac{\omega_\theta}{\omega_o}\right)^2 \tag{III-6}$$

$$A_2 = \left(\frac{\omega_\theta}{\omega_o}\right)^2 \left(\frac{\omega_z}{\omega_o}\right)^2 + \left(\frac{\omega_z}{\omega_o}\right)^2 \frac{\bar{x}_{ae}}{\bar{x}_{ac}} + \left(\frac{\omega_z}{\omega_o}\right)^2 \omega_o^2 \frac{\left(\bar{x}_e^2 + \bar{r}^2\right)}{\bar{x}_{ac}^2} \frac{C_{m_q}}{C_{L_\alpha}} + \left(\frac{\omega_\theta}{\omega_o}\right)^2 \frac{\bar{r}^2 \bar{\omega}_o^2}{\bar{x}_{ac}^2} \frac{C_{m_q}}{C_{L_\alpha}} \tag{III-7}$$

$$A_1 = -\frac{\bar{\omega}_o^2}{\bar{x}_{ac}} \left(\frac{\omega_z}{\omega_o}\right)^2 \left(\frac{\omega_\theta}{\omega_o}\right)^2 \left(\bar{x}_{ac}^2 + \bar{r}^2 - \bar{x}_{ac} \frac{C_{L_q}}{C_{L_\alpha}} + \frac{C_{m_q}}{C_{L_\alpha}}\right) \tag{III-8}$$

$$A_o = \bar{\omega}_o^2 \left(\frac{\omega_z}{\omega_o}\right)^2 \left(\frac{\omega_\theta}{\omega_o}\right)^2 \left(1 + \frac{\bar{r}^2}{\bar{x}_{ac}^2} \bar{\omega}_o^2 \frac{C_{m_q}}{C_{L_\alpha}}\right) \tag{III-9}$$

Obviously, the characteristic polynomial has a pair of zero roots. These roots merely express the fact that all altitudes and all directions of flight are equivalent. There are several interesting special cases.

A. Suppose the torsional stiffness is infinite ($\bar{\omega}_\theta = \infty$).

In this case the characteristic polynomial is

$$\bar{s}^3 + b_2 \bar{s}^2 + b_1 \bar{s} + b_o = 0, \tag{III-10}$$

where

$$b_2 = -\frac{\bar{x}_{ac}}{\bar{r}^2} \left(\frac{\omega_z}{\omega_o}\right)^2 + \frac{\bar{\omega}_o^2}{\bar{x}_{ac}} \frac{C_{m_q}}{C_{L_\alpha}} \tag{III-11}$$

$$b_1 = \frac{\bar{\omega}_o^2}{\bar{r}^2} \left(\frac{\omega_z}{\omega_o}\right)^2 \left(\bar{x}_{ac}^2 + \bar{r}^2 - \bar{x}_{ac} \frac{C_{L_q}}{C_{L_\alpha}} + \frac{C_{m_q}}{C_{L_\alpha}}\right) \tag{III-12}$$

$$b_o = -\frac{\bar{x}_{ac}}{\bar{r}^2} \bar{\omega}_o^2 \left(\frac{\omega_z}{\omega_o}\right)^2 \left(1 + \frac{\bar{r}^2}{\bar{x}_{ac}^2} \bar{\omega}_o^2 \frac{C_{m_q}}{C_{L_\alpha}}\right) \tag{III-13}$$

For a given airframe, it is convenient to take the frequency ratio $\frac{\omega_o}{\omega_z}$ as a measure of velocity. Since ω_z is known and is independent of velocity, $\frac{\omega_o}{\omega_z}$ is proportional to velocity V. The value of V at which the airframe is neutrally stable is of particular interest, and can be determined as follows. Suppose the airframe is neutrally stable, then there is at least one root of the form $\bar{s} = i\bar{\omega}$ where $\bar{\omega}$ is real. It follows immediately from the characteristic polynomial that if $\omega \neq 0$:

$$\bar{\omega}^2 = b_1$$

$$\bar{\omega}^2 = \frac{b_o}{b_2}$$

or

$$b_1 b_2 = b_o.$$

This condition determines the value of $\frac{\omega_o}{\omega_z}$ at neutral stability:

$$\left(\frac{\omega_z}{\omega_o}\right)^2 = \frac{r^2}{x_{ac}^2}\left[\bar{\omega}_o^2 \frac{C_{m_q}}{C_{L_\alpha}} + \frac{1 + \frac{r^2}{x_{ac}^2}\bar{\omega}_o^2 \frac{C_{m_q}}{C_{L_\alpha}}}{\frac{r^2}{x_{ac}^2} + 1 - \frac{1}{\bar{x}_{ac}}\frac{C_{L_q}}{C_{L_\alpha}} + \frac{1}{\bar{x}_{ac}^2}\frac{C_{m_q}}{C_{L_\alpha}}}\right] \qquad \text{(III-14)}$$

In many cases, especially in cases where the surface is mounted well aft of the center of mass of the airframe, the effects of C_{L_q} and C_{m_q} (pitch damping coefficients) will be negligible compared to the effects of C_L. In such a case we can ignore the ratios $\frac{C_{L_q}}{C_{L_\alpha}}$, $\frac{C_{m_q}}{C_{L_\alpha}}$, and an especially simple expression for the frequency ratio $\frac{\omega_z}{\omega_o}$ (at neutral stability) is obtained:

$$\left(\frac{\omega_z}{\omega_o}\right)^2 = \frac{r^2}{r^2 + x_{ac}^2} . \qquad \text{(III-15)}$$

This criterion can be given a simple physical characterization. Imagine the aerodynamic center to be rigidly constrained, the airframe being otherwise free of forces and constraints, then the natural frequency of the system is

$$\omega^* = \omega_z \left(\frac{r^2 + x_{ac}^2}{r^2}\right)^{\frac{1}{2}} \qquad \text{(III-16)}$$

Therefore, when the short period frequency ω_o (computed as though the airframe were rigid) equals the frequency ω^*, neutral stability occurs. The frequency of the neutrally stable oscillations of the airframe is simply $\omega^2 = \frac{b_o}{b_2} = \omega_o^2$, the short period frequency computed by assuming the airframe to be rigid. Although the presence of pitch damping due to C_{L_q} and C_{m_q} will modify these conclusions slightly, the basic mechanism of the instability for practical cases is revealed by (III-15) and (III-16).

Notice that the frequency ratio at neutral stability can be expressed in terms of four dimensionless parameters:

$$\frac{r^2}{x_{ac}^2}$$

$$\bar{\omega}_o^2 \frac{C_{m_q}}{C_{L_\alpha}}$$

$$\frac{1}{\bar{x}_{ac}} \frac{C_{L_q}}{C_{L_\alpha}}$$

$$\frac{1}{\bar{x}_{ac}^2}\frac{C_{m_q}}{C_{L_\alpha}}$$

and if damping terms are small, only a single parameter is involved, $\frac{r^2}{x_{ac}^2}$.

B. Infinite plunge stiffness ($\bar{\omega}_z = \infty$).

The characteristic polynomial is again of third order:

$$c_3 \bar{s}^3 + c_2 \bar{s}^2 + c_1 \bar{s} + c_0 = 0, \tag{III-17}$$

where

$$c_3 = \frac{1}{\bar{x}_{ac}}\left(\bar{x}_{ae}^2 - \bar{x}_{ae}\frac{C_{L_q}}{C_{L_\alpha}} + \frac{C_{m_q}}{C_{L_\alpha}}\right) \tag{III-18}$$

$$c_2 = -\left[\left(\frac{\omega_\theta}{\omega_o}\right)^2 + \frac{\bar{x}_{ae}}{\bar{x}_{ac}} + \bar{\omega}_o^2\,\frac{\bar{x}_e^2 + \bar{r}^2}{\bar{x}_{ac}^2}\,\frac{C_{m_q}}{C_{L_\alpha}}\right] \tag{III-19}$$

$$c_1 = \frac{\bar{\omega}_o^2}{\bar{x}_{ac}}\left(\frac{\omega_\theta}{\omega_o}\right)^2\left(\bar{x}_{ac}^2 + \bar{r}^2 - \bar{x}_{ac}\frac{C_{L_q}}{C_{L_\alpha}} + \frac{C_{m_q}}{C_{L_\alpha}}\right) \tag{III-20}$$

$$c_o = -\bar{\omega}_o^2\left(\frac{\omega_\theta}{\omega_o}\right)^2\left(1 + \bar{\omega}_o^2\,\frac{\bar{r}^2}{\bar{x}_{ac}^2}\,\frac{C_{m_q}}{C_{L_\alpha}}\right) \tag{III-21}$$

Suppose $\bar{s} = i\bar{\omega}$, $\bar{\omega}$ real. Then

$$-c_3\bar{\omega}^3 + c_1\bar{\omega} = 0,$$

$$-c_2\bar{\omega}^2 + c_o = 0.$$

Obviously, $\bar{\omega} = 0$ implies $c_o = 0$, and this is not possible unless $\frac{\omega_\theta}{\omega_o} = 0$. This last condition implies that the surface is connected to the airframe by means of a torsional spring of zero stiffness or else the velocity is infinite. If $\bar{\omega} \neq 0$ then

$$\frac{c_2}{c_o} = \frac{c_3}{c_1}$$

and we get for $\frac{\omega_\theta}{\omega_o}$:

$$\left(\frac{\omega_\theta}{\omega_o}\right)^2 = -\frac{\bar{x}_{ae}}{\bar{x}_{ac}} - \bar{\omega}_o^2 \frac{\bar{x}_e^2 + \bar{r}^2}{\bar{x}_{ac}^2} \frac{C_{m_q}}{C_{L_\alpha}} + \left(1 + \bar{\omega}_o^2 \frac{\bar{r}^2}{\bar{x}_{ac}^2} \frac{C_{m_q}}{C_{L_\alpha}}\right) \frac{\bar{x}_{ae}^2 - \bar{x}_{ae} \frac{C_{L_q}}{C_{L_\alpha}} + \frac{C_{m_q}}{C_{L_\alpha}}}{\bar{r}^2 + \bar{x}_{ac}^2 - \bar{x}_{ac} \frac{C_{L_q}}{C_{L_\alpha}} + \frac{C_{m_q}}{C_{L_\alpha}}} \qquad \text{(III-22)}$$

Now $\bar{x}_{ac}$ is negative if the airframe has a positive static margin. Therefore if the elastic axis is aft of the aerodynamic center, $-\frac{\bar{x}_{ae}}{\bar{x}_{ac}}$ is positive, and instability is certainly possible. It appears that the existence of an instability is closely connected with the divergence properties of the lifting surface. Thus, if $-\bar{x}_{ae}$ is positive, the surface is capable of divergence when the fuselage of the airframe is restrained. The instability predicted by (III-22) is as close as the free system can come to divergence. The instability is not ordinary divergence since the frequency of the instability is greater than zero.

It is not generally possible to ignore the pitch damping terms C_{L_q}, C_{m_q} in equation (III-22), since the character of the instability can be drastically modified by these terms. In fact, there is one interesting case where the pitch damping terms can produce instability at a very low airspeed. Suppose we position the aerodynamic center with respect to the elastic axis in such a way that

$$\bar{x}_{ae}^2 - \bar{x}_{ae} \frac{C_{L_q}}{C_{L_\alpha}} + \frac{C_{m_q}}{C_{L_\alpha}} = 0 \qquad \text{(III-23)}$$

We can then position the lifting surface with respect to the center of gravity of the airframe so that

$$\bar{r}^2 + \bar{x}_{ac}^{\,2} - \bar{x}_{ac}\frac{C_{L_q}}{C_{L_\alpha}} + \frac{C_{m_q}}{C_{L_\alpha}} = 0 \qquad \text{(III-24)}$$

Then it is obvious from the expressions given for the coefficients of the characteristic polynomial that

$$\left[\left(\frac{\omega_\theta}{\omega_o}\right)^2 + \frac{\bar{x}_{ae}}{\bar{x}_{ac}} + \bar{\omega}_o^{\,2}\frac{\bar{x}_e^{\,2}+\bar{r}^2}{\bar{x}_{ac}^{\,2}}\frac{C_{m_q}}{C_{L_\alpha}}\right]\bar{s}^2 + \bar{\omega}_o^{\,2}\left(\frac{\omega_\theta}{\omega_o}\right)^2\left(1 + \bar{\omega}_o^{\,2}\frac{\bar{r}^2}{\bar{x}_{ac}^{\,2}}\frac{C_{m_q}}{C_{L_\alpha}}\right) = 0, \qquad \text{(III-25)}$$

and therefore the system can be neutrally stable for <u>all</u> values of $\left(\frac{\omega_\theta}{\omega_o}\right)^2$ (e.g. the system is neutrally stable at every airspeed from 0 to ∞). Notice that C_{L_q} is crucial to this phenomenon. If $C_{L_q} = 0$ it is not possible to satisfy either of equations (III-23) or (III-24). It would, of course, be rare to encounter an airframe which satisfied the conditions of equations (III-23), (III-24) exactly. However the example does show that the effects of pitch damping can be very important. Note also that structural damping (dashpot in parallel with the torsional spring of Figure 13) would tend to eliminate this instability at low airspeeds.

The frequency of the instability is apparent from equation (III-25).

In the general case, where both ω_θ and ω_z are finite, the substitution $\bar{s} = i\bar{\omega}$ into the characteristic equation (III-4) yields

$$-A_3\bar{\omega}^3 + A_1\bar{\omega} = 0$$

$$A_4\bar{\omega}^4 - A_2\bar{\omega}^2 + A_o = 0$$

where the A's are given by equations (III-5), (III-6), (III-7), (III-8), (III-9). If $\bar{\omega} \neq 0$, these two equations can be combined into

$$A_4 \left(\frac{A_1}{A_3}\right)^2 - A_2 \frac{A_1}{A_3} + A_0 = 0.$$

Happily, if this equation is rearranged, it becomes linear in $\left(\frac{\omega_\theta}{\omega_o}\right)^2$, and we find

$$\left(\frac{\omega_z}{\omega_o}\right)^2 = -\left(\frac{\omega_z}{\omega_\theta}\right)^2 \left[\frac{\bar{x}_{ae}}{\bar{x}_{ac}} + \frac{\bar{x}_e^2 + \bar{r}^2}{\bar{x}_{ac}^2} \bar{\omega}_o^2 \frac{C_{m_q}}{C_{L_\alpha}}\right] - \frac{\bar{r}^2}{\bar{x}_{ac}^2} \bar{\omega}_o^2 \frac{C_{m_q}}{C_{L_\alpha}}$$

$$+ \bar{\omega}_o^2 \frac{C_{m_q}}{C_{L_\alpha}} \frac{\bar{r}^2}{\bar{x}_{ac}^2} \cdot \frac{\bar{r}^2 + \bar{x}_{ac}^2 - \bar{x}_{ac} \frac{C_{L_q}}{C_{L_\alpha}} + \frac{C_{m_q}}{C_{L_\alpha}}}{\bar{r}^2 \left(\frac{\omega_\theta}{\omega_z}\right)^2 + \bar{x}_{ae}^2 - \bar{x}_{ae} \frac{C_{L_q}}{C_{L_\alpha}} + \frac{C_{m_q}}{C_{L_\alpha}}}$$

$$+ \left(1 + \frac{\bar{r}^2}{\bar{x}_{ac}^2} \bar{\omega}_o^2 \frac{C_{m_q}}{C_{L_\alpha}}\right) \cdot \frac{r^2 + \left(\frac{\omega_z}{\omega_\theta}\right)^2 \left(\bar{x}_{ae}^2 - \bar{x}_{ae} \frac{C_{L_q}}{C_{L_\alpha}} + \frac{C_{m_q}}{C_{L_\alpha}}\right)}{\bar{x}_{ac}^2 + \bar{r}^2 - \bar{x}_{ac} \frac{C_{L_q}}{C_{L_\alpha}} + \frac{C_{m_q}}{C_{L_\alpha}}} \qquad \text{(III-26)}$$

The frequency of oscillation is obtained from $\bar{\omega}^2 = \frac{A_1}{A_3}$:

$$\left(\frac{\omega}{\omega_\theta}\right)^2 = \frac{\left(\bar{r}^2 + \bar{x}_{ac}^2 - \bar{x}_{ac} \frac{C_{L_q}}{C_{L_\alpha}} + \frac{C_{m_q}}{C_{L_\alpha}}\right)}{\left(\frac{\omega_\theta}{\omega_z}\right)^2 \bar{r}^2 + \left(\bar{x}_{ae}^2 - \bar{x}_{ae} \frac{C_{L_q}}{C_{L_\alpha}} + \frac{C_{m_q}}{C_{L_\alpha}}\right)} \qquad \text{(III-27)}$$

The frequency ratio $\frac{\omega_\theta}{\omega_o}$ at neutral stability is determined by the following set of seven non-dimensional parameters:

$$\frac{r^2}{x_{ac}^2}$$

$$\frac{x_{ae}}{x_{ac}}$$

$$\frac{1}{\bar{x}_{ac}} \frac{C_{L_q}}{C_{L_\alpha}}$$

$$\frac{1}{\bar{x}_{ac}^2} \frac{C_{m_q}}{C_{L_\alpha}}$$

$$\bar{\omega}_o^2 \frac{C_{m_q}}{C_{L_\alpha}}$$

$$\frac{\omega_z}{\omega_\theta}$$

$$\frac{x_e^2 + r^2}{x_{ac}^2}$$

Our conclusions regarding airframes which consist of a single light lifting surface elastically mounted to a rigid fuselage may be summarized as follows:

A. The system may be dynamically unstable even though it is statically stable.

B. The velocity at which the airframe becomes neutrally stable can be determined from the frequency ratio $\frac{\omega_\theta}{\omega_o}$, which can be expressed in terms of the seven non-dimensional parameters listed above. The parameter $\bar{\omega}_o^2 \frac{C_{m_q}}{C_{L_\alpha}}$ is usually quite small and is less important than the other parameters.

C. If the torsional stiffness between the lifting surface and the fuselage is infinite, an instability will occur when the short period frequency ω_o equals the frequency ω^*. The latter frequency is simply the natural frequency of the fuselage on the

plunge stiffness when the displacement of the lifting surface at the aerodynamic center is restrained. This simple criterion is strictly correct only if the effects of aerodynamic pitch damping are ignored; however, the criterion is not sensitive to pitch damping for practical airframes.

D. If the plunge stiffness between the lifting surface and the fuselage is infinite, either of two types of instability may occur. If the aerodynamic center is forward of the elastic axis ($x_{ae} < 0$), an instability occurs which is connected with the possibility of lifting surface divergence. In addition, by careful positioning of the elastic axis with respect to the aerodynamic center and the center of gravity, it is possible to obtain an airframe which is neutrally stable at all airspeeds. This type of instability can only be produced if C_{L_q} is different from zero.

E. None of the above instabilities can be predicted on the basis of frequency coalescence methods. We can describe the instabilities as being due to aerodynamic coupling between zero frequency modes (rigid motions) and infinite-frequency modes, since the structure in vacuo possesses only these types of modes.

F. The conclusions of this section should apply to airframes with a simple, light, lifting surface and a fairly rigid fuselage. A more realistic type of airframe is analyzed in Section IV.

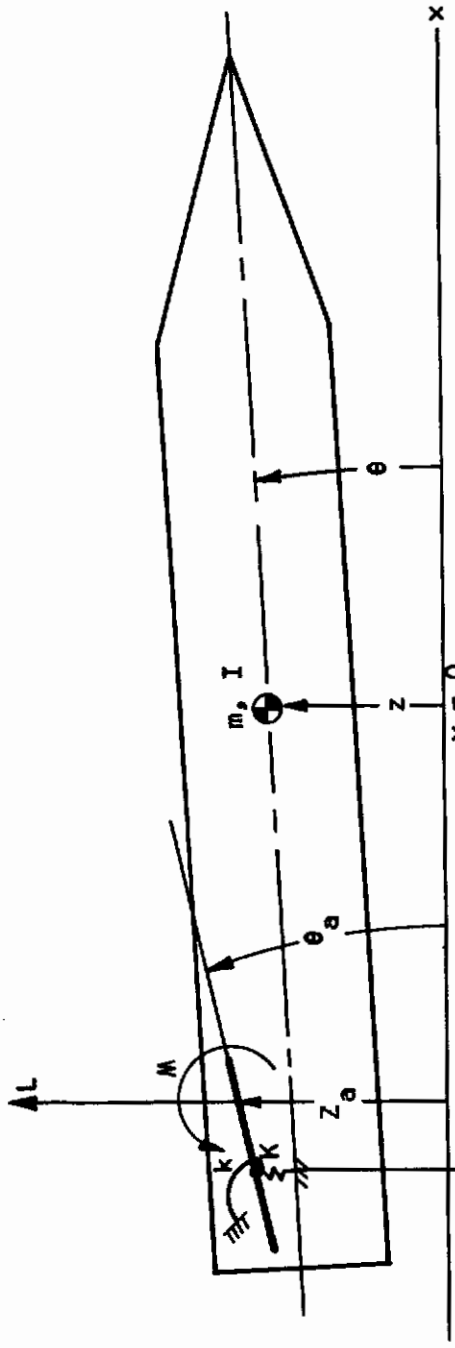

Note: $x_{ae} = x_{ac} - x_e$ and positive x is forward of the center of mass.

Figure 13. Airframe Consisting of a Simple Airfoil Flexibly Attached to a Rigid Fuselage

IV. ANALYSIS OF AN AIRFRAME HAVING TWO RIGID BODY MODES AND ONE ELASTIC MODE

The configuration shown in Figure 14 is in some ways more general than the configuration analyzed in Section III and is also a configuration which frequently occurs in practice. A detailed analysis should therefore be useful. It is convenient to give the equations of motion in modal form. There are two rigid body modes and one elastic mode. If the rigid mode shapes are properly normalized, the equations of motion of such a system can always be written in the form

$$\left.\begin{aligned} m\ddot{z} &= \int p(x, y)\,dS \\ I\ddot{\theta} &= \int x p(x, y)\,dS \\ m_e(\ddot{\xi} + \omega_e^2 \xi) &= \int \Phi(x, y) p(x, y)\,dS \end{aligned}\right\} \qquad \text{(IV-1)}$$

where

m = the total mass of the system

I = the total pitching inertia about the center of mass

m_e = the generalized mass of the elastic mode

$p(x, y)$ = net vertical pressure on the element of area dS at the point (x, y)

$\Phi(x, y)$ = mode shape of the elastic mode

If $\xi = 0$, then the two normal coordinates z and θ have a simple geometrical significance, z being the vertical displacement of the center of mass and θ the pitch angle of the fuselage. The geometrical significance of ξ depends upon the way in which the mode shape $\Phi(x, y)$ is normalized. We shall assume that a single rigid lifting surface is mounted at some point on the fuselage as shown in Figure 14. Then the vertical displacement of any point of the surface is

$$z + x\theta + \Phi(x, y)\xi$$

and the slope of the lifting surface is

$$\theta + \frac{\partial \Phi}{\partial x} \xi ,$$

obtained by taking the partial derivative of the vertical deflection with respect to x. Since the surface is assumed to be rigid, $\frac{\partial \Phi}{\partial x}$ must be a constant over the surface. If we normalize the elastic mode shape by setting $\frac{\partial \Phi}{\partial x} = 1$, then ξ has a simple geometrical significance. When $\theta = 0$, ξ is simply the pitch angle of the lifting surface. It follows from $\frac{\partial \Phi}{\partial x} = 1$ that $\Phi(x, y) = x +$ constant. It is convenient to express this constant in terms of the position of the node line of the elastic mode. When $z = 0$, $\theta = 0$, the vertical deflection of the node line is, by definition, zero. Therefore $\Phi(x, y) = x - x_{n\ell}$ over the lifting surface and the vertical deflection of any point on the lifting surface is

$$z + x\theta + (x - x_{n\ell})\xi$$

while the slope of the lifting surface is $\theta + \xi$.

The total lift, L, and the moment about the aerodynamic center of the lifting surface, M, can be expressed in terms of $p(x, y)$:

$$L = \int p(x, y)\, dS$$

$$M = \int (x - x_{ac}) p(x, y)\, dS = \int x p(x, y)\, dS - x_{ac} L$$

It follows that the equations of motion can be written

$$\left.\begin{aligned} m\ddot{z} &= L \\ I\ddot{\theta} &= M + x_{ac} L \\ m_e(\ddot{\xi} + \omega_e^2 \xi) &= M + x_{an} L \end{aligned}\right\} \qquad \text{(IV-2)}$$

where $x_{an} = x_{ac} - x_{n\ell}$. The lift and moment on the lifting surface can be expressed in terms of the vertical displacement of the aerodynamic center, the pitch angle of the surface, and the derivatives of these

quantities:

$$\left.\begin{aligned} L &= qS\left(C_{L_\alpha}\,\theta_a - C_{L_{\dot\alpha}}\frac{\dot z_a}{V} + C_{L_q}\frac{c\dot\theta_a}{V}\right) \\ M &= -\,qS\,C_{m_q}\frac{c^2\,\dot\theta_a}{V} \end{aligned}\right\} \qquad \text{(IV-3)}$$

where

$$z_a = z + x_{ac}\,\theta + (x_{ac} - x_{n_\delta})\xi = z + x_{ac}\,\theta + x_{an}\,\xi$$

$$\theta_a = \theta + \xi$$

$$q = \tfrac{1}{2}\rho V^2$$

In matrix form, the equations of motion are

$$\begin{bmatrix} ms^2 & 0 & 0 \\ 0 & Is^2 & 0 \\ 0 & 0 & m_e(s^2+\omega_e^2) \end{bmatrix}\begin{bmatrix} z \\ \theta \\ \xi \end{bmatrix} \qquad \text{(IV-4)}$$

$$= qS\begin{bmatrix} -C_{L_{\dot\alpha}}\frac{s}{V} & C_{L_\alpha} - \left(x_{ac}C_{L_{\dot\alpha}} - cC_{L_q}\right)\frac{s}{V} & C_{L_\alpha} - \left(x_{an}C_{L_{\dot\alpha}} - cC_{L_q}\right)\frac{s}{V} \\ -x_{ac}C_{L_{\dot\alpha}}\frac{s}{V} & x_{ac}C_{L_\alpha} - \left(x_{ac}^2C_{L_{\dot\alpha}} - x_{ac}cC_{L_q} + c^2C_{m_q}\right)\frac{s}{V} & x_{ac}C_{L_\alpha} - \left(x_{ac}x_{an}C_{L_{\dot\alpha}} - x_{ac}cC_{L_q} + c^2C_{m_q}\right)\frac{s}{V} \\ -x_{an}C_{L_{\dot\alpha}}\frac{s}{V} & x_{an}C_{L_\alpha} - \left(x_{an}x_{ac}C_{L_{\dot\alpha}} - x_{an}cC_{L_q} + c^2C_{m_q}\right)\frac{s}{V} & x_{an}C_{L_\alpha} - \left(x_{an}^2C_{L_{\dot\alpha}} - x_{an}cC_{L_q} + c^2C_{m_q}\right)\frac{s}{V} \end{bmatrix}\begin{bmatrix} z \\ \theta \\ \xi \end{bmatrix}$$

Introduce c as a unit of length, $\frac{c}{V}$ as a unit of time, and ρSc as a unit of mass. Also, introduce the radii of gyration

$$r^2 = I/m$$

$$r_e^2 = m_e/m$$

Then the following are convenient non-dimensional quantities:

$$\bar{r} = r/c \qquad \bar{s} = cs/V \qquad \bar{m} = m/\rho Sc$$

$$\bar{r}_e = r_e/c \qquad \bar{\omega}_e = c\omega_e/V \qquad \bar{C}_{L_\alpha} = C_{L_\alpha}/2\bar{m}$$

$$\bar{x}_{ac} = x_{ac}/c \qquad \bar{z} = z/c \qquad \bar{C}_{L_q} = C_{L_q}/2\bar{m}$$

$$\bar{x}_{an} = x_{an}/c \qquad\qquad \bar{C}_{m_q} = C_{m_q}/2\bar{m}$$

The equations of motion can now be written

$$\begin{bmatrix} -\left(\bar{s}^2 + \bar{C}_{L_\alpha}\bar{s}\right) & \bar{C}_{L_\alpha} - \left(\bar{x}_{ac}\bar{C}_{L_\alpha} - \bar{C}_{L_q}\right)\bar{s} & \bar{C}_{L_\alpha} - \left(\bar{x}_{an}\bar{C}_{L_\alpha} - \bar{C}_{L_q}\right)\bar{s} \\ -\bar{x}_{ac}\bar{C}_{L_\alpha}\bar{s} & \bar{x}_{ac}\bar{C}_{L_\alpha} - \left(\bar{x}_{ac}^2\bar{C}_{L_\alpha} - \bar{x}_{ac}\bar{C}_{L_q} + \bar{C}_{m_q}\right)\bar{s} - \bar{r}^2\bar{s}^2 & \bar{x}_{ac}\bar{C}_{L_\alpha} - \left(\bar{x}_{ac}\bar{x}_{an}\bar{C}_{L_\alpha} - \bar{x}_{ac}\bar{C}_{L_q} + \bar{C}_{m_q}\right)\bar{s} \\ -\bar{x}_{an}\bar{C}_{L_\alpha}\bar{s} & \bar{x}_{an}\bar{C}_{L_\alpha} - \left(\bar{x}_{an}\bar{x}_{ac}\bar{C}_{L_\alpha} - \bar{x}_{an}\bar{C}_{L_q} + \bar{C}_{m_q}\right)\bar{s} & \bar{x}_{an}\bar{C}_{L_\alpha} - \left(\bar{x}_{an}^2\bar{C}_{L_\alpha} - \bar{x}_{an}\bar{C}_{L_q} + \bar{C}_{m_q}\right)\bar{s} \\ & & -\bar{r}_e^2\left(\bar{s}^2 + \bar{\omega}_e^2\right) \end{bmatrix} \begin{bmatrix} \bar{z} \\ \theta \\ \xi \end{bmatrix} = 0$$

(IV-5)

The characteristic equation is obtained from the determinant of the matrix of coefficients in (IV-5):

$$\bar{s}^2\left(\bar{s}^4 + A_3\bar{s}^3 + A_2\bar{s}^2 + A_1\bar{s} + A_o\right) = 0 \qquad \text{(IV-6)}$$

$$A_3 = -\frac{\bar{\omega}_o^2}{\bar{x}_{ac}}\left[\bar{r}^2 + \bar{x}_{ac}^2 - \bar{x}_{ac}^2\frac{C_{L_q}}{C_{L_\alpha}} + \frac{C_{m_q}}{C_{L_\alpha}} + \frac{\bar{r}^2}{\bar{r}_e^2}\left(\bar{x}_{an}^2 - \bar{x}_{an}\frac{C_{L_q}}{C_{L_\alpha}} + \frac{C_{m_q}}{C_{L_\alpha}}\right)\right]$$

$$A_2 = \bar{\omega}_o^2\left[1 + \left(\frac{\omega_e}{\omega_o}\right)^2 + \frac{\bar{r}^2}{\bar{r}_e^2}\frac{\bar{x}_{an}}{\bar{x}_{ac}} + \bar{\omega}_o^2\frac{\bar{r}^2}{\bar{x}_{ac}^2}\frac{C_{m_q}}{C_{L_\alpha}}\left(1 + \frac{\bar{r}^2}{\bar{r}_e^2} + \frac{\bar{x}_n^2}{\bar{r}_e^2}\right)\right]$$

$$A_1 = -\frac{\bar{\omega}_o^4}{\bar{x}_{ac}}\left(\bar{r}^2 + \bar{x}_{ac}^2 - \bar{x}_{ac}\frac{C_{L_q}}{C_{L_\alpha}} + \frac{C_{m_q}}{C_{L_\alpha}}\right)\left(\frac{\omega_e}{\omega_o}\right)^2$$

$$A_o = \bar{\omega}_o^4\left(1 + \bar{\omega}_o^2\frac{\bar{r}^2}{\bar{x}_{ac}^2}\frac{C_{m_q}}{C_{L_\alpha}}\right)\left(\frac{\omega_e}{\omega_o}\right)^2$$

where ω_o and $\bar{\omega}_o$ are defined as in Section III of this report:

$$\omega_o = \sqrt{- \frac{\left(\frac{1}{2} \rho V^2\right) S C_{L_\alpha} x_{ac}}{m r^2}}$$

In order to determine the velocity at which the airframe becomes neutrally stable, substitute $\bar{s} = i\bar{\omega}$ in the characteristic equation, then if $\bar{\omega} \neq 0$:

$$- A_3 \bar{\omega}^2 + A_1 = 0$$

$$\bar{\omega}^4 - A_2 \bar{\omega}^2 + A_o = 0$$

or

$$\left(\frac{A_1}{A_3}\right)^2 - A_2 \left(\frac{A_1}{A_3}\right) + A_o = 0 \qquad \text{(IV-7)}$$

This equation is linear in $\left(\frac{\omega_e}{\omega_o}\right)^2$ if we divide through by $\left(\frac{\omega_e}{\omega_o}\right)^2$. If ω_e is given, then ω_o can be determined from the ratio $\frac{\omega_e}{\omega_o}$. Furthermore, since

$$\omega_o = \sqrt{- \frac{1}{2} \rho V^2 S \frac{x_{ac} C_{L_\alpha}}{mr^2}} = \sqrt{- \frac{1}{2} \rho S \frac{x_{ac} C_{L_\alpha}}{mr^2}}\, V$$

is a linear function of V for a given airframe, it follows that the velocity at neutral stability can be determined from (IV-7). Note that the frequency ω_o does not represent the short period frequency of the airframe except in the trivial case where the airframe is rigid. ω_o is simply a convenient way of specifying the velocity V. From (IV-7) we get

$$\left(\frac{\omega_o}{\omega_e}\right)^2 = \frac{a^2 - a}{ab - c} \qquad \text{(IV-8)}$$

where

$$a = \frac{1 + \left(\frac{\bar{r}}{\bar{x}_{ac}}\right)^2 - \frac{1}{\bar{x}_{ac}}\frac{C_{L_q}}{C_{L_\alpha}} + \frac{1}{\bar{x}_{ac}^2}\frac{C_{m_q}}{C_{L_\alpha}}}{1 + \left(\frac{\bar{r}}{\bar{x}_{ac}}\right)^2 - \frac{1}{\bar{x}_{ac}}\frac{C_{L_q}}{C_{L_\alpha}} + \frac{1}{\bar{x}_{ac}^2}\frac{C_{m_q}}{C_{L_\alpha}}\left(\frac{\bar{r}}{\bar{r}_e}\right)^2\left(\frac{\bar{x}_{an}^2}{\bar{x}_{ac}^2} - \frac{\bar{x}_{an}}{\bar{x}_{ac}}\frac{1}{\bar{x}_{ac}}\frac{C_{L_q}}{C_{L_\alpha}} + \frac{1}{\bar{x}_{ac}^2}\frac{C_{m_q}}{C_{L_\alpha}}\right)} \qquad \text{(IV-9)}$$

$$b = 1 + \left(\frac{\bar{r}}{\bar{r}_e}\right)^2 \frac{x_{an}}{x_{ac}} + \bar{\omega}_o^2 \frac{\bar{r}^2}{\bar{x}_{ac}^2}\frac{C_{m_q}}{C_{L_\alpha}}\left[1 + \frac{\bar{r}^2}{\bar{r}_e^2}\left(1 + \frac{\bar{x}_{n\ell}^2}{\bar{r}^2}\right)\right] \qquad \text{(IV-10)}$$

$$c = 1 + \bar{\omega}_o^2 \frac{\bar{r}^2}{\bar{x}_{ac}^2}\frac{C_{m_q}}{C_{L_\alpha}} \qquad \text{(IV-11)}$$

Equations (IV-8), (IV-9), (IV-10), and (IV-11) were used to construct the stability boundaries presented in the Appendix. The frequency of the neutrally stable oscillation is obtained from $\bar{\omega} = \frac{A_1}{A_3}$:

$$\left(\frac{\omega_e}{\omega}\right)^2 = 1 + \frac{\bar{r}^2}{\bar{r}_e^2}\,\frac{\frac{\bar{x}_{an}^2}{\bar{x}_{ac}^2} - \frac{\bar{x}_{an}}{\bar{x}_{ac}}\frac{1}{\bar{x}_{ac}}\frac{C_{L_q}}{C_{L_\alpha}} + \frac{1}{\bar{x}_{ac}^2}\frac{C_{m_q}}{C_{L_\alpha}}}{1 + \frac{\bar{r}^2}{\bar{x}_{ac}^2} - \frac{1}{\bar{x}_{ac}}\frac{C_{L_q}}{C_{L_\alpha}} + \frac{1}{\bar{x}_{ac}^2}\frac{C_{m_q}}{C_{L_\alpha}}} \qquad \text{(IV-12)}$$

Six parameters suffice to determine the frequency ratios $\frac{\omega_e}{\omega_o}$ and $\frac{\omega_e}{\omega}$. They are

$$\frac{\bar{x}_{an}}{\bar{x}_{ac}}$$

$$\frac{\bar{r}^2}{\bar{r}_e^2} \equiv R$$

$$\frac{\bar{r}^2}{\bar{x}_{ac}^2}$$

$$\frac{1}{\bar{x}_{ac}} \frac{C_{L_q}}{C_{L_\alpha}}$$

$$\frac{1}{\bar{x}_{ac}^2} \frac{C_{m_q}}{C_{L_\alpha}}$$

$$\bar{\omega}_o^2 \frac{\bar{r}^2}{\bar{x}_{ac}^2} \frac{C_{m_q}}{C_{L_\alpha}} = \frac{C_{m_q}}{\bar{m}\,\bar{x}_{ac}}$$

where m is the mass parameter, $\bar{m} = m/\rho Sc$. These parameters are the same as appeared in connection with the simple airframe discussed in Section III of the report, except that the parameter $\frac{\bar{r}^2}{\bar{r}_e^2}$ replaces the frequency ratio parameter $\frac{\omega_z}{\omega_\theta}$, and the node line position $\bar{x}_{n\ell}$ replaces the elastic axis position $\bar{x}_e$.

In the limiting case, where the generalized mass of the elastic mode is allowed to approach zero ($\bar{r}_e^2 \rightarrow 0$), equation (IV-6) becomes identical with equation (III-17) of Section III, provided we identify the node line position $\bar{x}_{n\ell}$ with the elastic axis position $\bar{x}_e$.

As was found previously, the presence of aerodynamic damping can have a profound influence on the stability of the airframe. Consider, for example, the case where

$$\bar{x}_{an}^2 - \bar{x}_{an} \frac{C_{L_q}}{C_{L_\alpha}} + \frac{C_{m_q}}{C_{L_\alpha}} = 0; \qquad \text{(IV-13)}$$

then

$$\left(\frac{\omega_o}{\omega_e}\right)^2 = 0,$$

which shows that the airframe is neutrally stable at <u>zero</u> airspeed. This instability is caused by the loss of aerodynamic damping on the elastic mode due to the destabilizing effect of C_{L_q}. Thus, since structural damping is ignored, the structural mode is neutrally stable in the absence of aerodynamic damping. Now the aerodynamic damping can be positive or negative in general, and the condition (IV-13) is just the condition that the aerodynamic damping be zero. If $C_{L_q} = 0$, the instability cannot occur since equation (IV-13) cannot be satisfied. This type of instability is entirely similar to one of the instabilities discussed in Section III and accounts for a prominent feature of the stability boundaries presented in the Appendix. The curves of $\frac{\omega_o}{\omega_{ofc}}^*$ given in the Appendix for the case of subsonic aerodynamics display a sharp dip. The value of $\bar{x}_{an}$ at which the dip occurs is correctly predicted by equation (IV-13). The curves drawn for supersonic aerodynamics do not exhibit this feature, since $C_{L_q} = 0$ for these curves. Instability due to loss of aerodynamic damping is very sensitive to the presence of structural damping and may be masked at low airspeeds by the structural damping.

A much more violent instability will be exhibited by the airframe of Figure 14 if the aerodynamic center is forward of the node line. In this case the short period frequency and the elastic mode frequency will come close together at a sufficiently large airspeed. At higher airspeeds, one of these two roots will become quite unstable. It is useful to examine this type of instability by the frequency coalescence technique.

*ω_{ofc} is defined in equation (IV-19).

ignore all damping terms in the equations of motion (IV-4). Then the characteristic equation can be obtained from (IV-6) by setting $C_{L_q} = C_{m_q} = 0$ and dropping the terms of odd order in $\bar{s}$. In this way we obtain the following characteristic equation:

$$\bar{s}^4 + A\,\bar{s}^2 + B = 0 \tag{IV-14}$$

$$A = \bar{\omega}_o^2 \left[1 + \left(\frac{\omega_e}{\omega_o} \right)^2 + R \frac{\bar{x}_{an}}{\bar{x}_{ac}} \right] \tag{IV-15}$$

$$B = \bar{\omega}_o^4 \left(\frac{\omega_e}{\omega_o} \right)^2 \tag{IV-16}$$

where $R = \dfrac{r^2}{\bar{r}_e^2}$.

$\bar{s}^2$ will be real and negative unless $A^2 - 4B$ is negative. If $A^2 - 4B$ is negative then two of the roots of equation (IV-14) will have a positive real part. The airframe is therefore on the verge of instability when

$$A^2 - 4B = 0 \tag{IV-17}$$

or, according to equations (IV-15) and (IV-16), when

$$\left[1 + \left(\frac{\omega_o}{\omega_e} \right)^2 + R \frac{\bar{x}_{an}}{\bar{x}_{ac}} \right]^2 = 4 \left(\frac{\omega_o}{\omega_e} \right)^2 \tag{IV-18}$$

To distinguish the value of ω_o determined by equation (IV-8) from the value given by equation (IV-18), denote the solution of (IV-18) by ω_{ofc}. Then

$$\frac{\omega_e}{\omega_{ofc}} = 1 + \sqrt{-R \frac{x_{an}}{x_{ac}}} \tag{IV-19}$$

Thus, according to the frequency coalescence criterion, there are only two parameters involved in the stability problem,

$$R = \frac{\bar{r}^2}{\bar{r}_e^2} \text{ (generalized mass ratio)}$$

$$\frac{x_{an}}{x_{ac}} = \frac{x_{ac} - x_{n\delta}}{x_{ac}}$$

The parameter $\frac{x_{an}}{x_{ac}}$ is negative if the aerodynamic center is forward of the node line. According to frequency coalescence, instability can occur only if the aerodynamic center is forward of the node line of the elastic mode. $\frac{\omega_{ofc}}{\omega_e}$ is plotted versus $\frac{x_{an}}{x_{ac}}$ in Figure 15 for several values of R. The frequency coalescence solution of the stability problem is remarkably simple, however it can be highly unconservative due to the fact that the effects of aerodynamic damping are entirely ignored. Also, only one of the two essentially distinct instability mechanisms is explained by the frequency coalescence approach.

The discrepancies between the predictions of the frequency coalescence method and predictions of the more exact theory are clearly exhibited in the stability boundaries of the Appendix. On the graphs presented in the Appendix the frequency coalescence solution is simply the straight line $\frac{\omega_o}{\omega_{ofc}} = 1$.

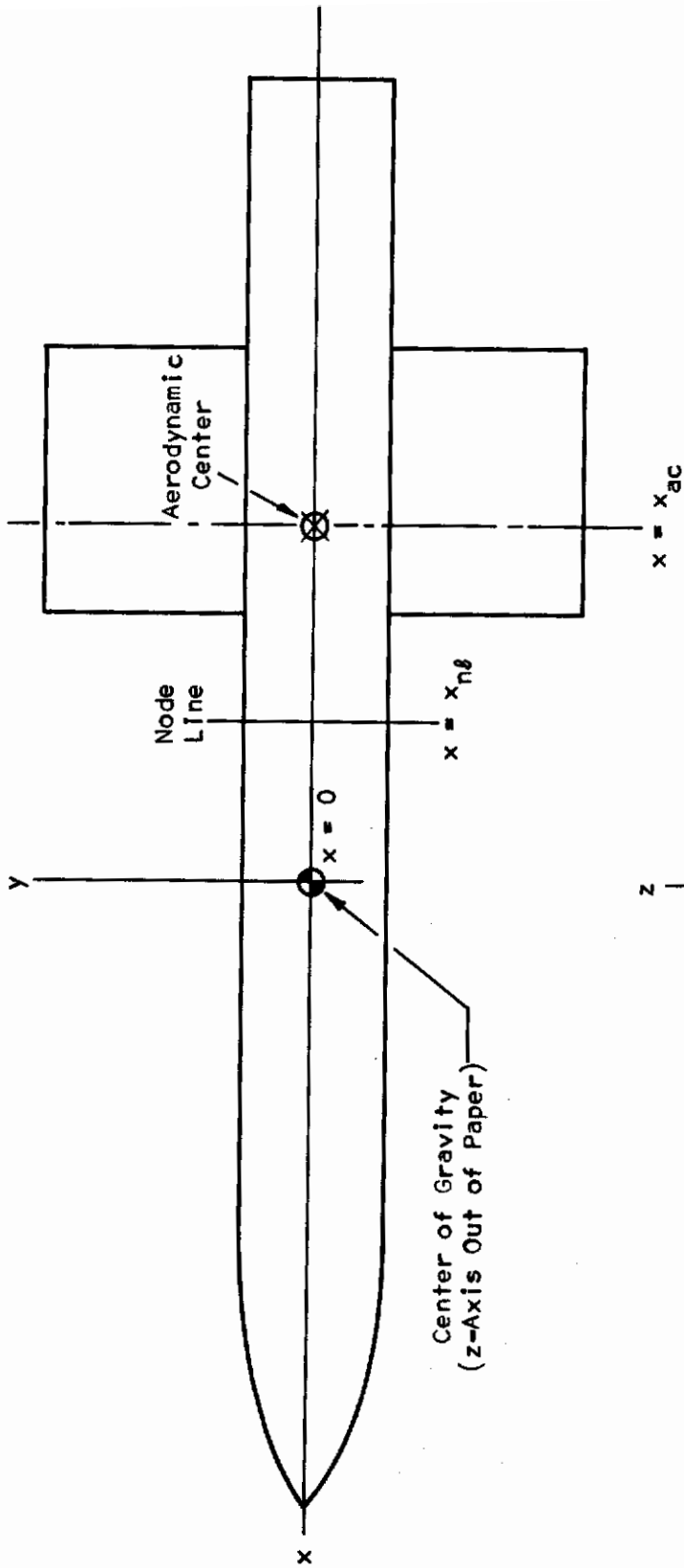

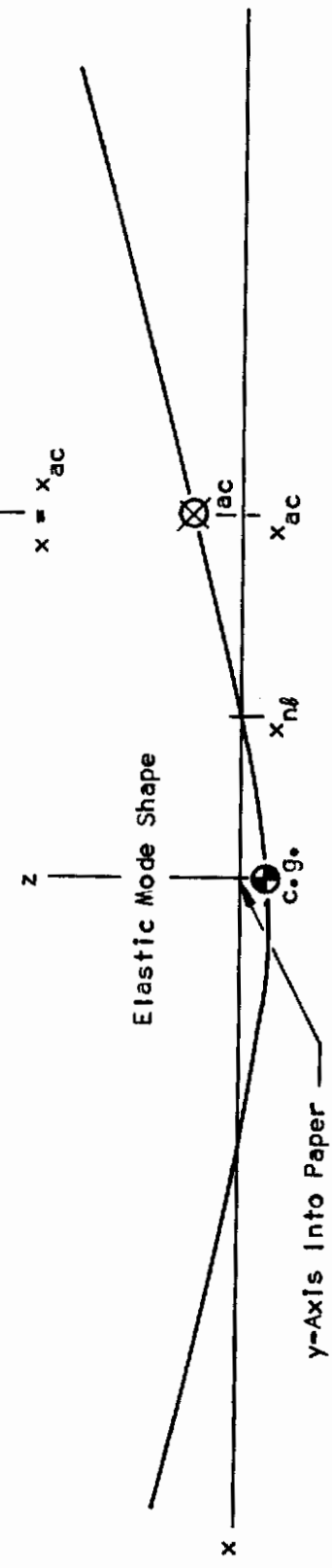

Figure 14. Flexible Airframe With a Rigid Lifting Surface

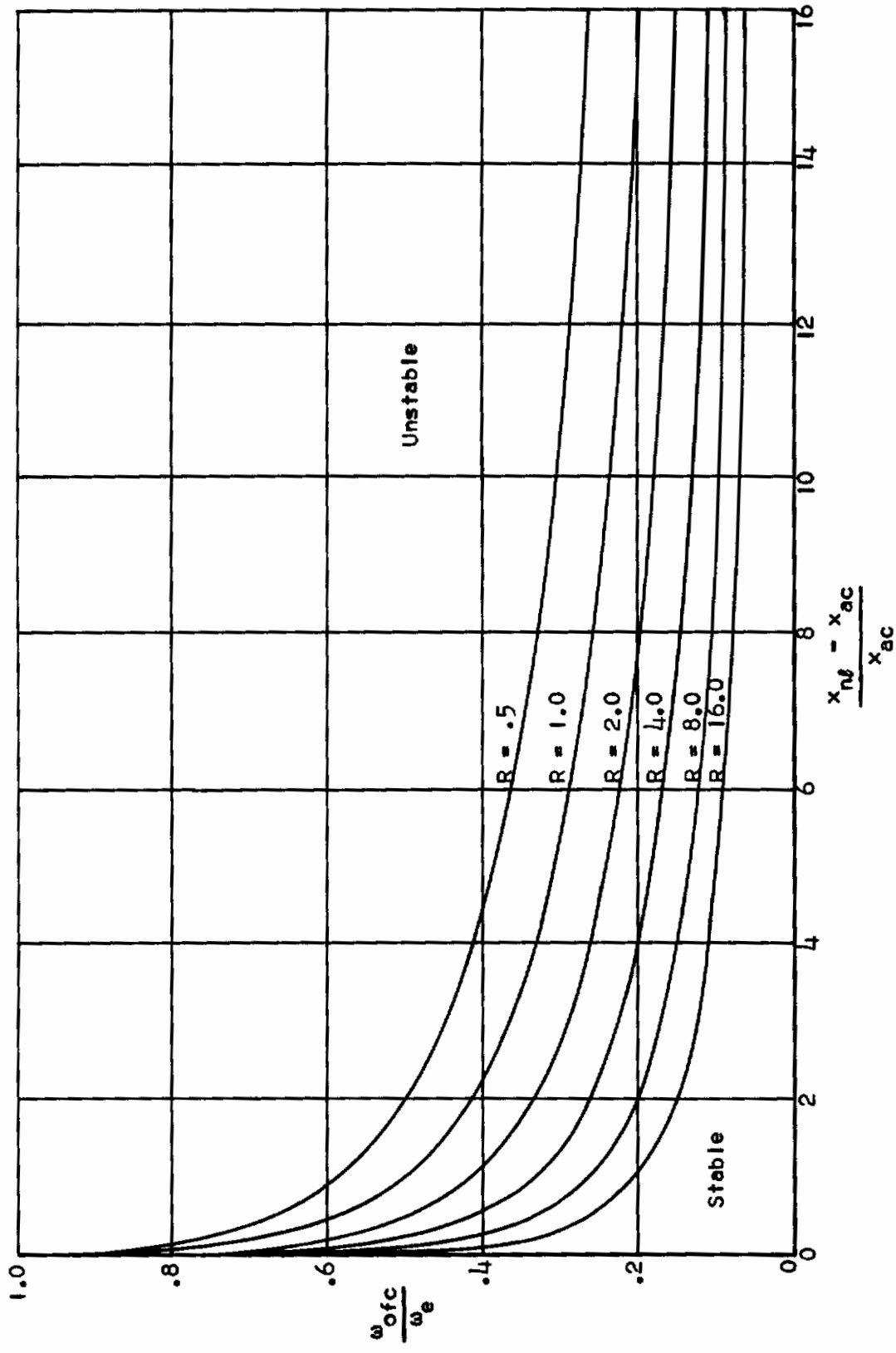

Figure 15. Stability Boundaries Constructed by the Frequency Coalescence Method

V. CLASSIFICATION OF AEROELASTIC STABILITY PROBLEMS

The study and analysis of the stability of airborne vehicles was historically divided into three fields of interest:

1. Stability and control.
2. Flutter.
3. Steady state aeroelasticity (divergence).

A definition of scopes of these fields has never been established; however, in their origin these areas of technology were directed at specific phenomena.

1. The analytical effort, most commonly called the study of "stability and control", was concentrated on aircraft stability problems which exist when the aircraft is a rigid body. The effects of elasticity have been incorporated into these analyses but often in such a manner as to exclude the dynamic response of the system in any of its finite frequency normal modes.
2. The field of flutter analysis has been limited to the study of aeroelastic instabilities which arise from the "coupling" of two or more finite frequency elastic modes of the aircraft. In many, and possibly most, flutter analyses of aircraft, the vehicle has been represented by a relatively small number of (10 or less) finite frequency elastic modes of the free system. Zero frequency modes have commonly been omitted from flutter analyses along with consideration of the generalized flexibility of modes higher than those specifically included in the analyses.
3. Steady state aeroelastic instability, commonly called divergence,

has been a recognized problem since the very early days of aircraft design. The analyses of steady state aeroelastic phenomena in essence ignore the inertia of the vehicle except for the consideration of "inertia relief" in free systems.

Recent years have brought about some changes in the analytical fields discussed above which tend to merge their technologies. The results of this study indicate that a unification of these analytical fields is desirable and necessary to produce a reliable aeroelastic stability analysis of a modern airborne system.

CLASSIFICATION OF AEROELASTIC PHENOMENA

Collar presented a classification of aeroelastic problems in the well known "Collar's triangle of forces" by which aeroelastic phenomena are described as being the result of various combinations of aerodynamic, elastic and inertia forces. We propose another aeroelastic triangle (Figure 16) for free systems as a supplement to Collar's triangle.

A classification of aeroelastic phenomena is made in the triangle of Figure 16 by the normal modes of the system which are required in a representation of the system to produce the phenomenon. The apexes of the triangle of Figure 16 are:

0 - zero frequency or rigid body modes

F - finite frequency modes

∞ - infinite frequency modes or residual flexibility

Since Figure 16 applies to aeroelastic problems, aerodynamic forces are involved in all phenomena described.

The problems included in the numbered boxes are:

1. Classical stability and control problems involving a rigid vehicle and aerodynamic forces.
2. Classical flutter problems involving 2 or more finite frequency modes and aerodynamic forces.
3. Classical steady state aeroelastic problems involving only elasticity and aerodynamic forces.
4. "Mode interaction." To a stability and control analyst this problem is described as one where elastic modes have a pronounced effect on the low frequency response of the system. To a flutter analyst this is a problem involving coupling of the rigid body modes with the elastic modes. This phenomenon is shown to be a stability problem in the analysis of Section IV of this report and is undoubtedly a problem in the prediction of the dynamic behavior of a system at a velocity below the flutter speed.

   The analysis of Section IV shows that this stability problem can be predicted, for many systems, by "frequency coalescence" methods (omitting damping terms) but for certain systems the damping terms can have a dominating effect on the solution.
5. "Elastic Interaction." This problem area will include the modification of "rigid body" dynamic response by the elasticity of the system and the stability problem shown by the analysis of Section III of this report where a free system can be unstable by virtue of only plunge or pitch flexibility of its aerodynamic surface.

This stability problem involving plunge flexibility is quite interesting because:

a. It is a flutter problem which can exist for an idealized system which has no finite frequency normal modes.

b. It is a flutter problem for which the "mechanism" of instability can be easily understood.

Most flutter phenomena are the result of complicated, relative phasing between structural motions which cause aerodynamic forces to either add or subtract energy from the system. For this case of "elastic interaction" the structural deflections have no relative phase angle and the phenomenon can be easily explained as follows.

Consider the airframe of Figure 13 with a rigid pitch spring (K_θ) and a flexible plunge spring (K_h). Figure 17 shows the airframe at the instant of maximum deflection (of unit pitch angle) in its short period mode for various values of velocity.

Figure 17a corresponds to a low value of velocity. The short period mode frequency is low as well as the lift force L. The short period mode is well damped by virtue of the lift due to the plunge velocity h.

Figure 17b corresponds to a higher value of velocity. The lift force has increased from that of Figure 17a; and, therefore, the short period mode frequency and the deflection of the spring K_h have increased. Since $\dot{h}$ is smaller, the damping of the short period mode has decreased.

Figure 17c corresponds to a higher velocity than Figure 17b. At this speed the lift force on the aerodynamic surface is sufficient to deflect the plunge spring (K_h) the distance y and therefore reduce the plunge of the surface to zero. Since the plunge of the surface is zero, the damping due to plunge is also zero. If this system is subjected to a still higher velocity the aerodynamic surface will plunge in a direction opposite from its attachment point. Since the plunge velocity $\dot{h}$ of Figure 17 contributed positive damping to the system, it is only reasonable that when the algebraic sign of $\dot{h}$ is changed the damping will be negative. Since the damping in the short period mode is attributable primarily to the plunge velocity, the system will be unstable at a dynamic pressure slightly higher than that depicted in Figure 17c.

6. "General Aeroelastic Problem." Section II of this report presented an analysis and comparison of the solution of configuration 4 of reference 1. It has been demonstrated that a reliable prediction of the dynamic response of this configuration can be attained only through the inclusion of zero frequency modes, finite frequency modes, and the residual flexibility of all higher modes of the system in the modal representation.

The analysis of Section II omitted the aerodynamic damping terms for simplicity. This assumption was apparently reasonable for the solution of configuration 4 because of the relatively high altitude considered. The analysis of Section III shows that this assumption cannot be used in the general

case and for many configurations can lead to an extremely unconservative prediction of the flutter speed.

7. The problem area described by area 7 of Figure 16 can be described as an aeroelastic instability which can be represented analytically when only an elastic mode and the residual flexibility of the system are included. Such a phenomenon is not known to exist but it is postulated that the problem area will be discovered in the future.

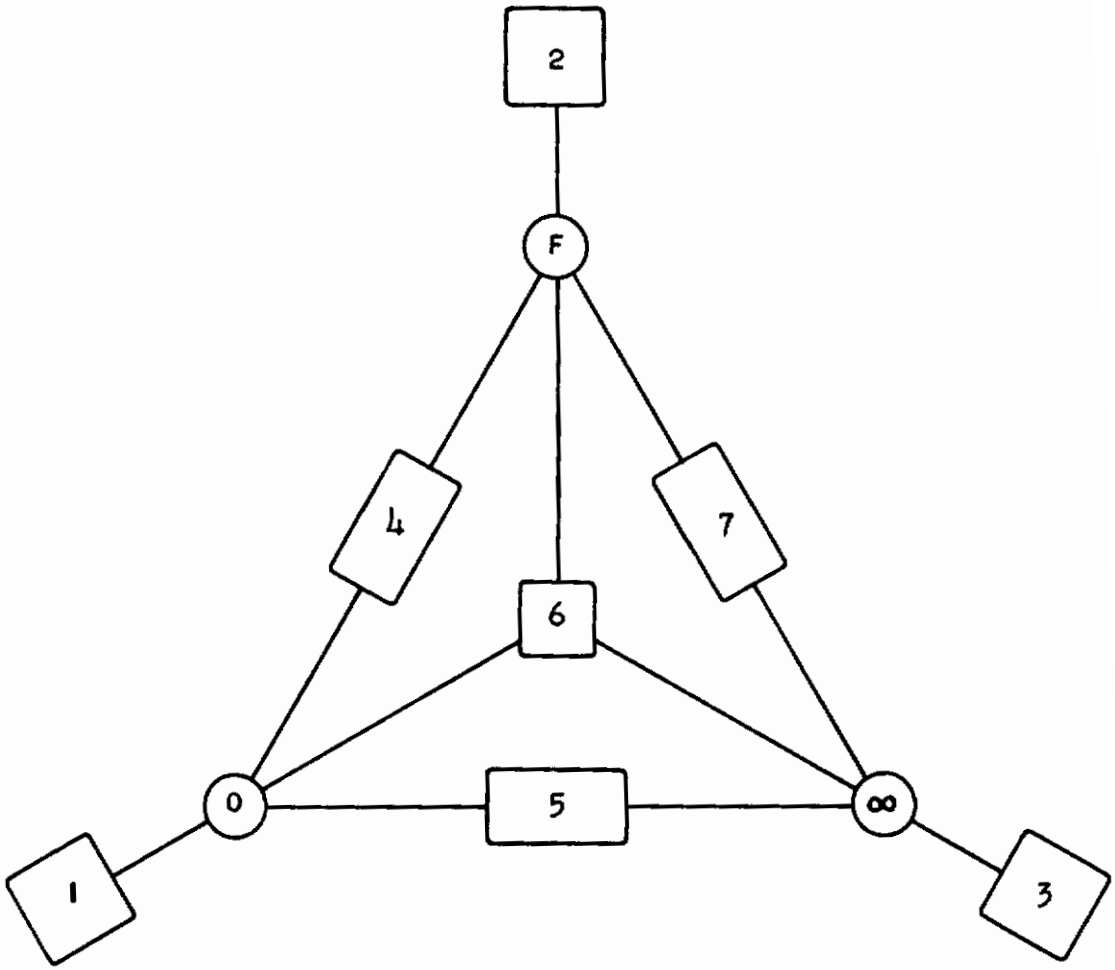

Figure 16. Diagram of Aeroelastic Phenomenon of Free Systems

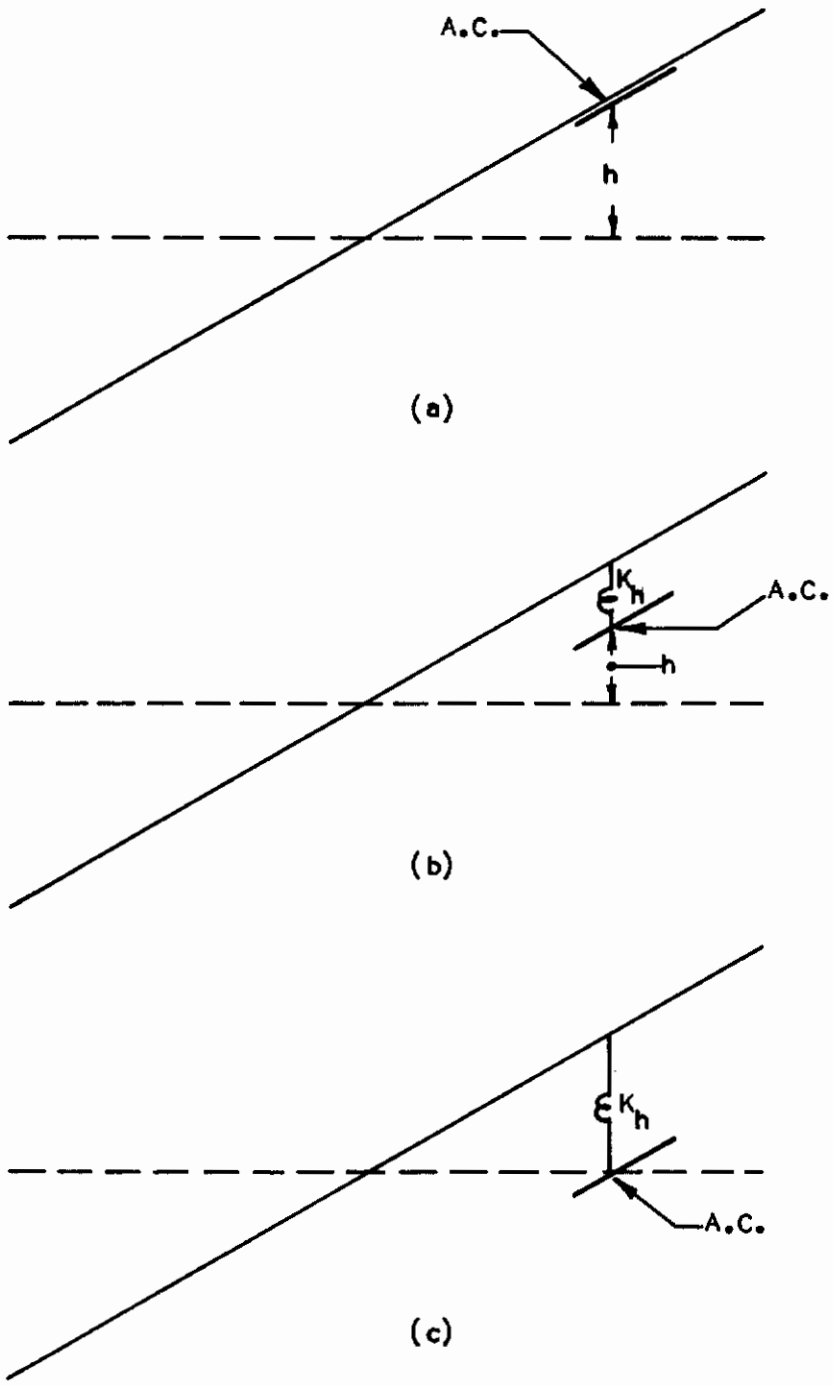

Figure 17. Missile With Elastically Attached Massless Lifting Surface

VI. COMPUTER STUDIES OF MISSILE CONFIGURATION AND COMPARISON WITH THEORY

Studies were made on the Computer Engineering Associates' passive analog computer of a number of "airborne missile" configurations. The purpose in making these computer studies was to provide a check or independent verification of the analyses of this report and to study the effects of parameters not included in these analyses.

The basic missile configuration considered in all computer studies was configuration 2 of reference 1. The geometry, mass and stiffness data for this basic configuration are repeated in Figures 18, 19, 20 and Table 1. During the conduct of this study numerous variations were made in this configuration. In most computer analyses the forward aerodynamic surface was omitted. All variations to the configuration are summarized in Table 2. In all cases the aerodynamic surfaces were considered to be rigid and elastically restrained by a "pitch" and "plunge" spring at the missile station listed in Table 2 as "e.a. Station".

The aerodynamic forces were represented as follows:

1. The forces on the body of the missile were assumed to be zero.
2. The lift forces on the surfaces, normal to the surfaces and positive upward are given by

$$L = \frac{1}{2} \rho V^2 S C_{L_\alpha} \left(\theta - \frac{sZ}{V} + \frac{cs\theta}{2V} \right)$$

where Z is the normal deflection (positive up) and θ is

the pitching slope (positive nose up) of the surface at the aerodynamic center of the surface.

3. The moments about the centers of pressure of the surface are given by:

$$M = -\frac{1}{2} \rho V^2 S \frac{\pi}{8} \frac{c^2}{V} s \theta$$

4. The effects of downwash were neglected.

The "basic" flight condition is defined by the following aerodynamic constants:

Velocity = 2250 mph

Altitude = sea level

Dynamic Pressure = q_o = 90 lb./in.^{2}

Lift Curve Slope = C_{L_α} = 1.5 per rad.

The flutter speeds measured in the studies were tabulated as a fraction of the basic velocity (V_o), thus flutter speed is listed as the ratio V/V_o.

The computer studies of the configurations listed in Table 2 determined the dynamic pressure corresponding to flutter. In all cases the flutter encountered was of the general type discussed in this report; that is, it involved the rigid body modes of the system as indicated by a flutter frequency below the lowest natural frequency of structure in a vacuum.

RIGID FUSELAGE - CASES 1 THROUGH 9

Cases 1 through 9 considered a rigid fuselage with a single aerodynamic surface elastically attached near the aft end of the missile.

Listed at the right side of Table 2 are the values of flutter speed measured on the analog computer, calculated from the criteria of Section III and from the criteria of Section IV.

Cases 1 through 5 considered an aerodynamic center which coincided with the elastic axis of the lifting surface.

Cases 1, 2 and 5 are identical except for the pitch inertia of the elastically supported aft surface. The correlation between theory and measurement was fair for cases 1 and 5 where the inertia was quite small (zero in case 5) but much poorer in case 2 where the inertia was 10 times larger. The flutter speed calculated from the criteria of Section III is identical for cases 1, 2 and 5 because the mass of the surface is completely ignored in the analysis of Section III. The discrepancy between the theory of Section III and measurement in case 2 is easily explained by omission of the mass from the Section III criteria but the discrepancy between the measurement and the criteria of Section IV cannot be explained.

Cases 3 and 4 are identical except that the mass of the lifting surface, elastically mounted by a plunge spring, was omitted in case 4. The identical flutter speed was measured on the computer for these 2 cases as also was, of course, predicted by the theory of Section III which ignored the mass completely. The criteria of Section IV could not be applied to cases 4 and 5 due to the absence of a finite frequency elastic mode. The correlation between theory and measurement is considered reasonably good for these cases. The discrepancies can be ascribed to the equivalent structural damping inherently present in

the passive analog computer.

Cases 4 and 5 are interesting specimens of flutter because in a vacuum the structures in both cases have no finite frequency modes. When described by their normal coordinates these configurations possess two zero frequency degrees of freedom and one infinite frequency degree of freedom. Nevertheless these configurations exhibit a flutter instability at a finite frequency.

Cases 6 and 7 are similar to cases 1 and 3, respectively, except that the aft aerodynamic surface was shifted forward 10% of its chord in cases 6 and 7 while retaining the attachment point of the surface to the fuselage at the same point on the fuselage. The effective elastic axis of the aerodynamic surface was, therefore, at the 60% chord, 10% of the chord aft of the aerodynamic center. The configurations of case 6, where the pitch restraint between the fuselage and the aerodynamic surface is flexible, tends toward steady state elastic divergence. Divergence would be encountered at a dynamic pressure corresponding to V/V_o of 1.39. Table 2 shows that a dynamic instability is encountered at a somewhat lower speed than the divergence speed.

The comparison of cases 6 and 7 to cases 1 and 3 demonstrate the sensitivity of the flutter phenomenon to the relative locations of the aerodynamic center and the elastic axis of the lifting surface. This extreme sensitivity may be considered as an explanation for some of the discrepancies in theoretical predictions and computer measurements shown in Table 2. The precise location of the aerodynamic center is difficult to control in the experimental procedure followed on the analog computer.

It seems also worthwhile to point out that the precise location of the aerodynamic center is generally not known for a physical system and, in fact, cannot be defined as physical point except for idealized systems.

Cases 8 and 9 are similar to cases 7 and 6, respectively, except that the lifting surface was moved aft 300 inches in cases 8 and 9. This variation affected the flutter speed very little in the computer measurements and had a somewhat larger effect on the theoretical predictions.

FUSELAGE WITH SINGLE BENDING DEGREE OF FREEDOM - CASE 10

Case 10 considered a configuration where the entire system was rigid except for a single flexibly restrained "hinge" at fuselage station 700. The purpose of studying this design was to experimentally evaluate the phenomenon shown on the charts of Section IV where the flutter speed is zero for specific parameter combinations. The flexibility of the system was reduced to the single flexibly restrained "hinge" in the fuselage to preclude considerations of "residual flexibility". The location of the lifting surface was varied in this case to provide a variation in the dimensionless parameter $\frac{x_{n\beta} - x_{ac}}{x_{ac}}$.

Figure 21 shows a comparison between the flutter speeds predicted by the theory of Section IV, frequency coalescence, and analog computer measurements. The radical difference between theoretical prediction by Section IV and computer measurements is easily explained by the presence of a small amount of equivalent structural damping in the computer solution.

Figure 22 shows some typical V-g diagrams for the configuration of case 10. The curve labeled "structural damping" shows the equivalent structural damping level which existed in the analog computer at the values of dimensionless velocity V/V_o. For the curve corresponding to $\frac{x_{n\delta} - x_{ac}}{x_{ac}}$ of 3.84 the intersection with the structural damping curve is at a value of V/V_o virtually identical to that at its intersection with the 0 damping axis which is considered to be the flutter speed. At this value of $\frac{x_{n\delta} - x_{ac}}{x_{n\delta}}$ theory and computer measurement are in reasonable agreement as shown in Figure 21.

The curve on Figure 22, corresponding to $\frac{x_{n\delta} - x_{ac}}{x_{ac}}$ of .264 never intersects with the "structural damping" curve; and if the structural damping curve were subtracted out of the solutions, this configuration would apparently be unstable at all finite velocities as shown in Figure 21.

This single example cannot be considered to prove that the low speed instability problem shown in Section IV can be completely ignored in the presence of a small amount of structural damping. This example does show that this problem may not be as serious as might be concluded from a consideration of only the results of Section IV.

EFFECT OF ALTITUDE - CASES 11 AND 12

Cases 11 and 12 may be compared with cases 1 and 3, respectively, to show the effect of an increase in altitude. Cases 11 and 12 correspond to an air density 1/10 of the air density considered in cases 1 and 3.

The change in the flutter speed is shown to be an increase of 12% to 16%. It may be concluded that the "mode interaction" phenomenon is not sensitive to air density or altitude parameters.

FLEXIBLE FUSELAGE - CASES 13 THROUGH 25

The comparison between theory and computer measurements for cases involving a flexible fuselage, in all cases, showed rather poor correlation. This lack of correlation is probably due to:

a. The presence of higher elastic modes in the computer representation which were ignored in the theoretical analyses.

b. Equivalent structural damping in the computer measurements which was ignored in the theoretical analyses.

The analyses of Sections II and III were not applied to these configurations because they were known to include assumptions which precluded their applicability. The analysis of Section II cannot be considered applicable to any cases of this configuration because it ignores aerodynamic damping. The results of cases 1 through 9 and the analysis of Section III identify the mode interaction phenomenon of this "missile configuration" to be intimately related to the aerodynamic damping. However the flutter phenomenon observed in some cases of this configuration were undoubtedly related to the instability studied in Section II.

EFFECT OF FLEXIBLY MOUNTED LIFTING SURFACE - CASES 13 THROUGH 16

Cases 13 and 14 consider configurations that are identical except for the flexibility of the attachment of the lifting surface to the fuselage. Case 13 considered the attachment to be rigid and case 14 considered the attachment in pitch and plunge to be of "basic" flexibility.

The flutter speeds measured for these cases were virtually identical, but the system damping at speeds less than the flutter speed were quite different. Figures 23 and 24 show the V-g diagrams for these cases including the "short period mode" and the lowest "elastic mode of the system". In case 13, where the aerodynamic surface was rigidly connected to the fuselage, the short period mode remained well damped throughout the speed range up to the vicinity of the flutter speed where its damping increased. In case 14, where the lifting surface was elastically connected to the fuselage, the damping in the short period mode became progressively smaller as velocity increased until it became unstable at the flutter speed.

The simplified analyses of this study are not capable of either predicting or providing an explanation for this difference between cases 13 and 14. The results of this study are capable, however, of defining the minimum complexity of an analysis which would be applicable to these cases as an analysis which includes consideration of

a. Two rigid body modes.

b. One elastic mode.

c. The residual flexibility of the higher modes of the system.

d. Aerodynamic damping terms.

e. Prediction of system damping at speeds less than the flutter speed.

Such an analysis of a specific configuration is not considered overly complex for practical solution, but the complexity does appear too great for the type of generally applicable solutions sought in this study. It should be noted that the intention of the analyses of this study

was to predict the susceptibility of a configuration to "mode interaction" and that the difficulties experienced in predicting precise flutter speeds or the response of the system at subcritical speeds does not impair the fulfillment of this intention.

A comparison of cases 15 and 16 show that when the rigidly mounted surface is moved aft of the node line of the first elastic mode, the instability disappears; but that when the flexible mounting of the lifting surface is introduced the system is again unstable at virtually the same speed as in cases 13 and 14 where the surface is forward of the node line.

EFFECTS OF CANARD SURFACE - CASES 18 AND 19

The configurations studied in cases 18 and 19 are identical to those considered in cases 14 and 13, respectively, except that the canard surface of the "basic" configuration is added in cases 18 and 19. The effects of the canard surface are simply to increase the flutter speed about 7%. The V-g curves of cases 18 and 19 are similar in character to those of cases 14 and 13, respectively, shown in Figures 23 and 24.

EFFECTS OF THE POSITION OF THE SINGLE LIFTING SURFACE - CASES 22 THROUGH 25

Cases 13 through 16 and cases 22 through 25 show the effect of positioning the lifting surface at four locations along the fuselage from station 800 to station 1000. At each location the effect of flexibility of the lifting surface attachment was investigated. As shown in Table 2, the flutter speed was affected very little by the variations in position

of the lifting surface or the flexibility of the aerodynamic surface attachment. In each case, when the attachment was rigid the short period mode damping remained constant over the speed range studied, and when the attachment was flexible the short period mode damping became progressively small as speed was increased until the short period mode became unstable at the flutter speed.

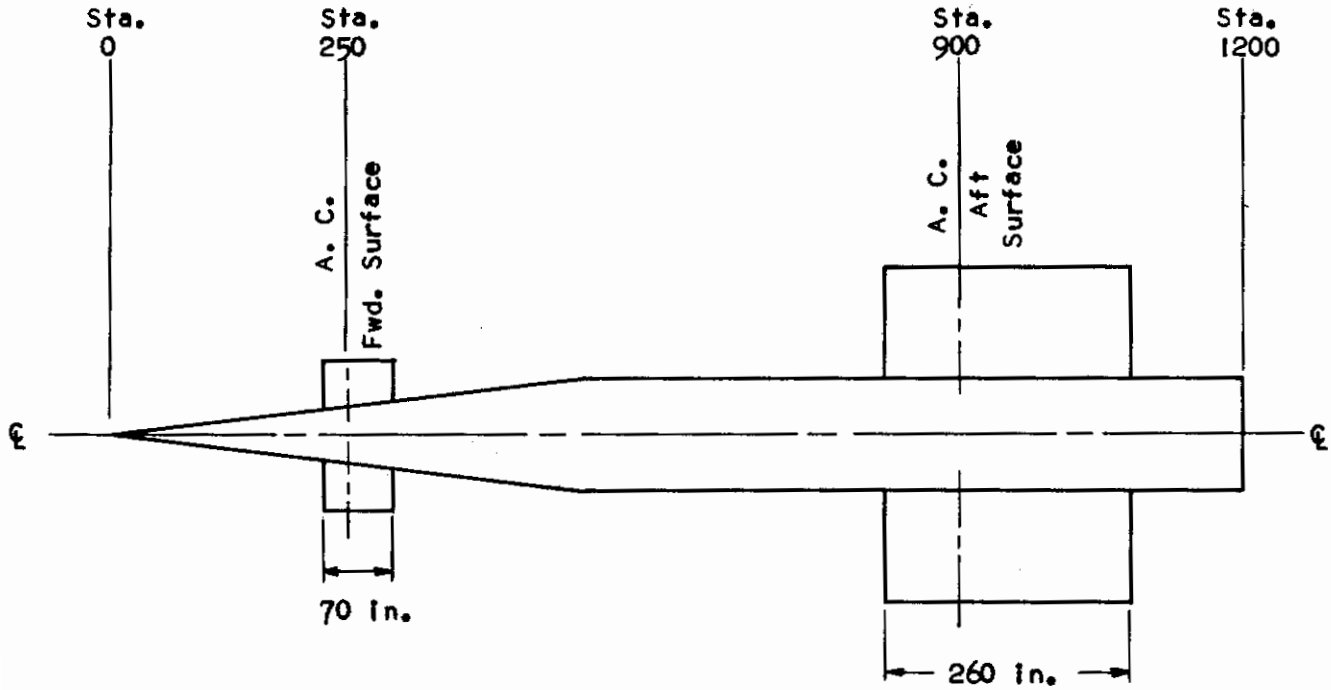

Note: Stations shown in inches.
Area of forward surface (total for both sides) = 7000 in.^{2}
Area of aft surface (total for both sides) = 62,400 in.^{2}

Figure 18. Configuration 2

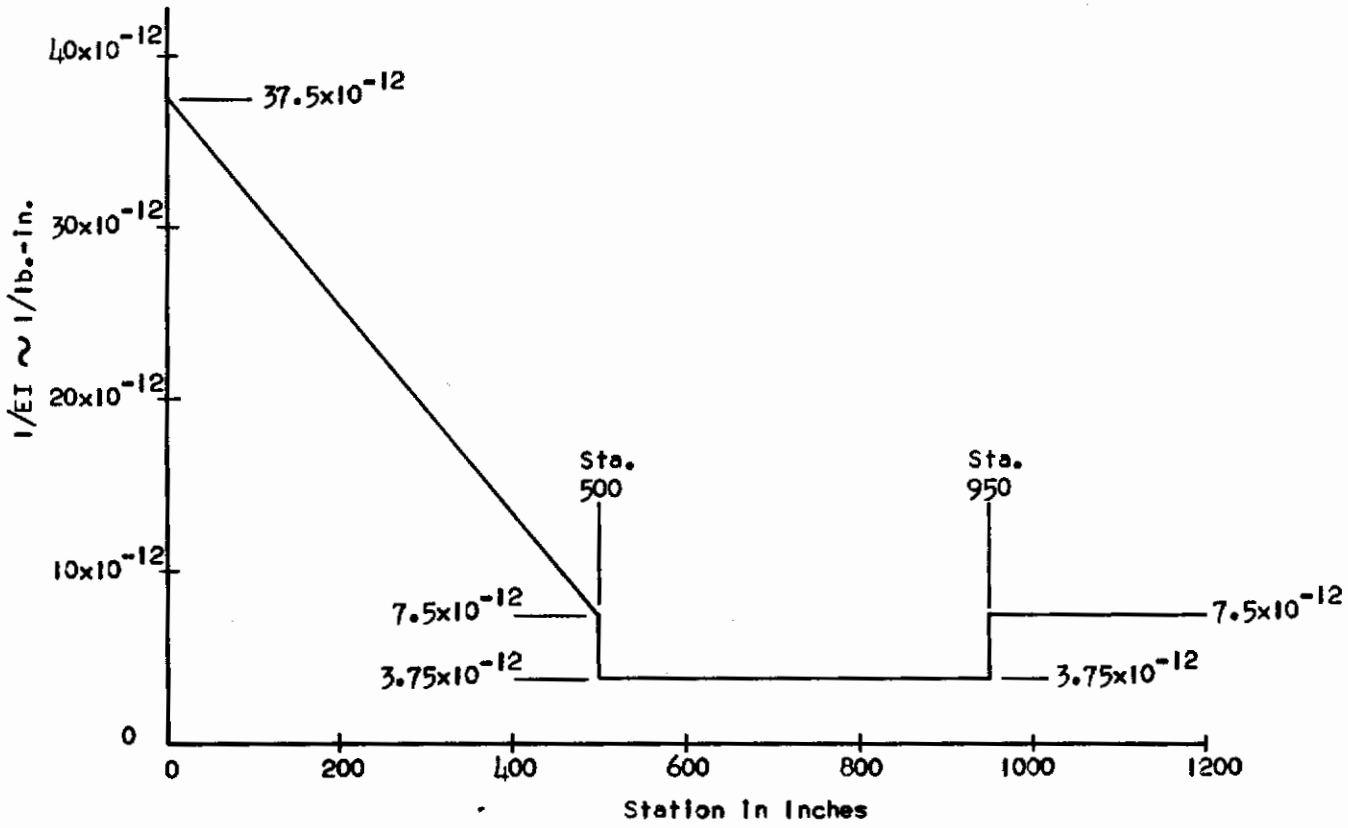

Figure 19. Body Flexibility of Configuration 2

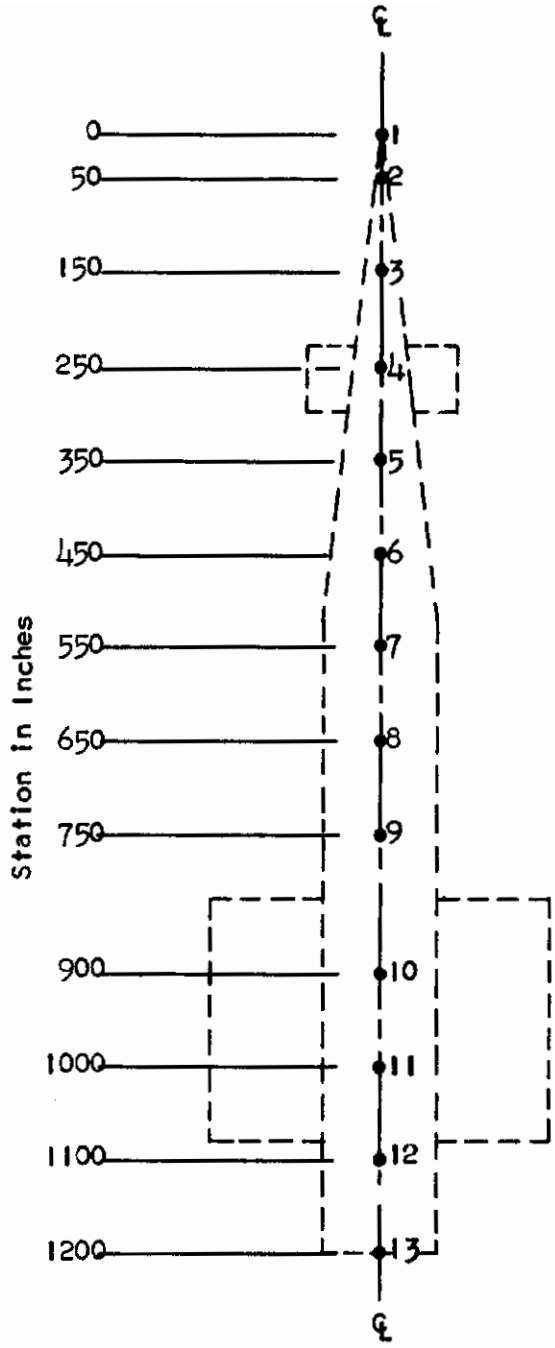

Figure 20. Mass Locations of Configuration 2

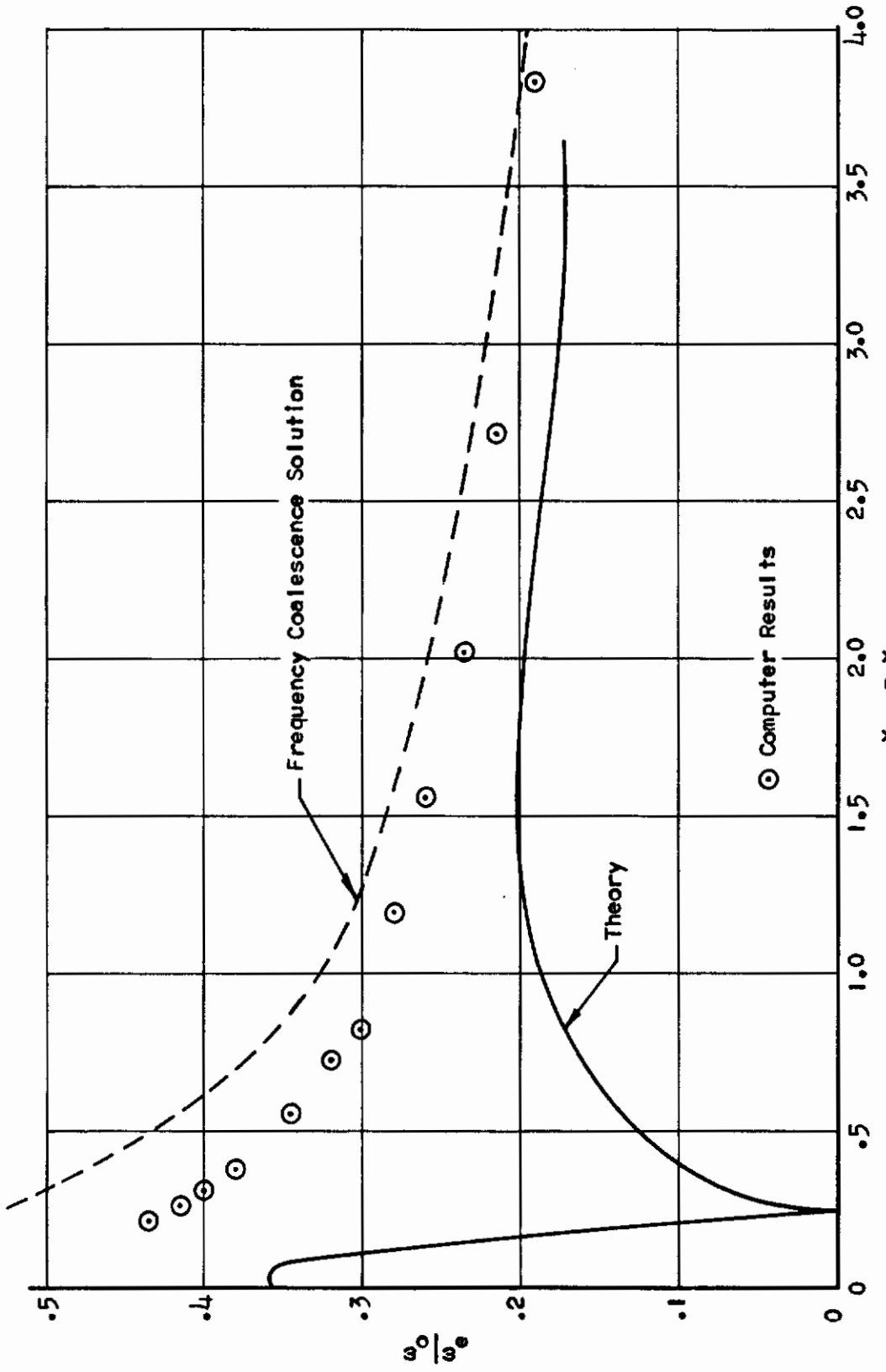

Figure 21. Comparison of Computer Results and Theory - Case 10

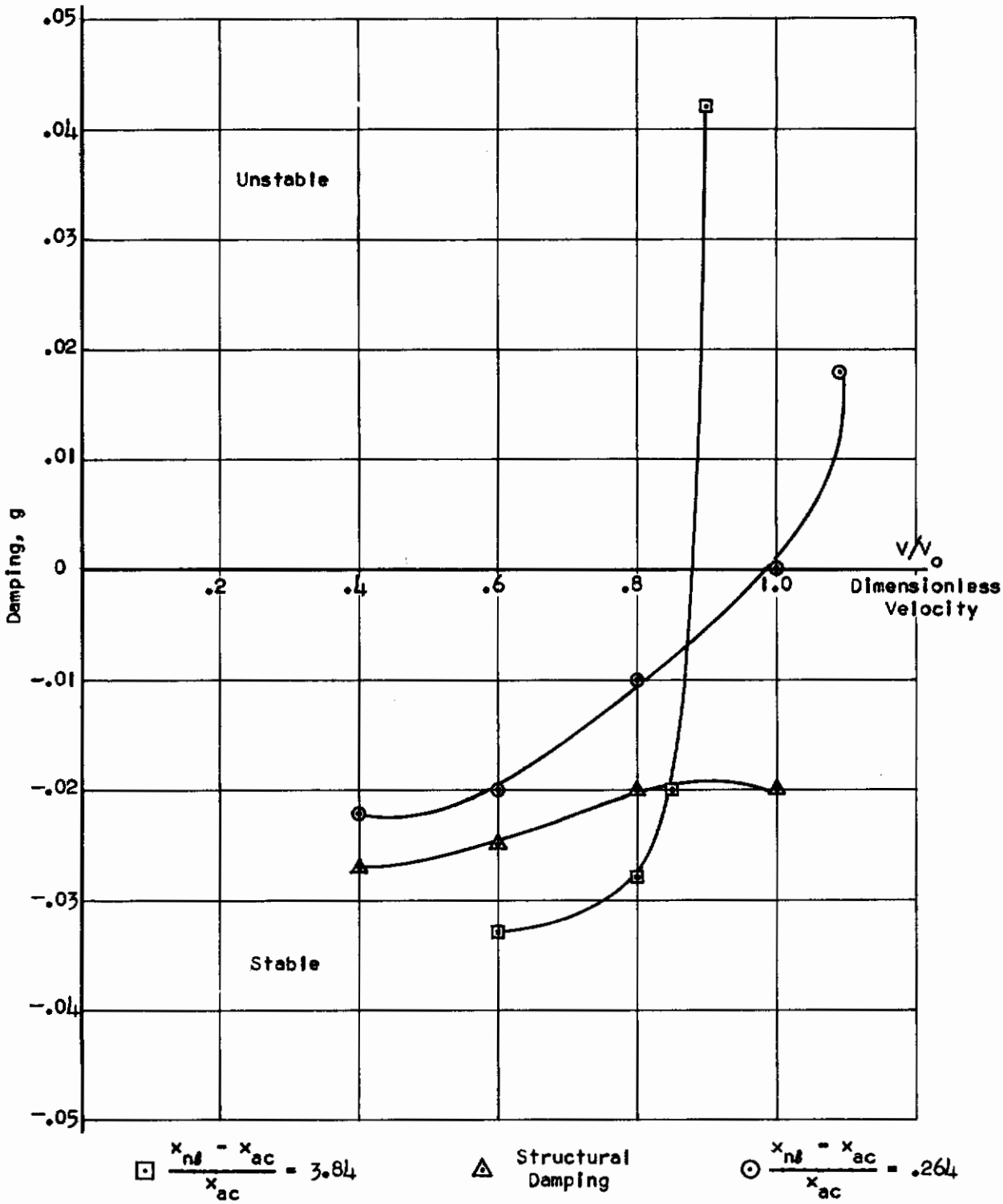

Figure 22. Effect of Parasitic Computer Damping Upon Neutral Stability Determination - Case 10

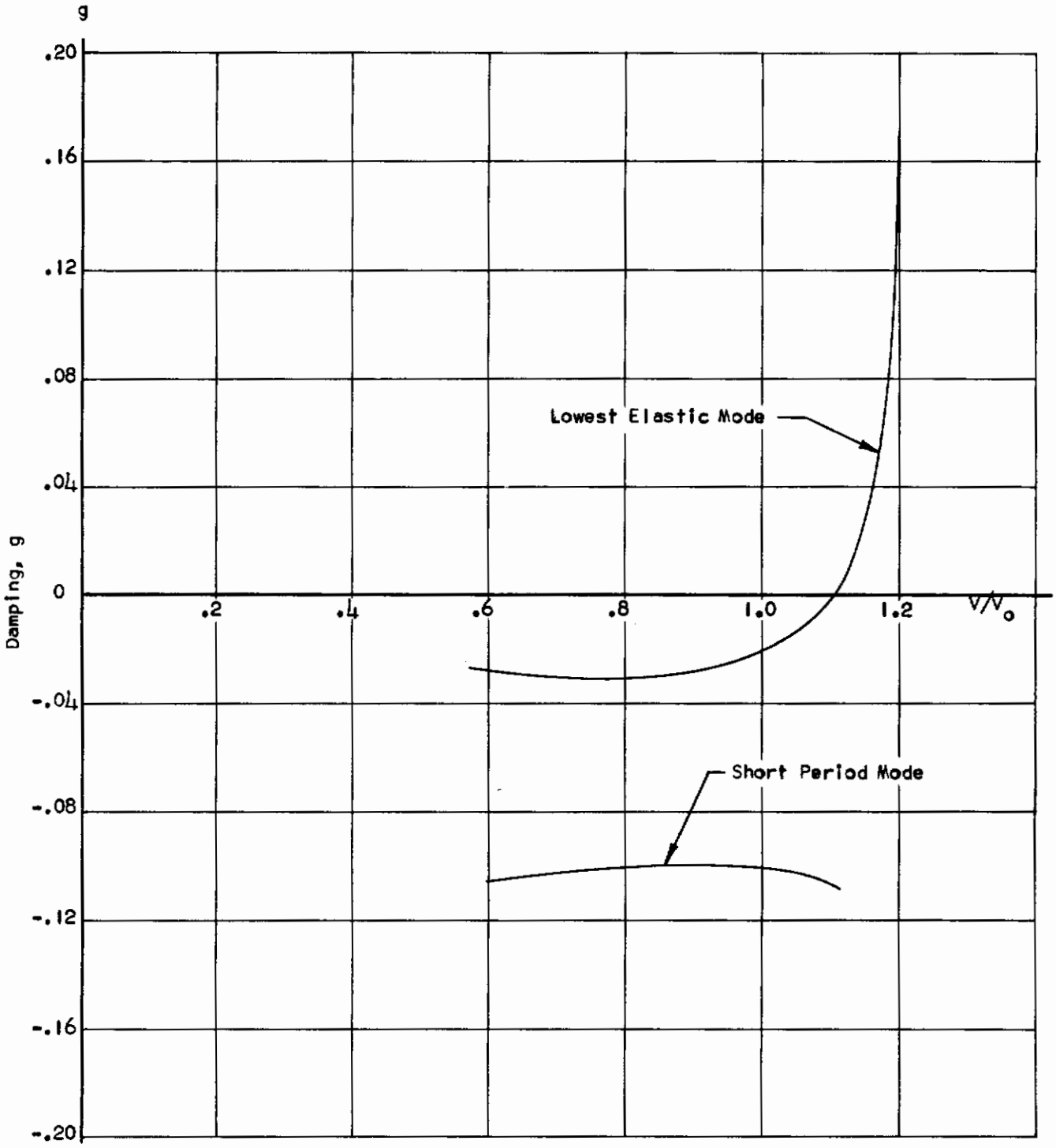

Figure 23. V-g Curve for Case 13

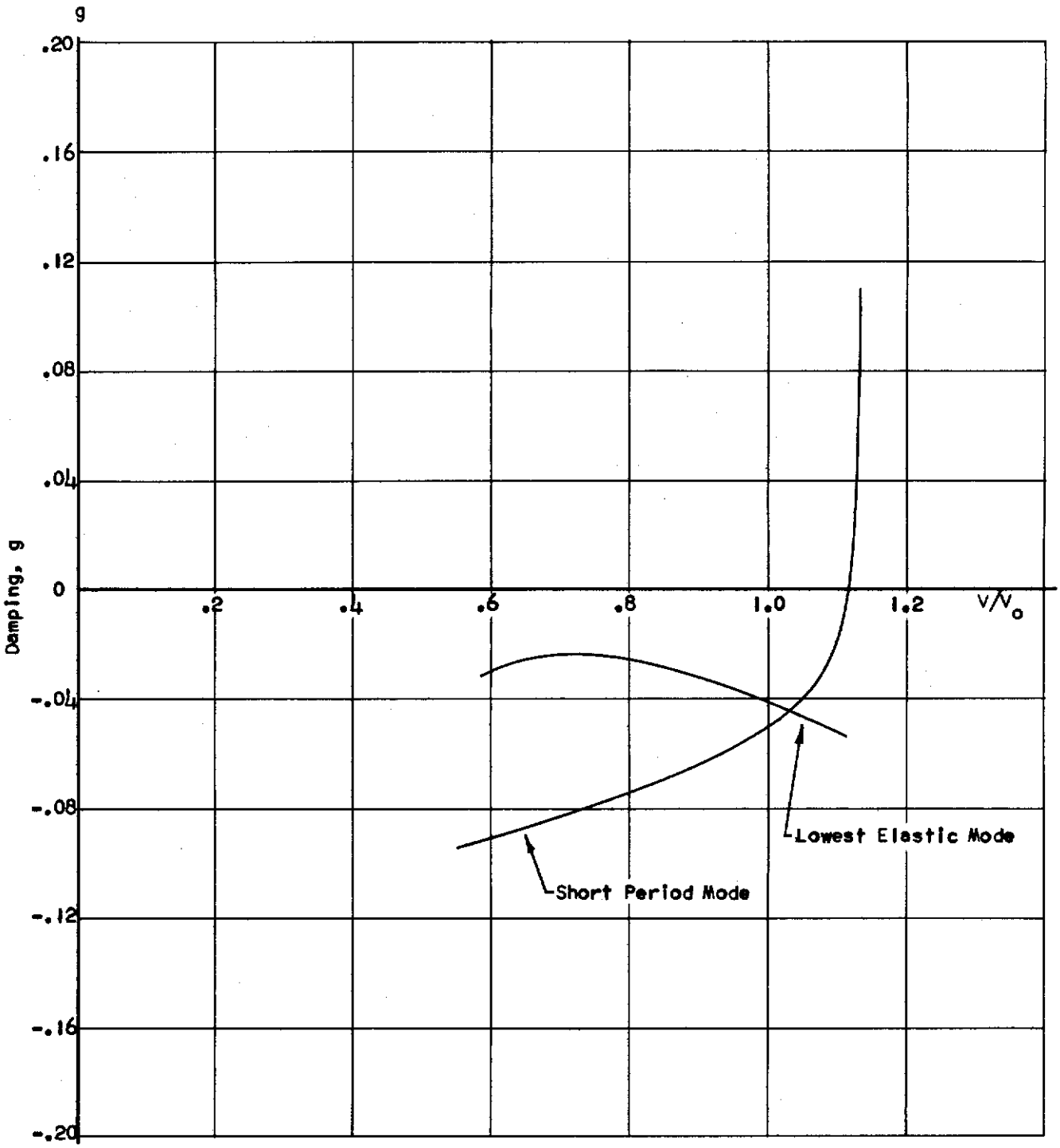

Figure 24. V-g Curve for Case 14

Table I. Mass Distribution for Configuration 2

Mass No. (Figure 20)	Station	Condition 30 Mass	Condition 31 Mass
	(in.)	lb.-sec.^{2}/in.	lb.-sec.^{2}/in.
1	0	4.728	4.728
2	50	18.911	18.911
3	150	18.911	18.911
4	250	31.605	31.605
5	350	56.734	18.911
6	450	82.122	27.374
7	550	94.816	31.605
8	650	94.816	31.605
9	750	51.812	17.270
10	900	51.812	17.270
11	1000	189.632	63.210
12	1100	45.854	15.285
13	1200	22.929	7.642
Forward Surface	250	1.554	1.554
Aft Surface	900	15.544	15.544
Pitching Mass Moment of Inertia			
		lb.-sec.^{2}-in.	lb.-sec.^{2}-in.
Forward Surface	250	155.4	155.4
Aft Surface	900	2487.	2487.

Table 2. Missile Configuration - Description of Cases

Case No.	Fuselage		Forward Surface		Aft Surface								Air Density	q/q_o at Flutter		
	Flexibility	Inertia	Position	Area	e.a. Station	e.a. Position in % Chord	a.c. Position in % Chord	Area	Plunge Inertia	Pitch Inertia	Plunge Flex.	Pitch Flex.		Measured	Calc. III	Calc. IV
1	Rigid	Basic	Off	- - -	900	50%	50%	Basic	Basic	Basic	Rigid	Basic	Basic	2.56	2.80	2.73
2				- - -					Basic	x 10	Rigid	Basic		1.66	2.80	2.24
3				- - -					Basic	Basic	Basic	Rigid		2.26	2.13	2.18
4				- - -					0	Basic	Basic	Rigid		2.26	2.13	
5				- - -		50%			Basic	0	Rigid	Basic		2.69	2.80	
6				- - -		60%				Basic	Rigid	Basic		1.11	1.19	1.22
7				- - -	900						Basic	Rigid		2.20	2.20	2.24
8				- - -	1200						Basic	Rigid		2.20	2.11	1.86
9				- - -	1200	60%	50%				Rigid	Basic		1.10	1.13	1.17
10				- - -		25%	25%				Rigid	Rigid	Basic			
11				- - -	900	50%	50%				Rigid	Basic	x .1	2.97		
12	Rigid			- - -						Basic	Basic	Rigid	x .1	2.53		
13	Basic			- - -						x .161	Rigid	Rigid	Basic	1.10		.586
14				- - -	900						Basic	Basic		1.12		
15				- - -	1000						Basic	Basic		1.16		
16	Basic	Basic	Off	- - -	1000	50%	50%	Basic	Basic	x .161	Rigid	Rigid	Basic	Stable		
18	Basic	Basic	Basic	Basic	900	50%	50%	Basic	Basic	x .161	Basic	Basic	Basic	1.18		
19	Basic	Basic	Basic	Basic	900	50%	50%	Basic	Basic	x .161	Rigid	Rigid	Basic	1.17		
22	Basic	Basic	Off	- - -	850	50%	50%	Basic	Basic	x .161	Rigid	Rigid	Basic	1.08		.546
23				- - -	850						Basic	Basic		1.09		.493
24				- - -	800						Basic	Basic		1.18		.549
25	Basic	Basic	Off	- - -	800	50%	50%	Basic	Basic	x .161	Rigid	Rigid	Basic	1.18		.920

VII. CONCLUSIONS

1. An accurate approximation for the aeroelastic behavior of a structure may be made in terms of its normal coordinates by including some of its modes explicitly and the "residual flexibility" approximation to all higher modes. This approximation for the system, derived in reference 1, is applicable in the presence of "mode interaction". This conclusion is drawn from the fact that "mode interaction" was found to depend on only the parameters listed in the foregoing approximation.

2. In the presence of "mode interaction," the accurate determination of "residual flexibility" is extremely important. In the presence of "mode interaction" the dynamics of a system can be very sensitive to slight changes in flexibility.

3. Systems which tend toward steady state divergence are particularly susceptible to "mode interaction."

4. In most free systems where steady state divergence is predicted to occur, a mode interaction or flutter instability will probably occur at a velocity lower than that predicted for steady state divergence.

5. Aerodynamic damping terms can have a destabilizing effect on a free system.

6. Aeroelastic systems which possess no finite frequency normal modes, can be susceptible to a finite frequency flutter instability.

7. A reliably accurate method for predicting the dynamic response of a general, free, aeroelastic system must include consideration of

    a. The rigid body modes of the system.

    b. The lowest elastic mode of the system.

    c. The "residual flexibility" of all higher modes.

    d. Aerodynamic damping.

    e. Structural damping.

8. Flutter analyses of free systems must include the zero frequency modes of the systems.

REFERENCES

1. Schwendler, R. G., and MacNeal, R. H., Optimum Structural Representation in Aeroelastic Analyses, ASD-TR-61-680, March, 1962.

2. Collar, A. R., The Expanding Domain of Aeroelasticity, Journal of the Royal Aeronautical Society, Volume 50, pp. 613-636, August, 1946.

3. Weiss, M. J., Higher Algebra for the Undergraduate, John Wiley and Sons, Inc., New York.

BIBLIOGRAPHY

1. Schwendler, R. G., and MacNeal, R. H., Optimum Structural Representation in Aeroelastic Analyses, ASD-TR-61-680, March, 1962.
2. MacNeal, Richard H., Electric Circuit Analogies for Elastic Structures, John Wiley and Sons, New York, 1962.
3. Collar, A. R., The Expanding Domain of Aeroelasticity, Journal of the Royal Aeronautical Society, Vol. 50, pp. 613-636, August, 1946.
4. MacNeal, R. H., Vibrations of Composite Systems, OSR TN-55-120, Air Research and Development Command Technical Report No. 4 under Contract No. AF18(600)-669, October, 1954.
5. Guillemin, E. A., The Mathematics of Circuit Analysis, Wiley and Sons, Inc., New York, 1949.
6. Hildebrand, F. B., Methods of Applied Mathematics, Prentice Hall, Inc., New York, 1952.
7. Pearce, B. F., Johnson, W. A., and Siskind, R. K., Analytical Study of Approximate Longitudinal Transfer Functions for a Flexible Airframe, Systems Technology Inc., ASD-TDR-62-279, June, 1962.
8. Jones, R. T., An Analysis of the Stability of an Airplane with Free Controls, NACA TR 709, 1941.
9. Serbin, H., Effect of Free Body Motion on Flutter, AFTR 5988, 1953.
10. Etkin, B., Dynamics of Flight, John Wiley and Sons, Inc., New York, 1959.
11. Hakkinen, R. J., and Richardson, A. S., Theoretical and Experimental Investigation of Random Gust Loads - Part I, NACA TN 3878, 1957.

12. Bisplinghoff, R. L., Ashley, H., and Halfman, R. L., Aeroelasticity, Addison-Wesley Publishing Co., Inc., Cambridge, Mass., 1955.

13. Cole, H. A., and Hollenan, E. C., Measured and Predicted Dynamic Response Characteristics of a Flexible Airplane to Elevator Control Over a Frequency Range Including Three Structural Modes, NACA TN 4147, 1958.

14. McCann, G. D., The Direct Analogy Electric Analog Computer, I. S. A. Journal, Instrument Society of America, April, 1956.

15. MacNeal, R. H., Direct Analog Method of Analysis of the Vertical Flight Dynamic Characteristics of the Lifting Rotor with Floating Hub, Journal of American Helicopter Society, Vol. 3, October, 1958.

16. Wilts, C. H., Aerodynamic Forces in Analog Computation, California Institute of Technology Computing Center Technical Report No. 116, September, 1959.

17. Cauer, W., Ein Reacktanztheorem, Sitz. d. Preuss. Akad der Wissen, Phys. Math., pp. 673-681, 1931.

18. MacNeal, R. H., and McCann, G. D., Ideal Transformers in the Synthesis of Analog Computer Circuits, Proceedings, Western Computer Conference, February, 1955.

19. MacNeal, R. H., McCann, G. D., and Wilts, C. H., The Solution of Aeroelastic Problems by Means of Electrical Analogies, Journal of Aero. Science, Vol. 18, December, 1951.

20. McCann, G. D., and MacNeal, R. H., Beam Vibration Analysis with the Electric Analog Computer, Journal of Applied Mechanics, Vol. 72, pp. 13-26, March, 1950.

21. Russell, W. T., and MacNeal, R. H., An Improved Electrical Analogy for the Analysis of Beams in Bending, Journal of Applied Mechanics, Vol. 20, p. 349, September, 1953.

22. Benscoter, S. U., and MacNeal, R. H., Equivalent Plate Theory for a Straight Multicell Wing, NACA TN 2786, September, 1952.

23. MacNeal, R. H., and Benscoter, S. U., Analysis of Multicell Delta Wings on Caltech Analog Computer, NACA TN 3114, January, 1954.

APPENDIX

STABILITY BOUNDARIES FOR AN AIRFRAME HAVING TWO RIGID BODY MODES AND ONE ELASTIC MODE

A brief summary of the analysis of section IV is first presented.

The aeroelastic system of Figure 25 is characterized by two rigid body modes and a single elastic mode. It is assumed that aerodynamic forces act only upon a rigid lifting surface and that these forces produce a lift and moment about the aerodynamic center which are given by

$$\begin{bmatrix} L \\ \hline M \end{bmatrix} = q\,S \left[\begin{array}{c|c} -C_{L_\alpha}\frac{s}{V} & C_{L_\alpha} + (1-2\bar{x})C_{L_\alpha}\frac{cs}{V} \\ \hline 0 & -C_{m_q}\frac{c^2 s}{V} \end{array}\right] \begin{bmatrix} z_{ac} \\ \hline \theta_{ac} \end{bmatrix}$$

where

$q = \frac{1}{2}\rho V^2$ is the dynamic pressure.

C_{L_α} is the lift coefficient.

$1 - 2\bar{x} = \frac{C_{L_q}}{C_{L_\alpha}}$ is the ratio of lift coefficient caused by pitch rate to the lift coefficient caused by angle of attack.

C_{m_q} is the pitch damping moment coefficient.

c is the chord length.

s is the Laplace transform differentiation operator $\left(s \sim \frac{d}{dt}\right)$.

The equations of motion for the system of Figure 25 can be written

$$m\ddot{z} = L$$

$$m r^2 \ddot{\theta} = M + x_{ac} L$$

$$m r_e^2(\ddot{\xi} + \omega_e^2 \xi) = M + (x_{ac} - x_{n\delta})L$$

and the motion of the lifting surface is related to the normal coordinates

z, θ, ξ as follows:

$$z_{ac} = z + x_{ac}\,\theta + (x_{ac} - x_{n\ell})\xi$$

$$\theta_{ac} = \theta + \xi$$

The symbols appearing in these equations have the following significance:

m is the total mass of the system (generalized mass of rigid plunge mode).

$m\,r^2$ is the total pitching inertia about the center of mass (generalized mass of rigid pitch mode).

$m\,r_e^2$ is the generalized mass of the elastic mode when the elastic mode shape is normalized by making the slope of the elastic mode unity at the node line.

ω_e^2 is the frequency of the elastic mode.

x_{ac} is the x-coordinate of the aerodynamic center relative to the coordinate system of Figure 25 (if the aerodynamic center is behind the center of mass, then x_{ac} will be negative).

$x_{n\ell}$ is the x-coordinate of the node line of the elastic mode (negative if the node line is behind the center of mass).

Analysis of the above system of equations produces the following results:

a. Let ω_o be a fictitious short period frequency defined by

$$\omega_o = \sqrt{-\frac{\left(\frac{1}{2}\rho V^2\right) S\, C_{L_\alpha}\, x_{ac}}{m\,r^2}} = V\sqrt{-\frac{\rho\, S\, C_{L_\alpha}\, x_{ac}}{2\,m\,r^2}}$$

Then the system is neutrally stable whenever the frequency ratio $\frac{\omega_o}{\omega_e}$

takes on the value given by

$$\left(\frac{\omega_o}{\omega_e}\right)^2 = \frac{a^2 - a}{ab - c}$$

where

$$a = \frac{1 + \left(\frac{r}{x_{ac}}\right)^2 - \frac{1 - 2\bar{x}}{\bar{x}_{ac}} + \frac{1}{\bar{x}_{ac}^2}\frac{C_{m_q}}{C_{L_\alpha}}}{1 + \left(\frac{r}{x_{ac}}\right)^2 - \frac{1 - 2\bar{x}}{\bar{x}_{ac}} + \frac{1}{\bar{x}_{ac}^2}\frac{C_{m_q}}{C_{L_\alpha}} + \frac{r^2}{r_e^2}\left[\left(\frac{x_{n\ell} - x_{ac}}{x_{ac}}\right)^2 + \left(\frac{x_{n\ell} - x_{ac}}{x_{ac}}\right)\left(\frac{1 - 2\bar{x}}{\bar{x}_{ac}}\right) + \frac{1}{\bar{x}_{ac}^2}\frac{C_{m_q}}{C_{L_\alpha}}\right]}$$

$$b = 1 - \frac{r^2}{r_e^2}\left(\frac{x_{n\ell} - x_{ac}}{x_{ac}}\right) - \frac{C_{m_q}}{2\mu\,\bar{x}_{ac}}\left[1 + \frac{r^2}{r_e^2}\left\langle 1 + \frac{\left(\frac{x_{n\ell} - x_{ac}}{x_{n\ell}} + 1\right)^2}{\left(\frac{r}{x_{ac}}\right)^2}\right\rangle\right]$$

$$c = 1 - \frac{C_{m_q}}{2\mu\,\bar{x}_{ac}}$$

b. As a corollary, it follows that the stability of the system of Figure 25 is determined by six parameters:

$$\frac{x_{n\ell} - x_{ac}}{x_{ac}}$$

$$\frac{r^2}{r_e^2} = R$$

$$\frac{r}{x_{ac}}$$

$$\frac{1 - 2\bar{x}}{\bar{x}_{ac}}$$

$$\frac{1}{\bar{x}_{ac}^2}\frac{C_{m_q}}{C_{L_\alpha}}$$

$$\frac{C_{m_q}}{\mu\,\bar{x}_{ac}}$$

The last of these parameters is much less important than the other five, and the first two parameters are decisive when the effects of damping are negligible.

c. If all damping terms are ignored in the equations of motion, then a frequency coalescence type of analysis can be applied, with the following result. Let ω_{ofc} be the value of ω_o at which the system is neutrally stable according to frequency coalescence. Then

$$\frac{\omega_{ofc}}{\omega_e} = \frac{1}{1 + \sqrt{R \frac{x_{n\ell} - x_{ac}}{x_{ac}}}}$$

In this case we see that the stability boundaries are especially simple, and only depend upon the first two of the six parameters listed above.

The above conclusions suggest the following as a reasonable approach to the construction of stability boundaries:

a. Plot $\frac{\omega_o}{\omega_{ofc}}$ versus the six parameters listed above. This mode of presentation has the advantage that the frequency coalescence solution appears as the straight line $\frac{\omega_o}{\omega_{ofc}} = 1$; thus, when the exact solutions deviate significantly from this line, we know that we are working in a regime where damping effects are significant. Since $\frac{\omega_o}{\omega_e} = \frac{\omega_o}{\omega_{ofc}} \frac{\omega_{ofc}}{\omega_e}$, it follows that the value of $\frac{\omega_o}{\omega_e}$ at neutral stability can be determined from $\frac{\omega_o}{\omega_{ofc}}$ provided that $\frac{\omega_{ofc}}{\omega_e}$ is plotted separately. The latter plot is extremely simple, since $\frac{\omega_{ofc}}{\omega_e}$ depends only upon two parameters, R and $\frac{x_{n\ell} - x_{ac}}{x_{ac}}$. Such a plot is presented in Figure 26.

Note that the velocity V corresponding to neutral stability can be found if the frequency of the elastic mode ω_e is known, since

$$\omega_o = \frac{\omega_o}{\omega_e}\,\omega_e \quad \text{and} \quad \omega_o = V\sqrt{-\frac{\rho S C_{L_\alpha} x_{ac}}{2m r^2}}$$

Note that ω_e is not a function of V, but is the frequency of the elastic mode in vacuo. If the frequency of instability ω is desired, it can be found from the equation

$$\left(\frac{\omega_e}{\omega}\right)^2 = 1 + \frac{r^2}{r_e^2}\,\frac{\left(\frac{x_{n\ell} - x_{ac}}{x_{ac}}\right)^2 + \frac{x_{n\ell} - x_{ac}}{x_{ac}}\,\frac{1 - 2\bar{x}}{\bar{x}_{ac}} + \frac{1}{\bar{x}_{ac}^2}\,\frac{C_{m_q}}{C_{L_\alpha}}}{1 + \left(\frac{r}{x_{ac}}\right)^2 - \frac{1}{\bar{x}_{ac}}\,\frac{1 - 2\bar{x}}{\bar{x}_{ac}} + \frac{1}{\bar{x}_{ac}^2}\,\frac{C_{m_q}}{C_{L_\alpha}}}$$

b. The three parameters $R = \frac{r^2}{r_e^2}$, $\frac{x_{n\ell} - x_{ac}}{x_{ac}}$, and $\frac{r}{x_{ac}}$ are important, and wide variation of these parameters must be taken into account. We need only consider negative values of x_{ac}, since otherwise the system is statically unstable.

c. The ratios of aerodynamic coefficients, $(1 - 2\bar{x})$ and $\frac{C_{m_q}}{C_{L_\alpha}}$, will be allowed to take on values characteristic of subsonic and supersonic conditions. Thus, for subsonic flow (Figures 27 through 35)

$$1 - 2\bar{x} = .5$$

$$\frac{C_{m_q}}{C_{L_\alpha}} = .0625$$

$$C_{L_\alpha} = 6.28$$

and for supersonic flow (Figures 36 through 44)

$$1 - 2\bar{x} = 0$$

$$\frac{C_{m_q}}{C_{L_\alpha}} = .0625$$

$$C_{L_\alpha} = 1.5$$

If we then allow $\bar{x}_{ac} = \frac{x_{ac}}{c}$ to vary over reasonable ranges, we obtain practical ranges for the aerodynamic stability parameters

$$\frac{1 - 2\bar{x}}{\bar{x}_{ac}}$$

$$\frac{1}{\bar{x}_{ac}^2} \frac{C_{m_q}}{C_{L_\alpha}}$$

d. The parameter $\frac{C_{m_q}}{\mu \bar{x}_{ac}}$ is not an important one for vehicles moving in air, since the mass parameter

$$\mu = \frac{m}{\rho S c}$$

is apt to be very large and $\bar{x}_{ac}$ will not be zero for statically stable vehicles. Thus, it suffices to choose a single value for μ ($\mu = 100$). The procedure of c above then determines the range of the parameter $\frac{C_{m_q}}{\mu \bar{x}_{ac}}$. Figure 45 shows that the effect of varying $\frac{C_{m_q}}{\mu \bar{x}_{ac}}$ by a factor of 100 produces less than 7% variation in $\frac{\omega_o}{\omega_{ofc}}$, except at points near $\frac{x_{n\ell} - x_{ac}}{x_{ac}} = 0$.

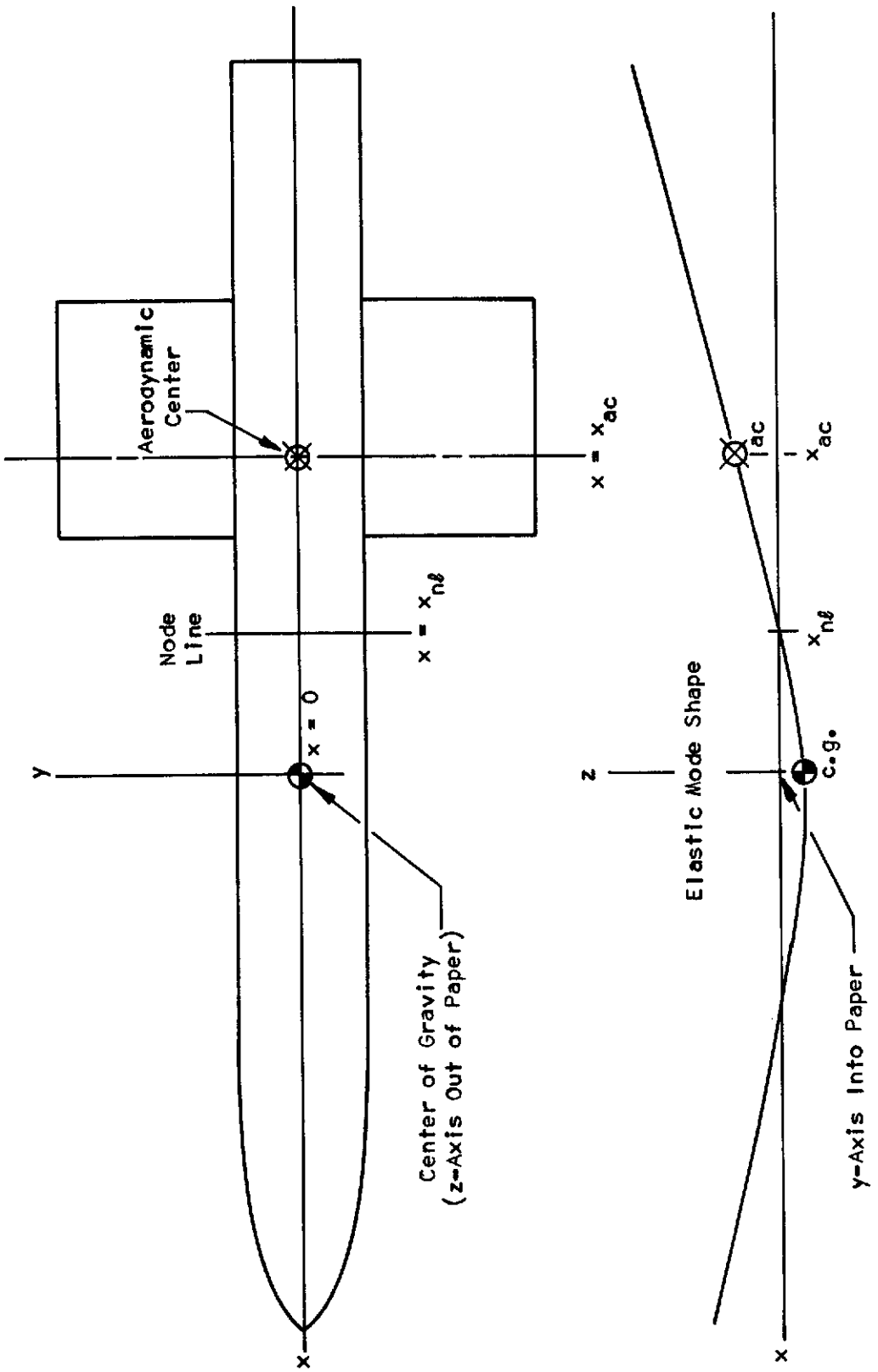

Figure 25. Flexible Airframe With a Rigid Lifting Surface

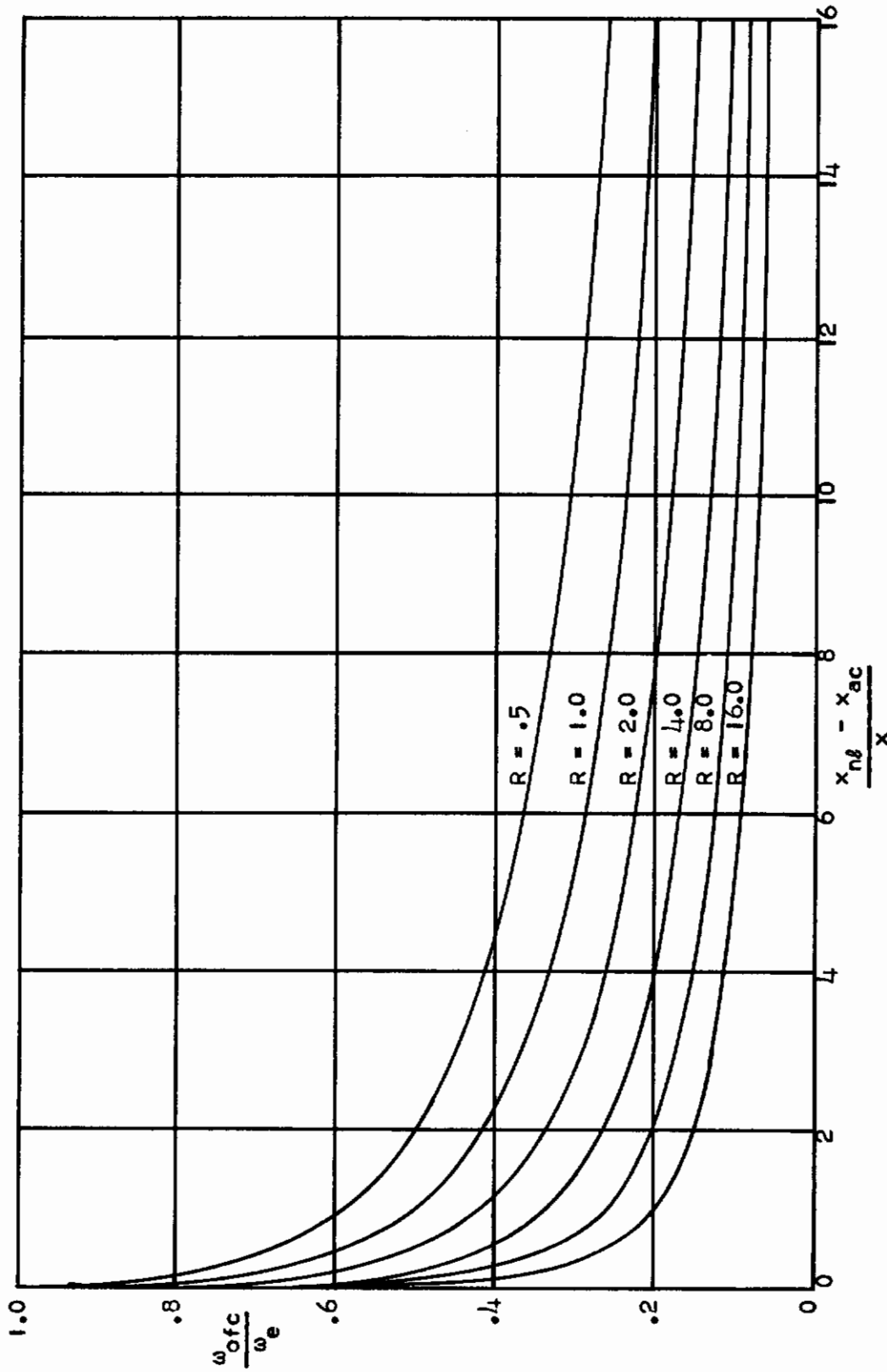

Figure 26. Frequency Coalescence Solution

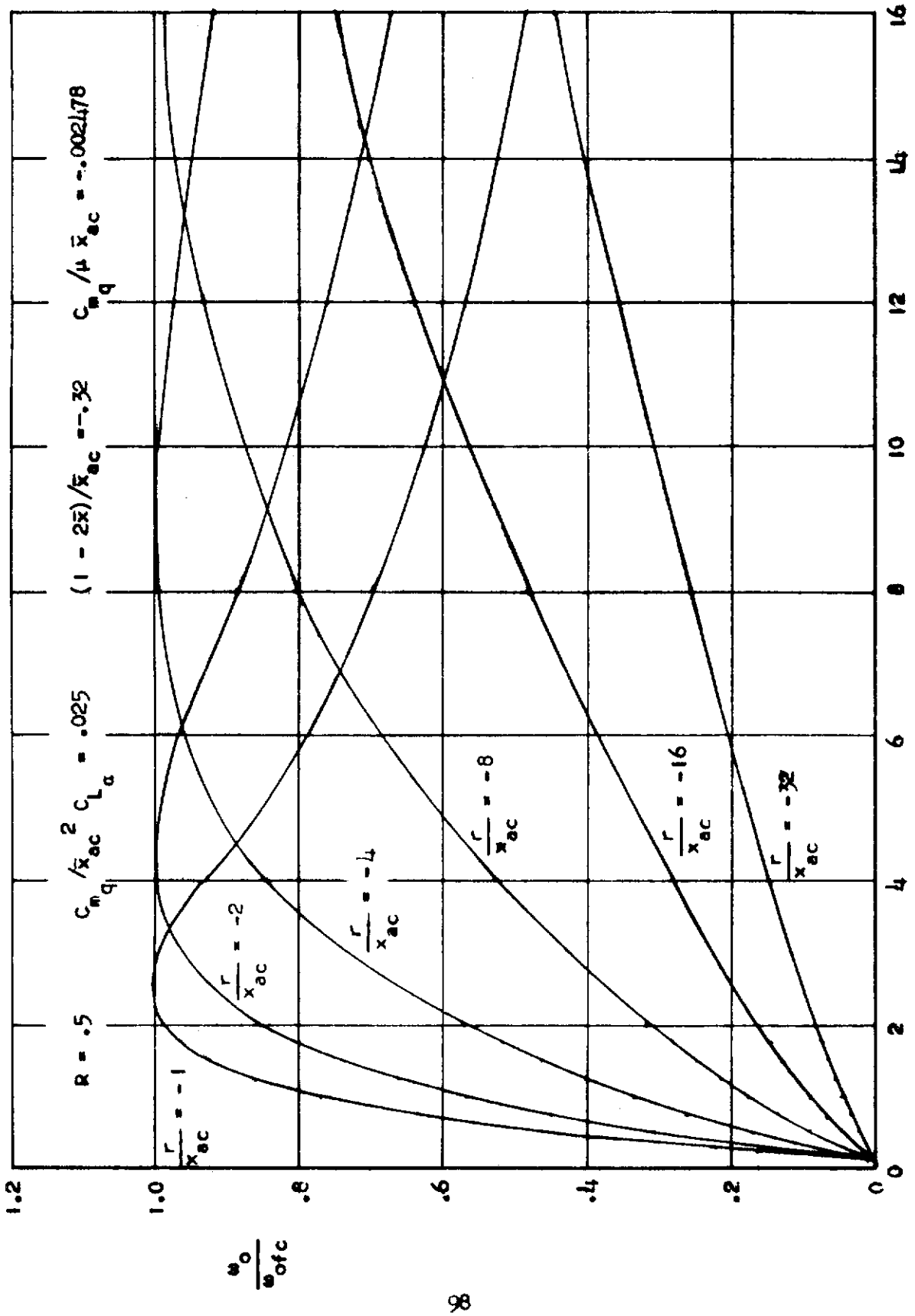

Figure 27. Frequency Coalescence Solution

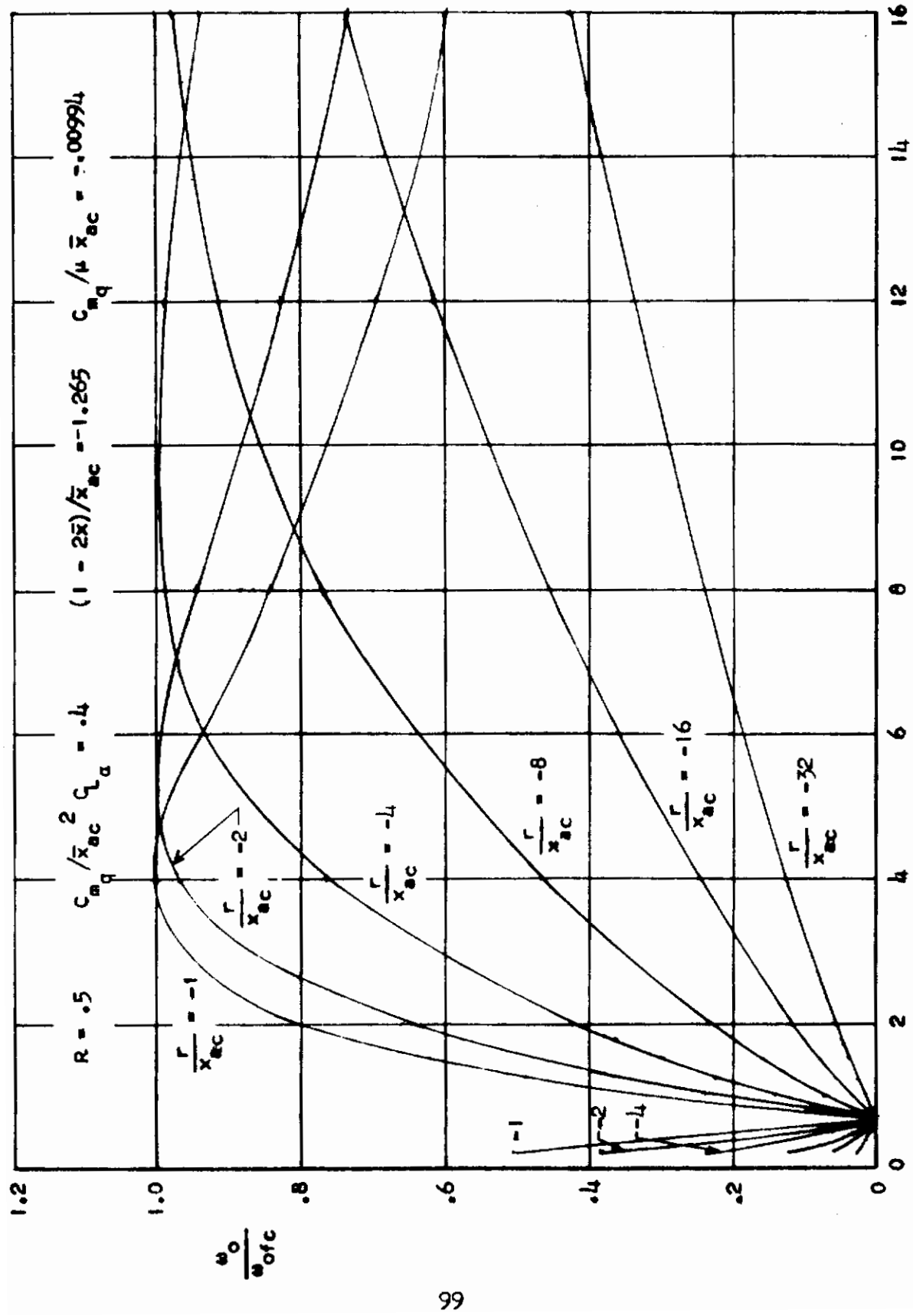

Figure 28. Frequency Coalescence Solution

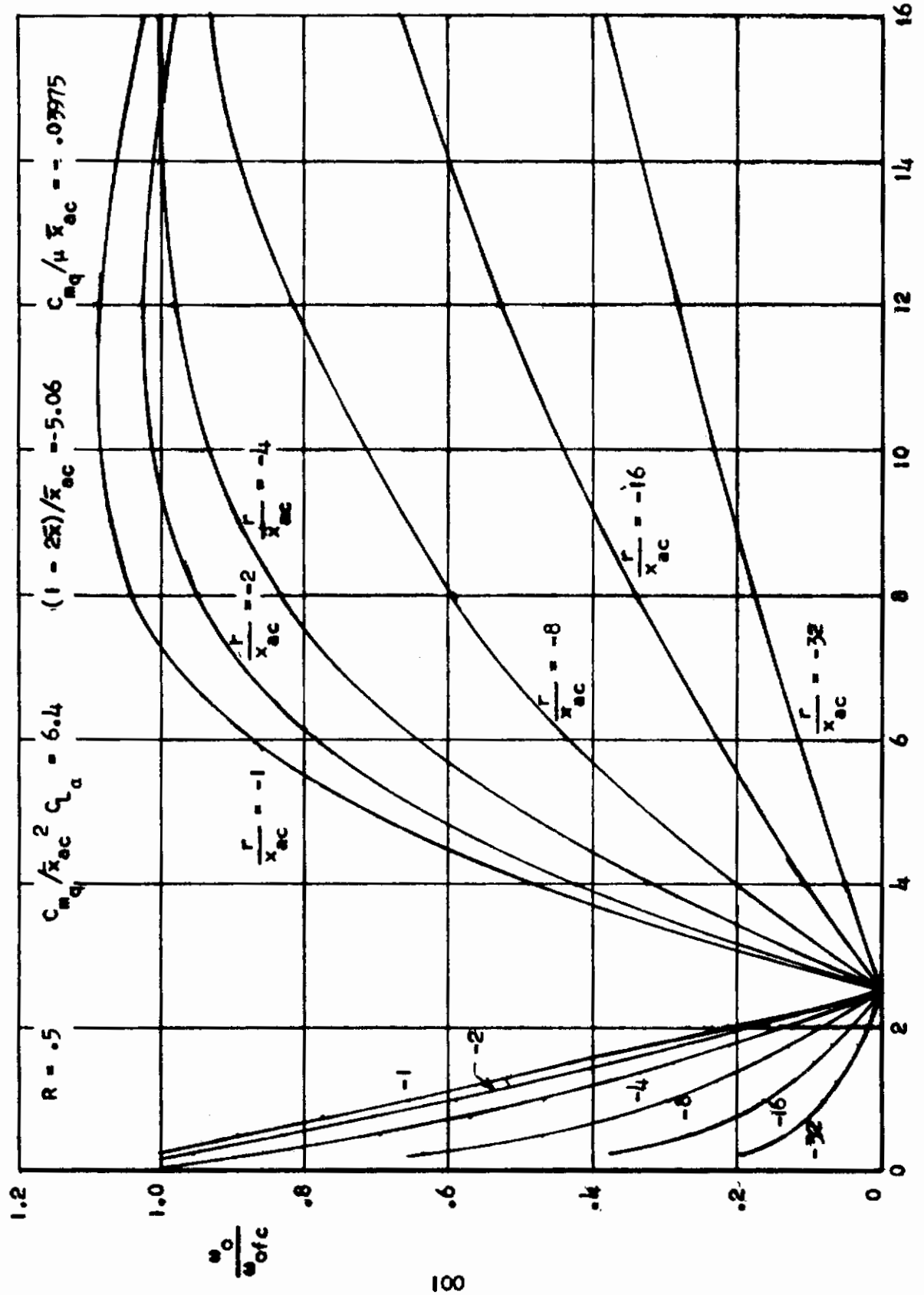

Figure 29. Frequency Coalescence Solution

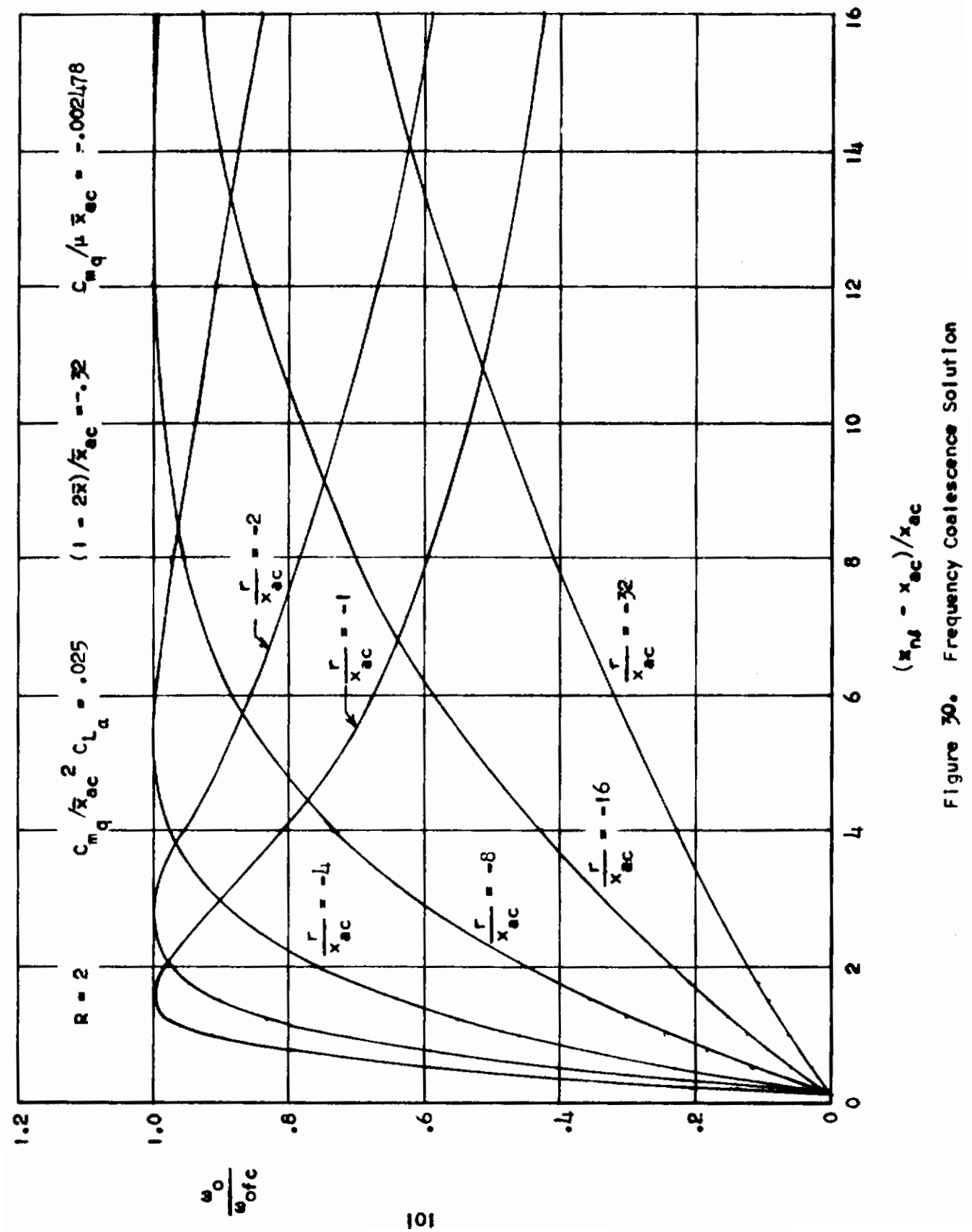

Figure 30. Frequency Coalescence Solution

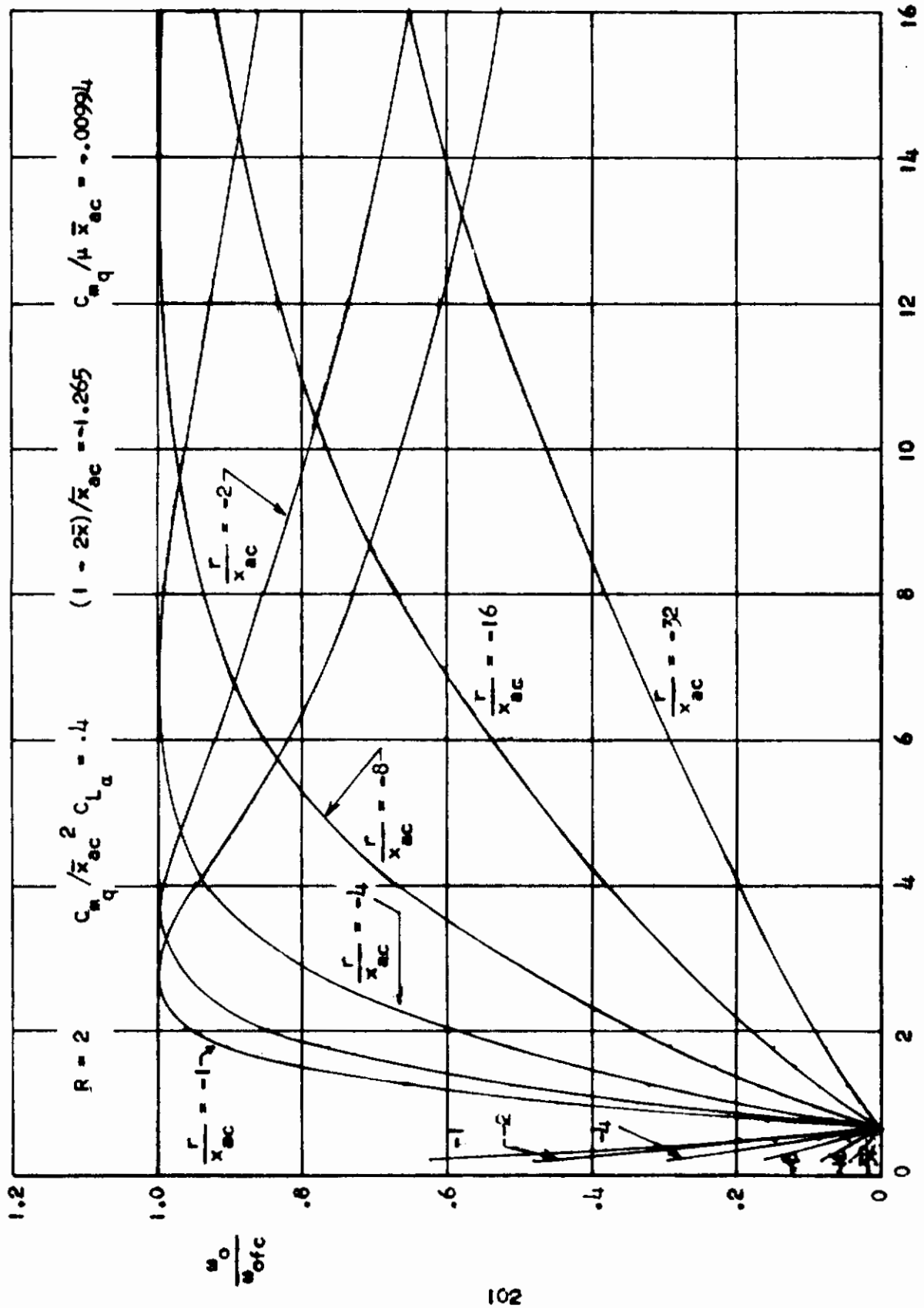

Figure 31. Frequency Coalescence Solution

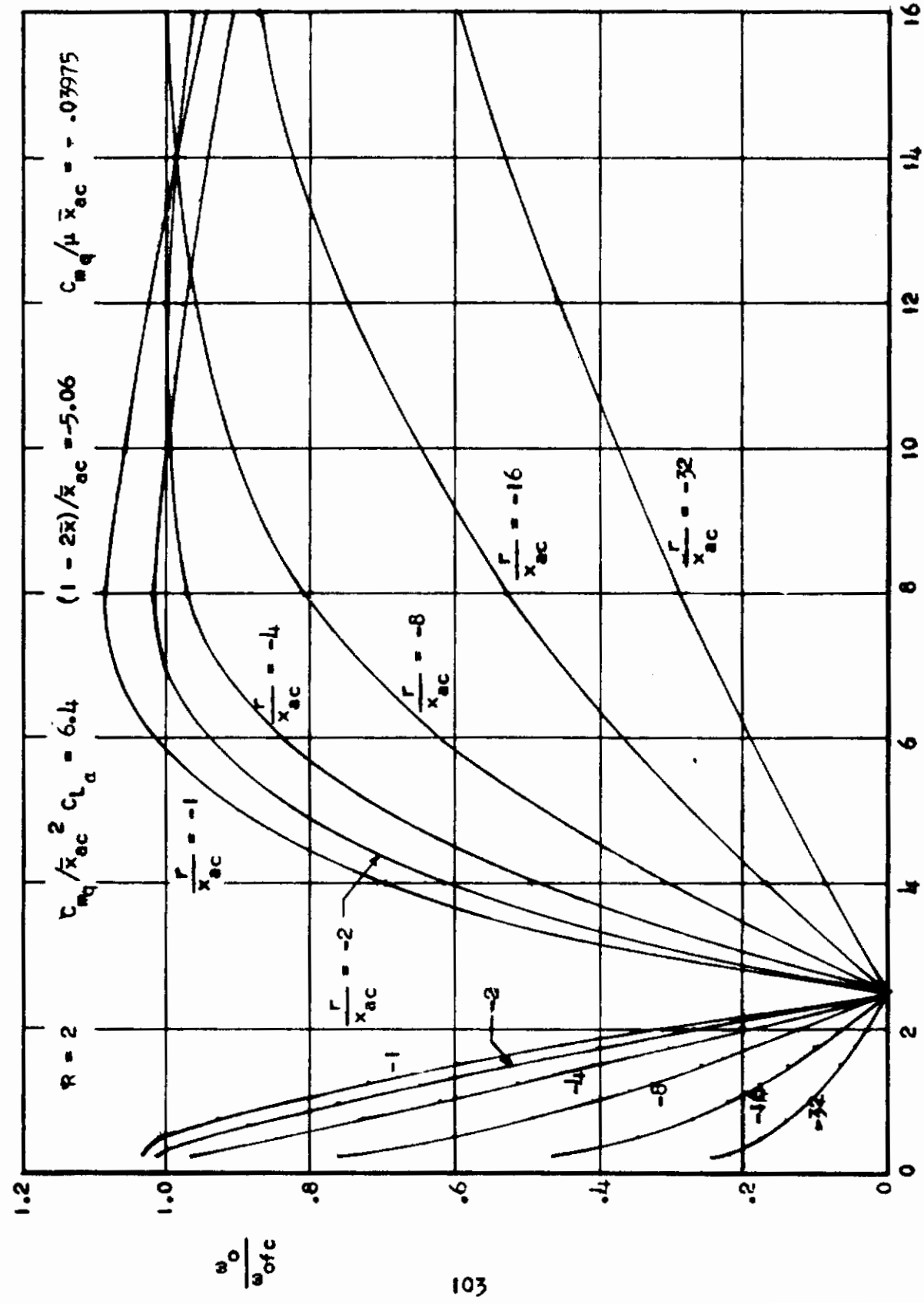

Figure 32. Frequency Coalescence Solution

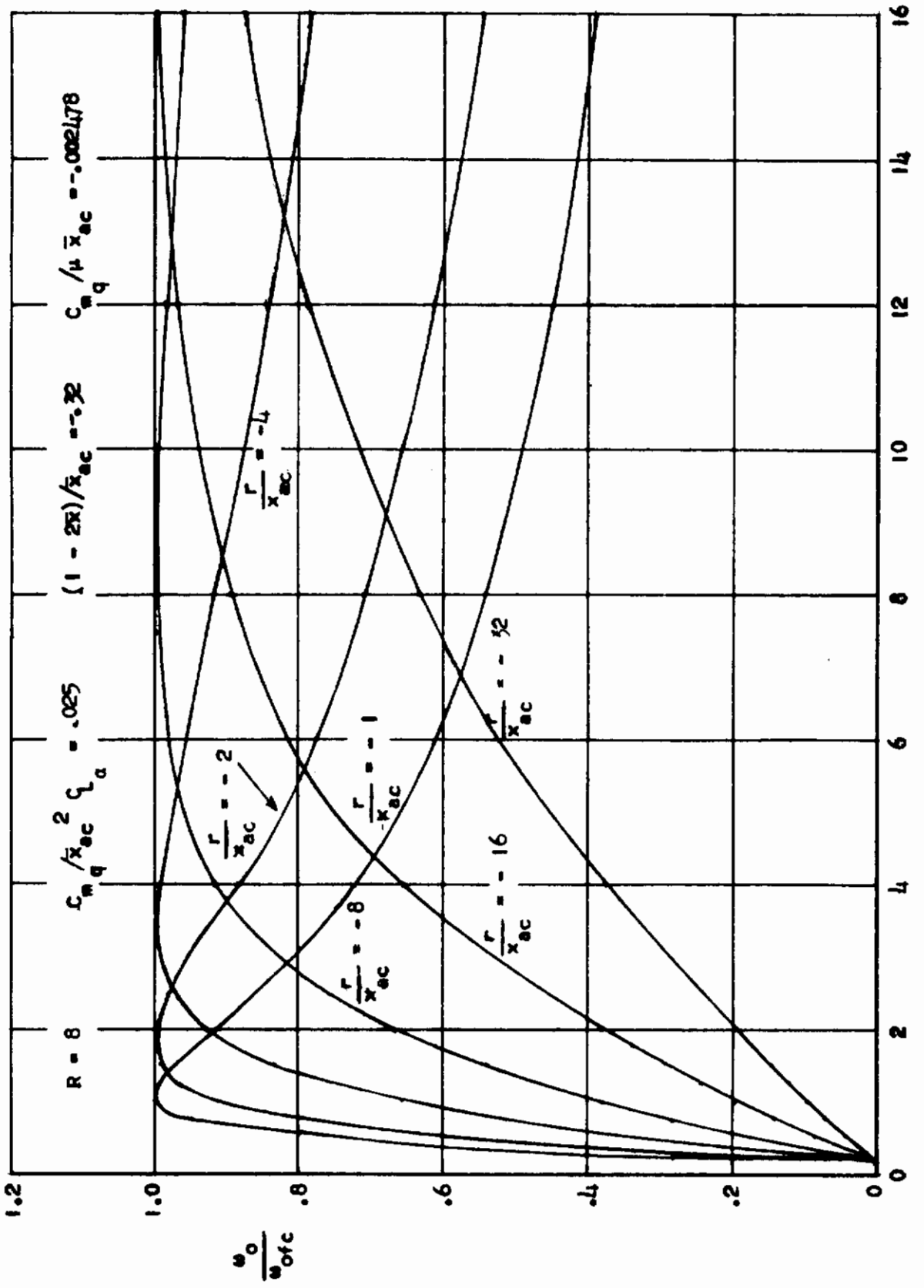

Figure 33. Frequency Coalescence Solution

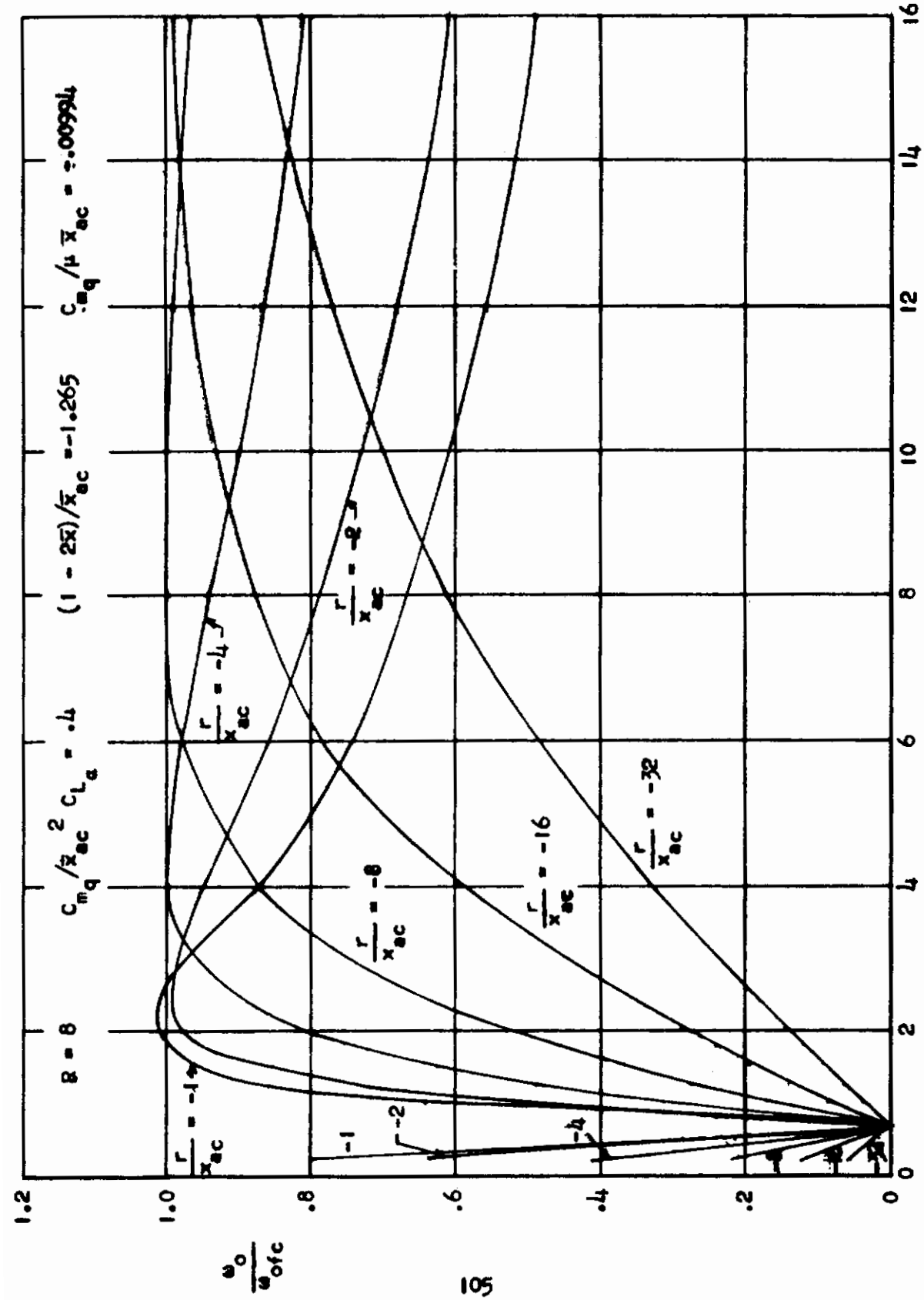

Figure 34. Frequency Coalescence Solution

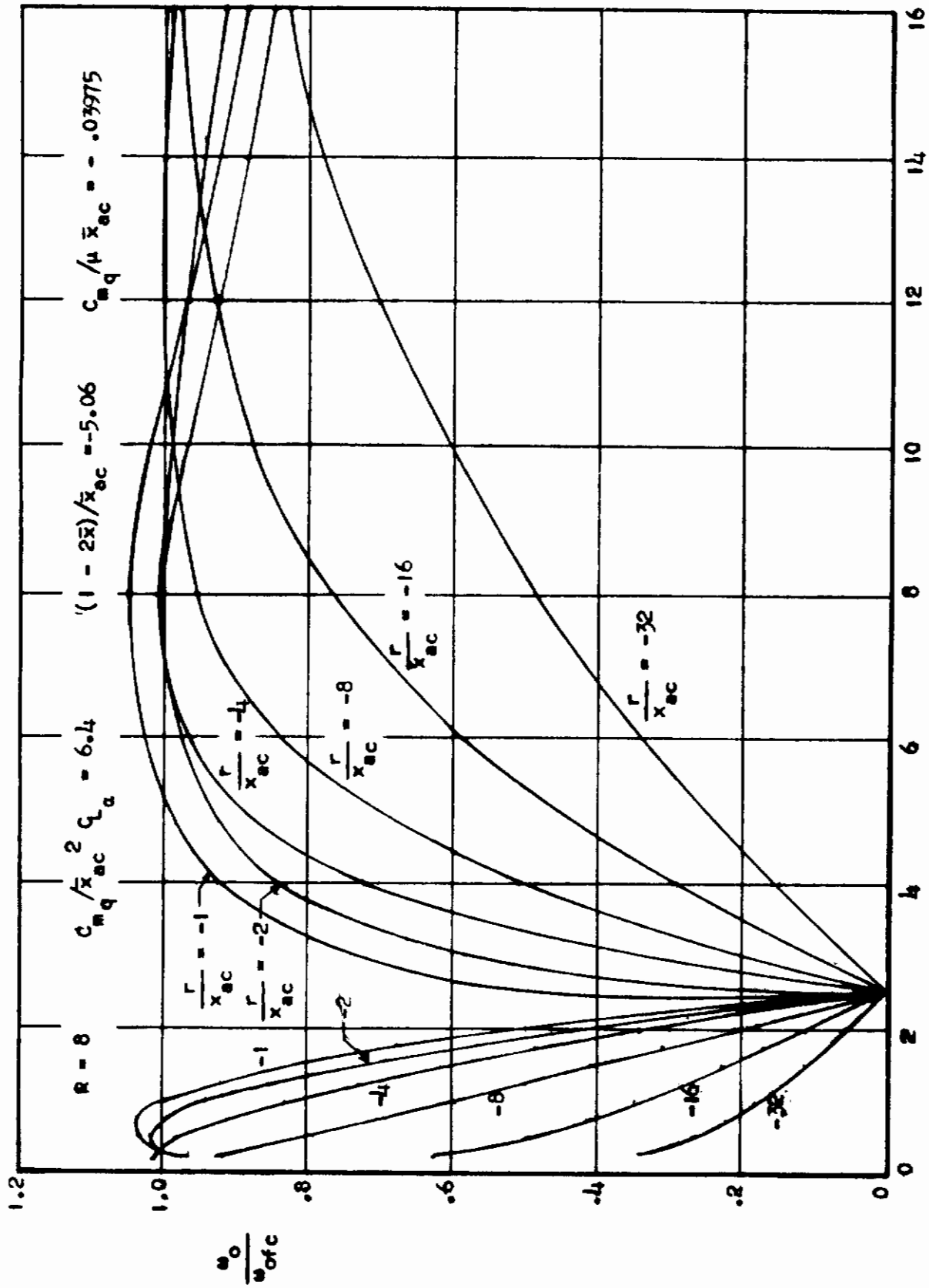

Figure 35. Frequency Coalescence Solution

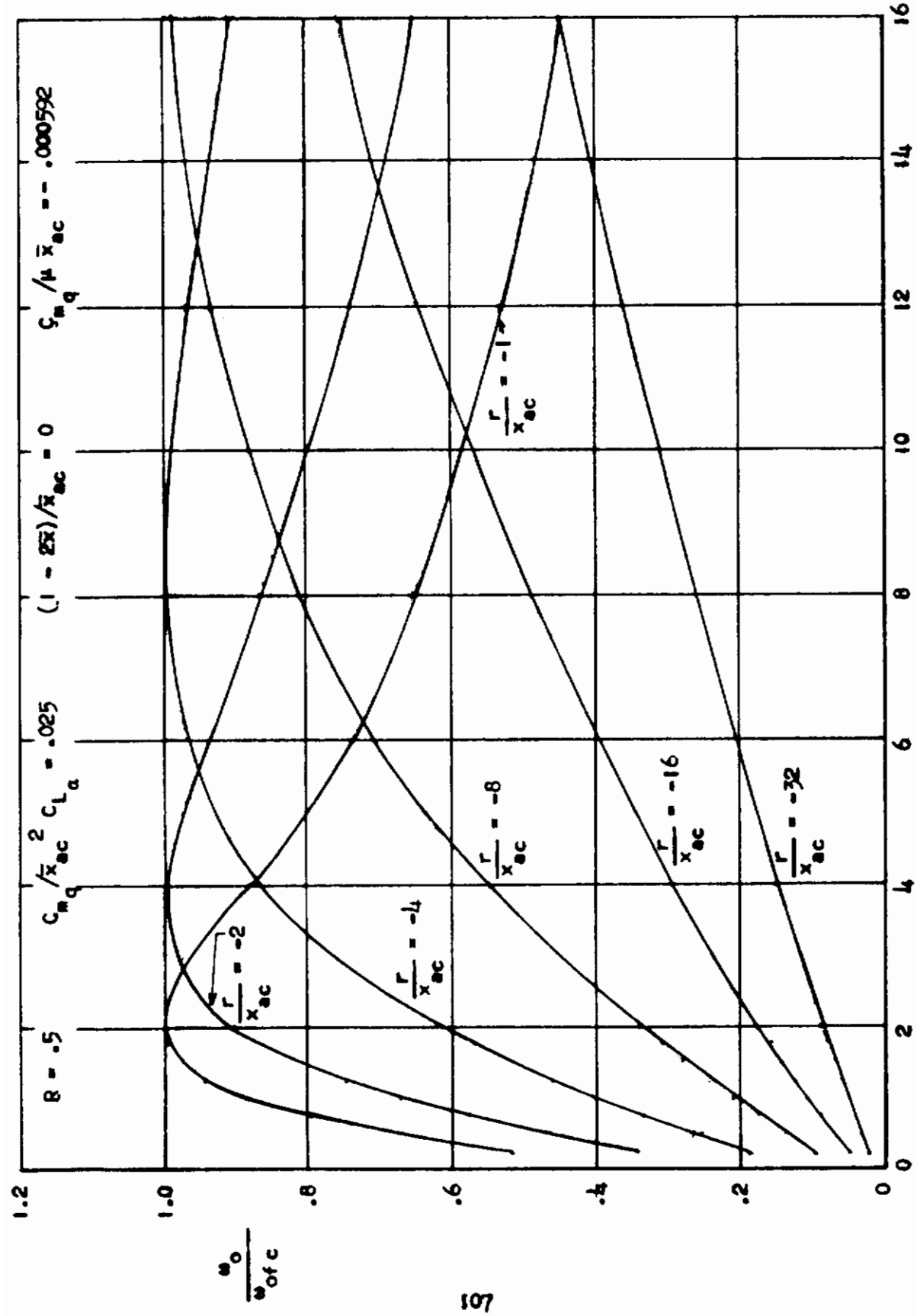

Figure 36. Frequency Coalescence Solution

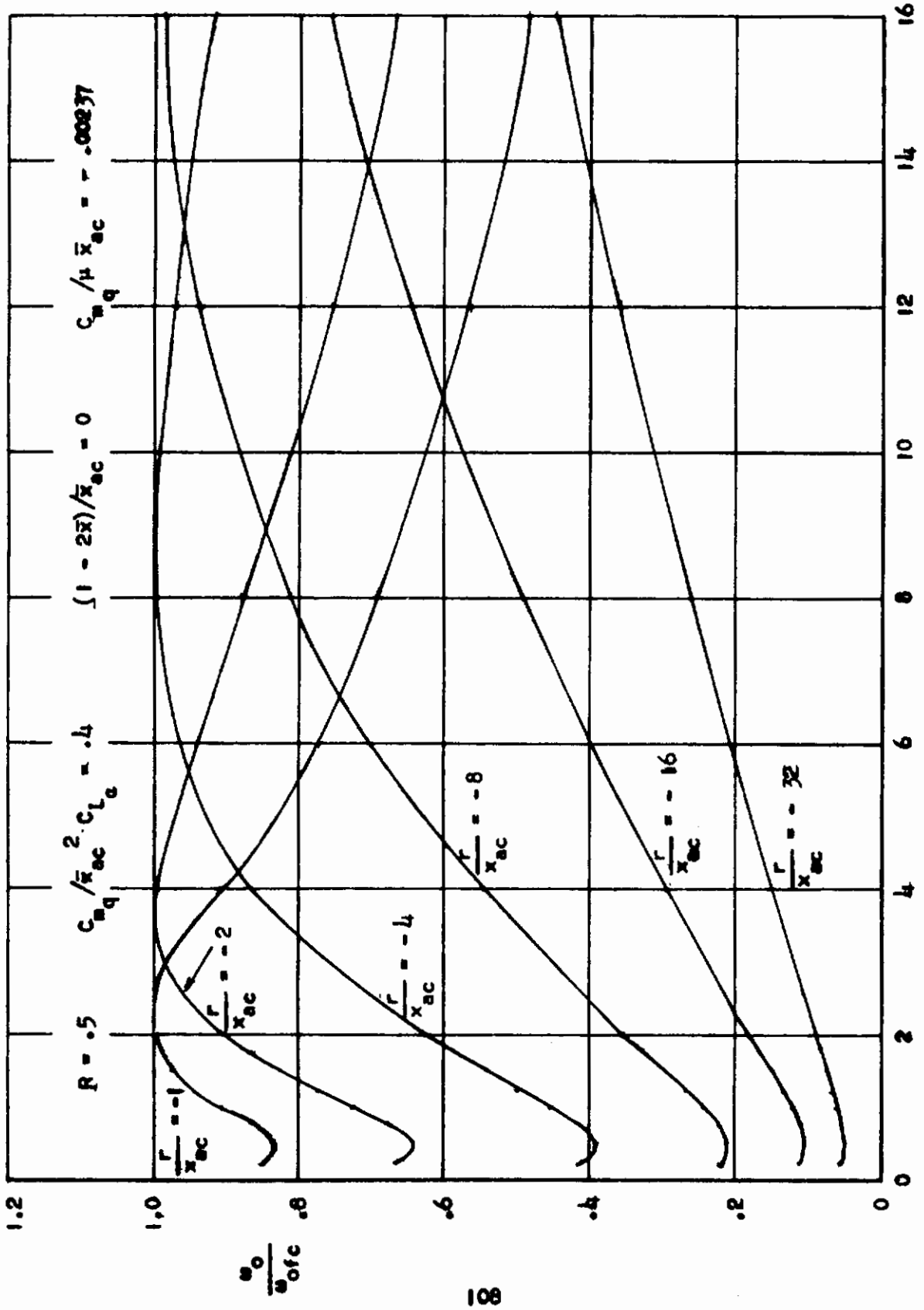

Figure 37. Frequency Coalescence Solution

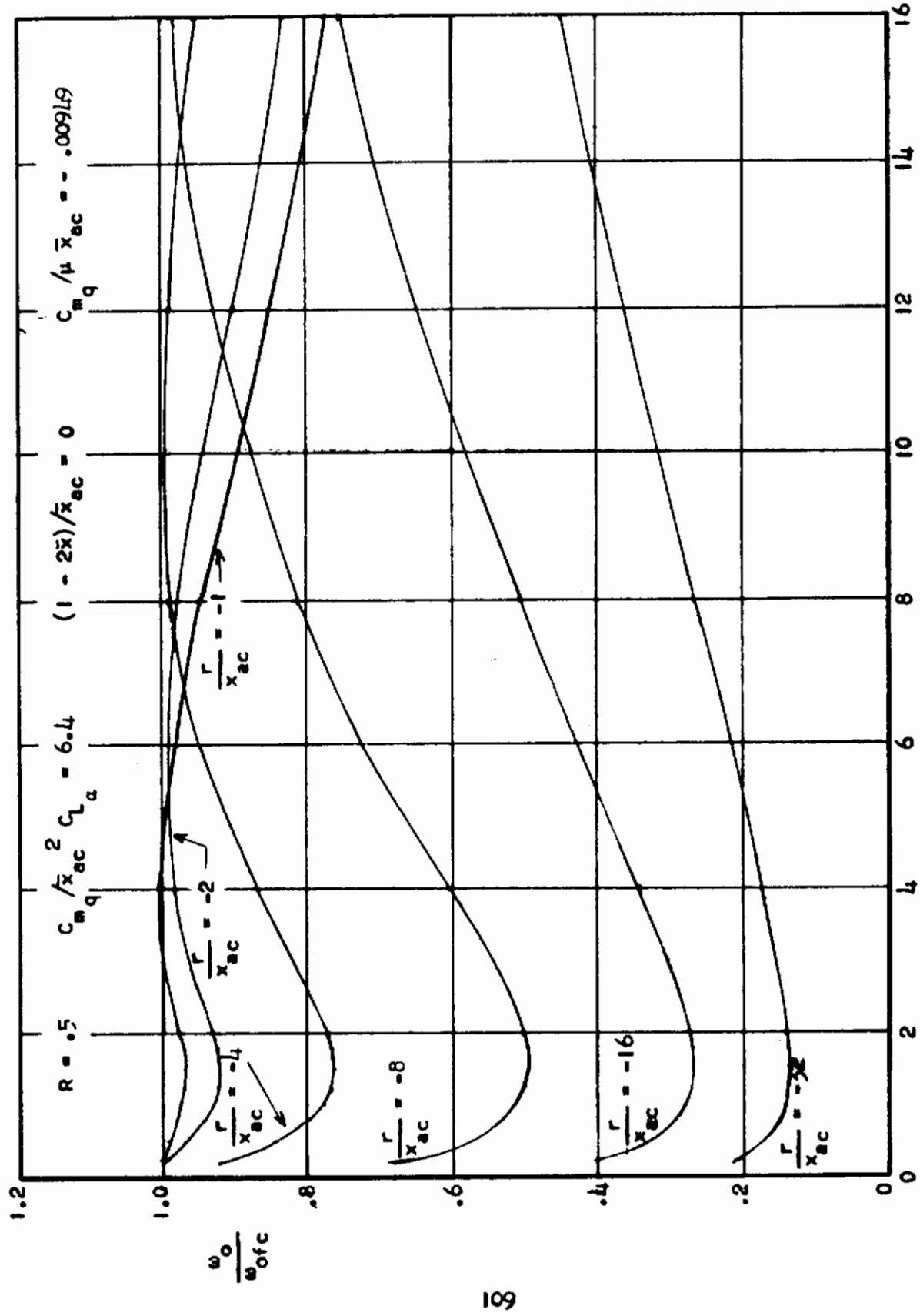

Figure 38. Frequency Coalescence Solution

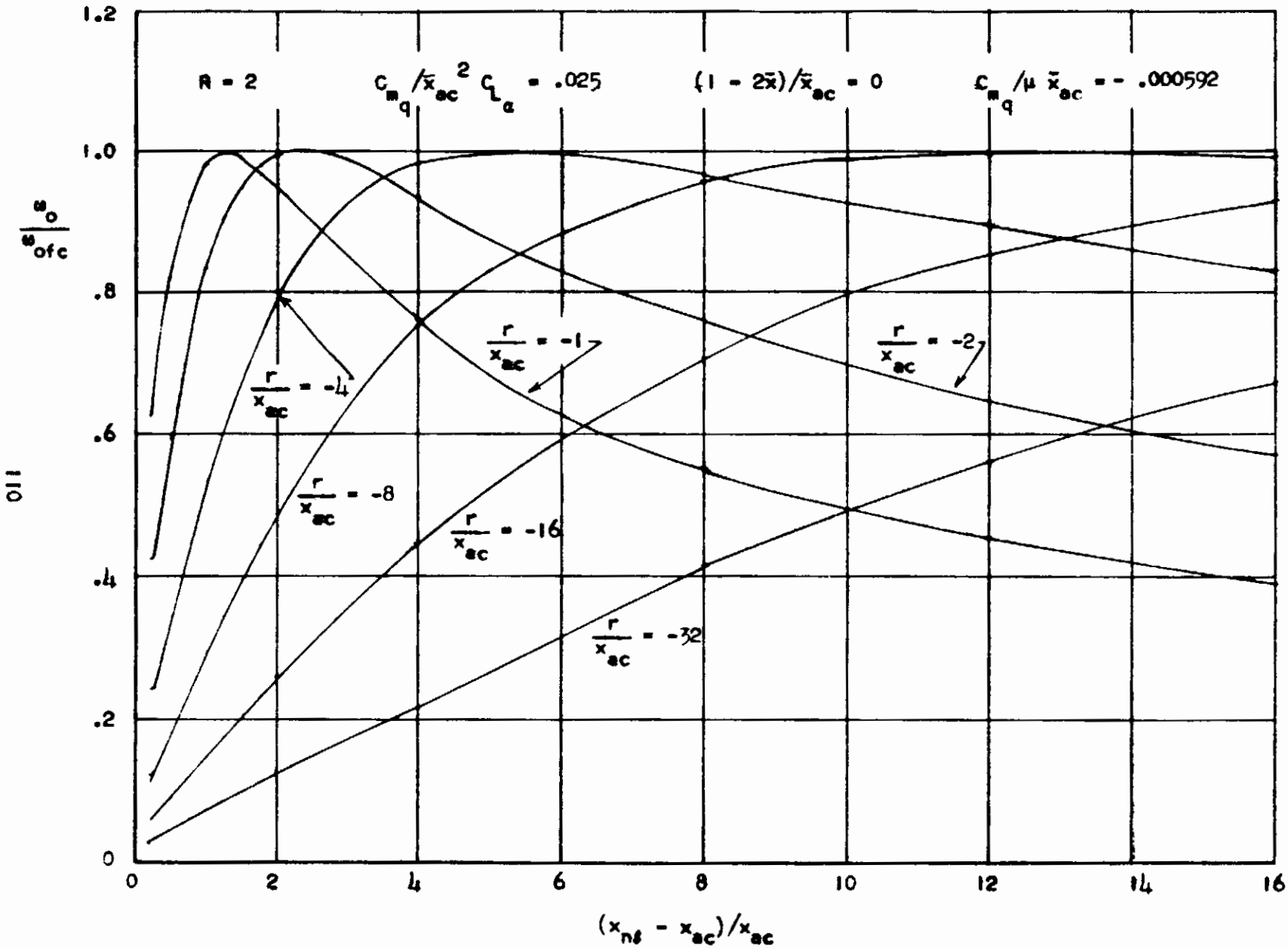

Figure 39. Frequency Coalescence Solution

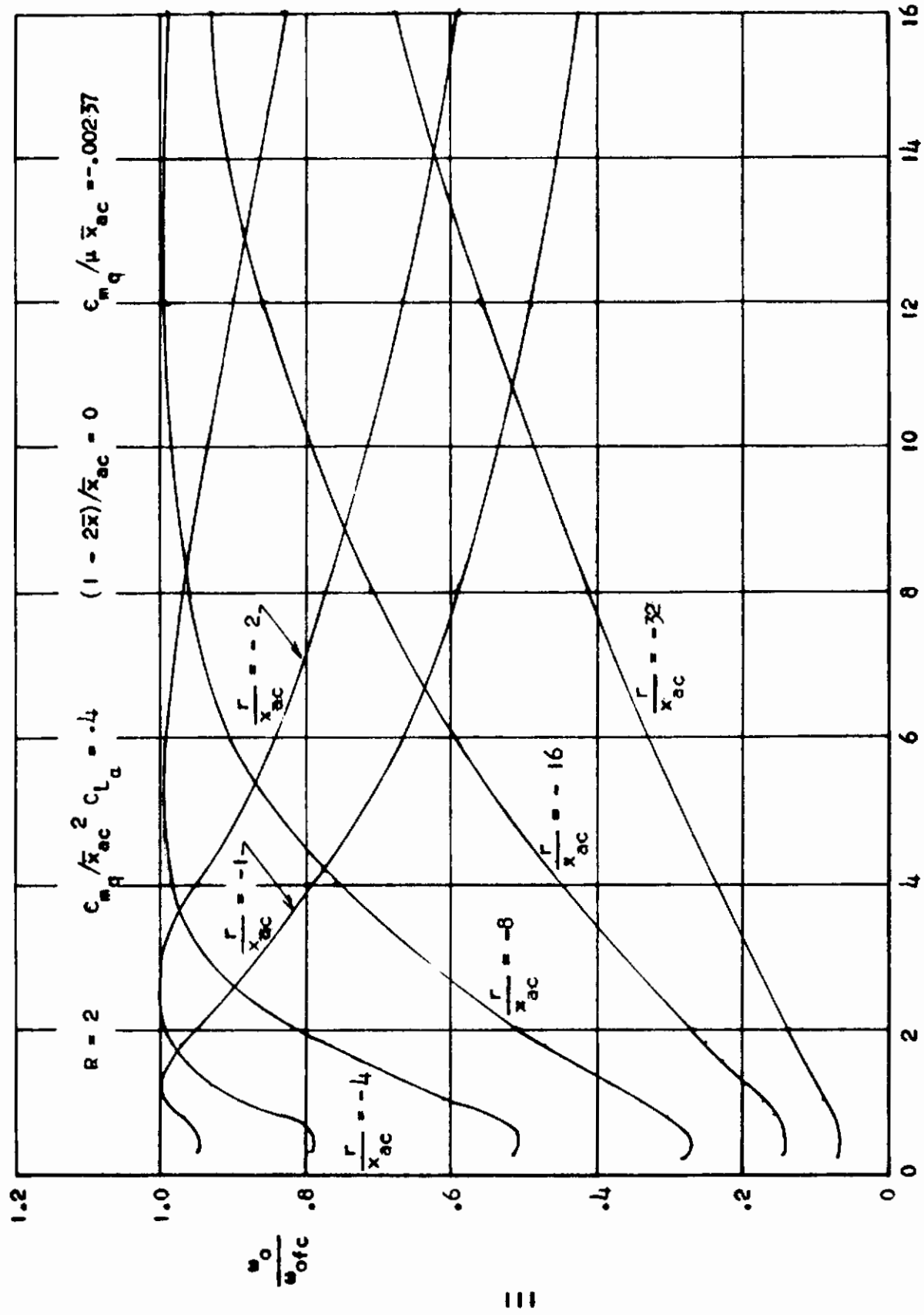

Figure 40. Frequency Coalescence Solution

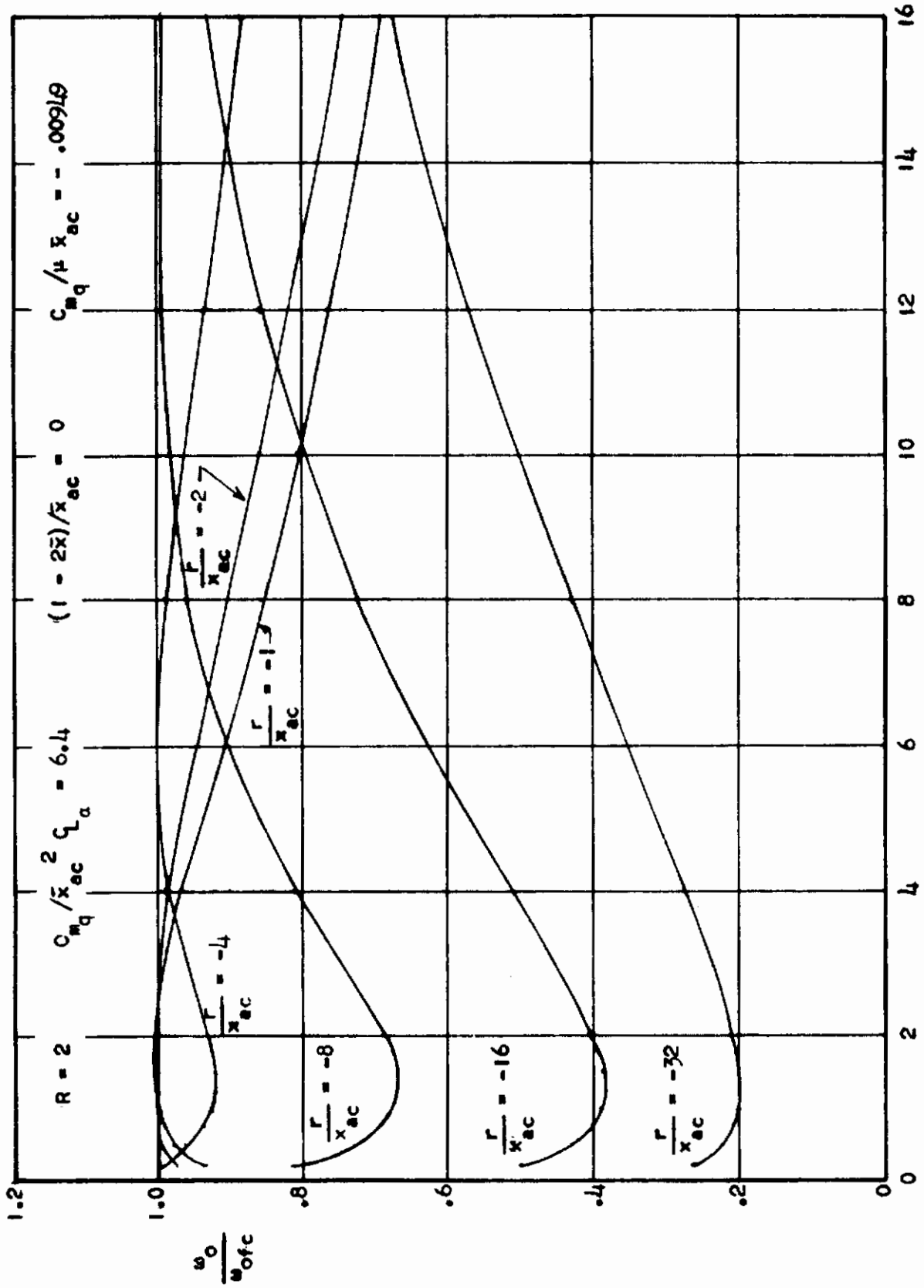

Figure 41. Frequency Coalescence Solution

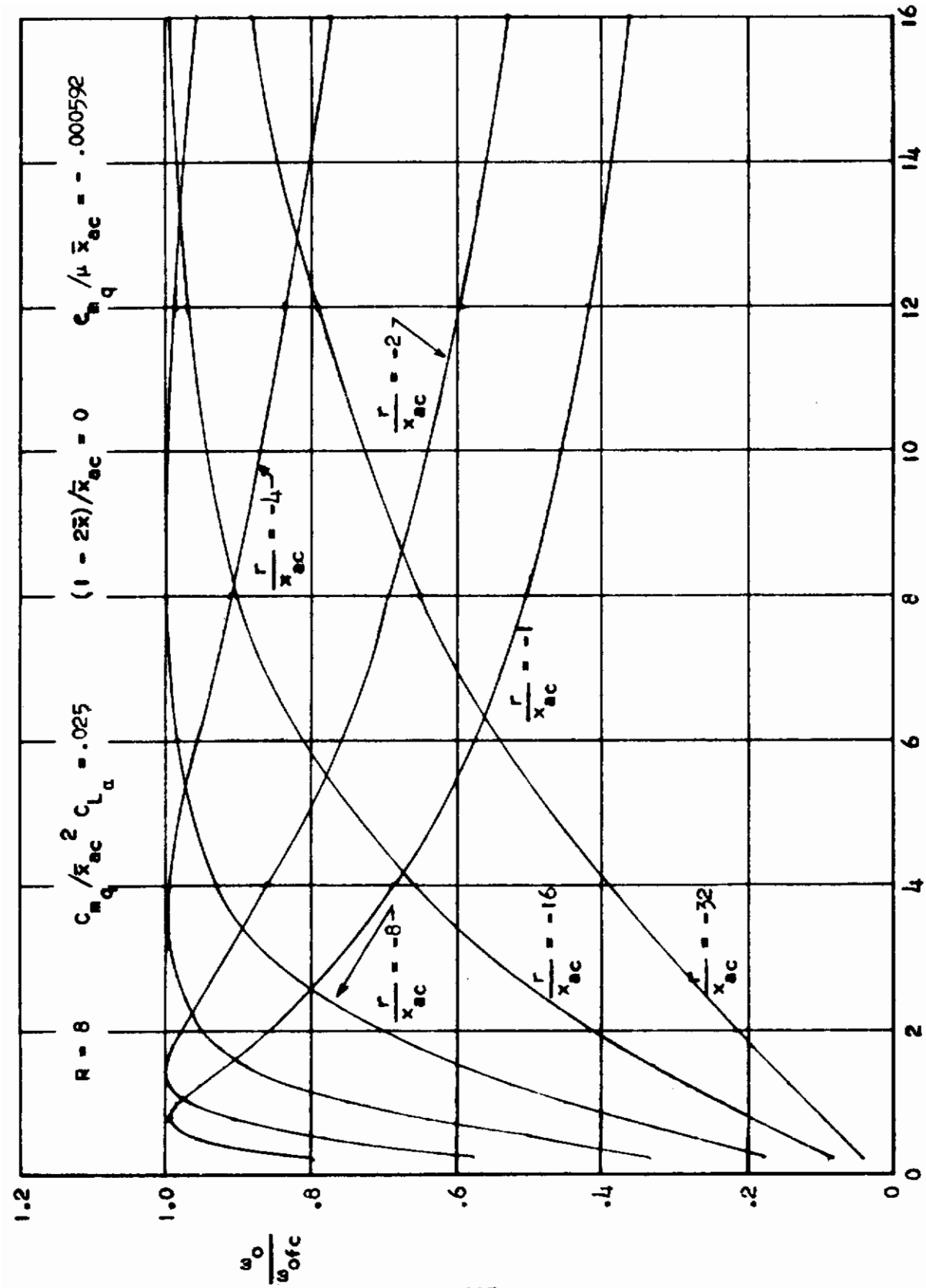

Figure 42. Frequency Coalescence Solution

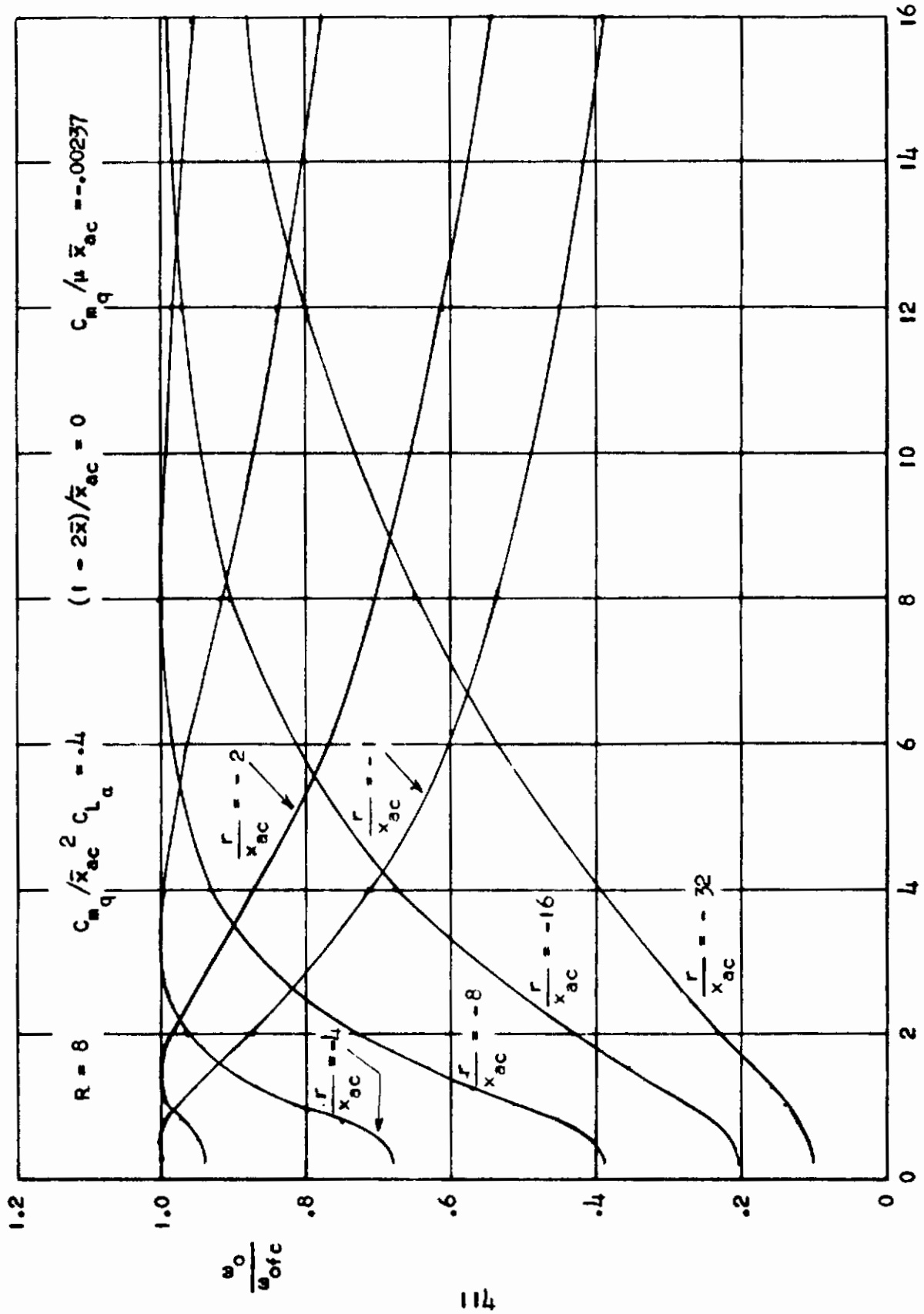

Figure 43. Frequency Coalescence Solution

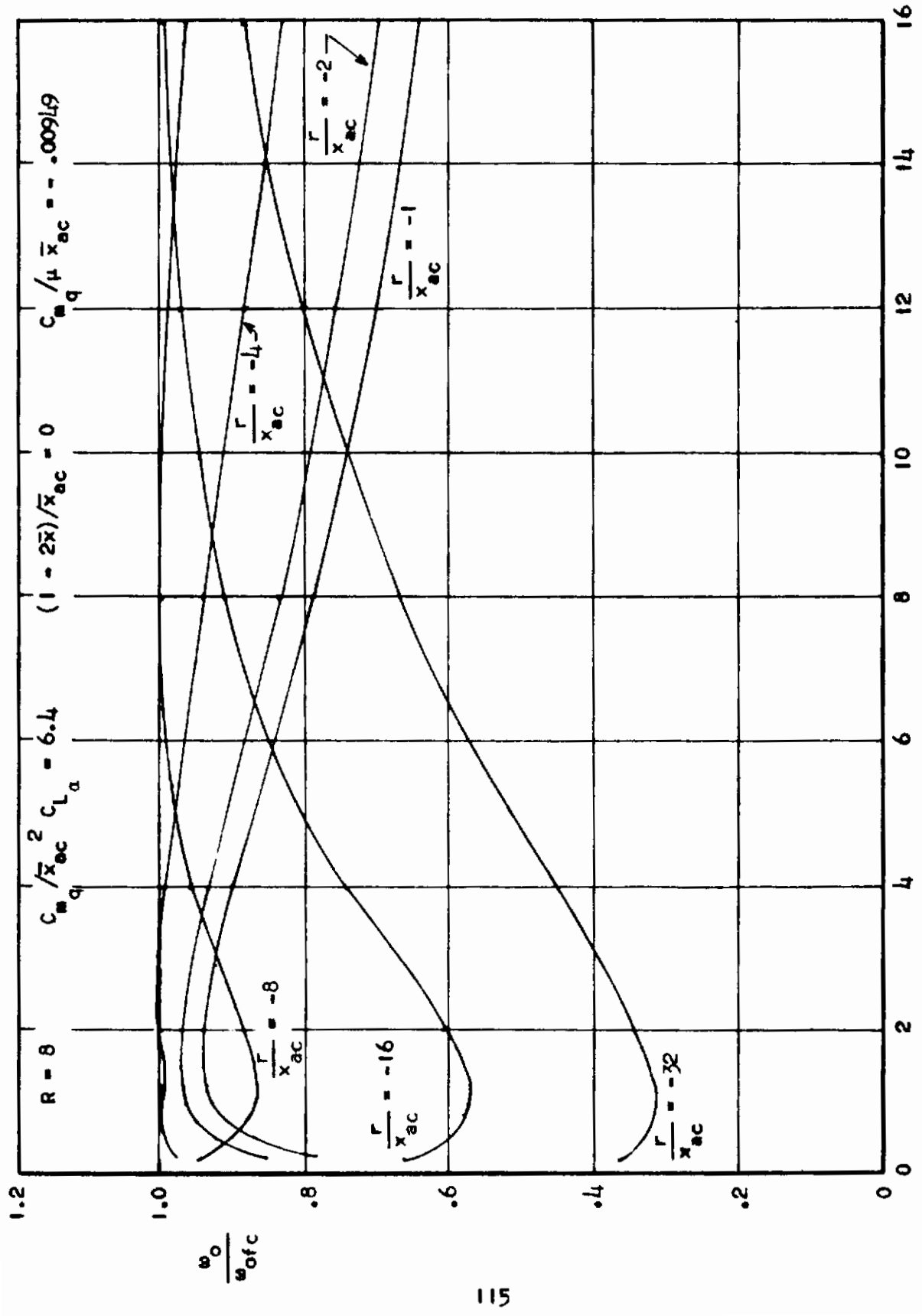

Figure 44. Frequency Coalescence Solution

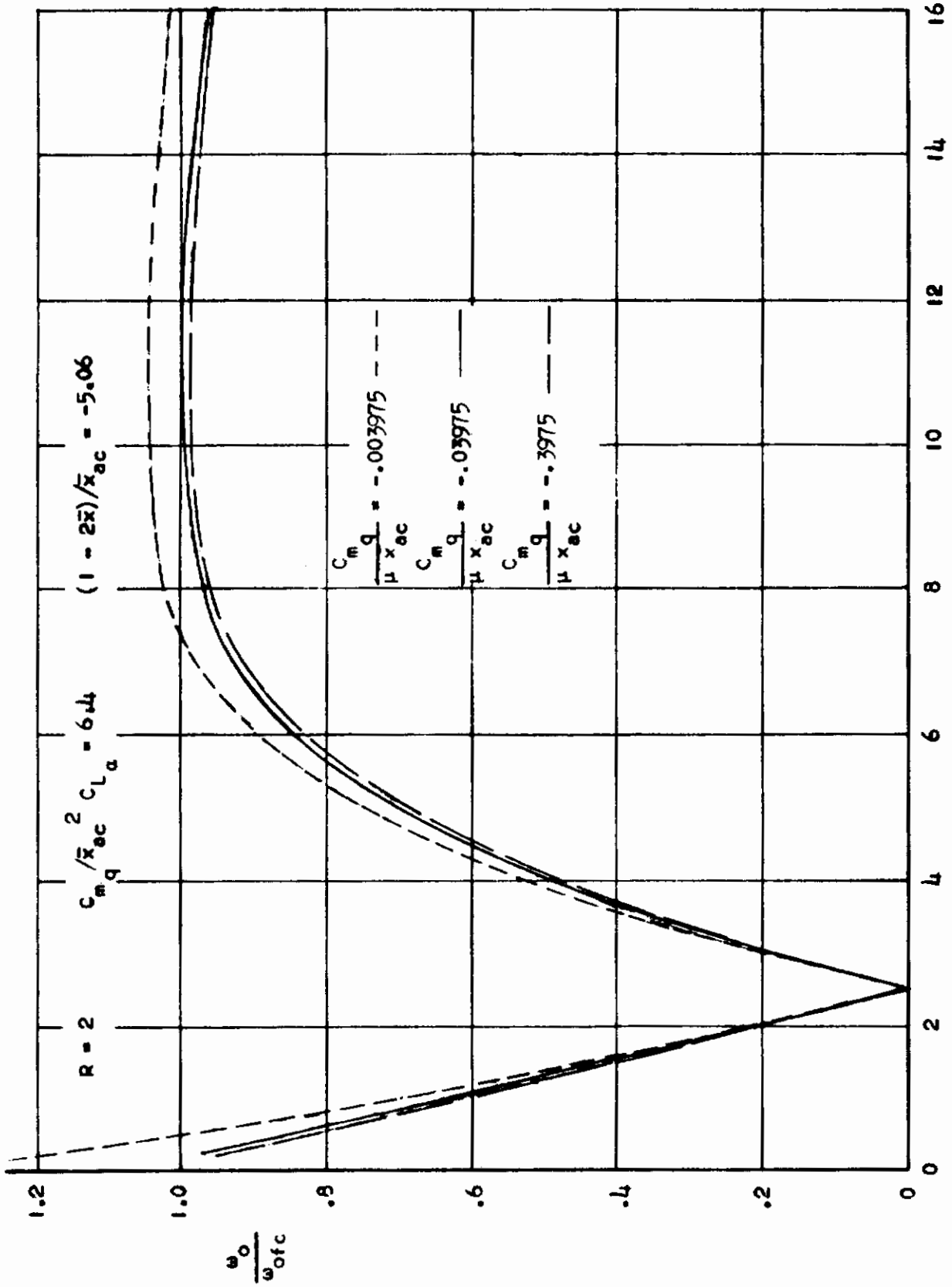

Figure 45. Effect of $(C_{m_q}/\mu\, \bar{x}_{ac})$